EXPLORING THE NEURAL CORRELATES OF OPENNESS/INTELLECT AND RELATED CONSTRUCTS USING NEW AND BEST PRACTICES IN PERSONALITY NEUROSCIENCE

A DISSERTATION
SUBMITTED TO THE FACULTY OF
UNIVERSITY OF MINNESOTA
BY

Tyler Adam Sassenberg

IN PARTIAL FULFILLMENT OF THE REQUIREMENTS
FOR THE DEGREE OF
DOCTOR OF PHILOSOPHY

Colin G. DeYoung, Ph.D., advisor

May 2024

Acknowledgements

First, I would like to thank Colin DeYoung for his support and mentorship in fMRI and personality research. Working with Colin has allowed my intellectual curiosity to flourish across a wide range of psychological, biological, and philosophical domains. Being part of his lab has helped sharpen my thinking and encouraged me to experiment with new ideas in a way that I am truly grateful for.

Thank you to Phil Burton for his mentorship, especially during my first few years in the program learning fMRI and GPIP. His guidance really helped me understand the complexities of fMRI research, and the research in this dissertation wouldn't have been possible without his help. I would also like to thank my committee members, Angus MacDonald III, Scott Sponheim, and Nate Helwig for their time and guidance on this research.

Thank you to Steve Malone for his help in navigating and analyzing data from MCTFR, as well as other collaborators that made this research possible: Rex Jung, Ranee Flores, Adam Safron, and Victoria Klimaj.

Thank you to Kerry Michael and Leslie Meek, my undergraduate advisors, for fueling my passions in biology and psychology, getting me started in psychological research, and supporting my grad school journey.

Thank you to Moin Syed and the illustrious grad seminar gang for providing a space to share, commiserate, ask questions, and celebrate the small victories throughout the past five years. Thank you to my peers and collaborators on various projects, Scott Blain, Aisha Udochi, Allison Dai, Magdalena March, Edward Chou, Matt Rogers, and Hannah Asis. Your perspectives, feedback, and conversations have truly enriched my experience as a PhD student.

Thank you to my friends for their support, especially Ben Mladenich, Jon Bostrom, Martin Zais, Abby Malleck, Nate Dvorak, Andy Rosenthal, and Hannah Wahlstrom for helping me stay mostly sane during the dark times. Lastly, thank you to my family, Kyle, Patience, mom, and dad, for always being there for me.

Abstract

Personality neuroscience aims to understand the associations of brain structure and function with stable patterns of thought, behavior, emotion, and motivation. One broad personality dimension of interest in this field is Openness/Intellect. This trait describes individual differences in engagement with semantic and perceptual information, and subsumes a variety of societally relevant facets pertaining to higher-order cognitive processing. This dissertation examines the functional neural correlates of a number of facets beneath Openness/Intellect, including intelligence, creativity, and Psychoticism (sub-clinical psychosis proneness). Across three studies, this research aims to expand on past findings demonstrating associations of these traits with functional properties among broad macroscale brain networks implicated in abstract higher-order cognition, all within the context of broader predictive processing accounts of brain function. The first study showcases a functional gradient approach to test associations of creative achievement with functional similarity of higher-order brain networks. The second study demonstrates associations of intelligence, Openness/Intellect, and Psychoticism with various forms of dynamic brain network flexibility. Lastly, the third study explores individual differences in signatures of self-organized criticality in the brain, and how it relates to intelligence and Psychoticism. Through a variety of methods, these findings converge on the notion of Openness/Intellect and its facets being associated with individual differences in abstract information processing capabilities among broad cortical networks. This research provides a more nuanced perspective of the neural correlates of Openness/Intellect by demonstrating how its adaptive and maladaptive facets are related to different and

complementary functional properties in the brain. Beyond Openness/Intellect, this research helps provide future avenues for understanding the associations of other normative and pathological personality dimensions with properties of brain function.

Table of Contents

List of Tables

Chapter II

Chapter III

Chapter IV

List of Figures

Chapter I

Chapter II

Chapter III

Chapter IV

Chapter I: General Introduction - Personality, Openness/Intellect, and the Brain

I looked up from under the evening
at the gear wheels of the skies -
from glistening threads of chance
the loom of the past was weaving law,
and again I looked up at the sky
from under the vapors of my dreams
and I saw that the fabric of the law
was always bursting apart somewhere.

-Attila József, *Consciousness*, 1934

Cybernetics and the Personality Hierarchy

Personality psychology is the discipline tasked with providing an integrative framework for understanding the whole person (McAdams & Pals, 2006). This is a daunting mission, but one that offers multiple avenues for understanding the ways in which each individual is like all others, like some others, and like no other. In seeking to identify and understand the nature of unique patterns of individual differences, personality psychology has benefited from the insights of kindred disciplines like cognitive science and neuroscience, and a consensus is gradually emerging across these domains, characterizing human experience as the consequence of biologically-based processes of probabilistic inference. This notion of predictive processing, or hierarchical predictive coding, is explicated through perspectives like control theory and cybernetics, and describes the complex interactions between nested biological and psychological

mechanisms to minimize prediction error. Although this particular notion has been applied under many different names and in different contexts, all are characterized by the general principle that human experience emerges from encounters with the unknown, in some form, and the management of that encounter (Austin & Vancouver, 1996; DeYoung, 2015; Safron & DeYoung, 2021; Hovhannisyan & Vervaeke, 2021).

In seeking to understand patterns of individual differences, personality psychologists have identified a reliable set of personality traits, describing individual differences in relatively stable patterns of cognition, emotion, motivation, and behavior, in response to persistent sets of stimuli over evolutionary time. These trait domains cohere with predictive processing accounts of human behavior and biology by representing individual differences as variation in cybernetic parameters that regulate behavior and cognition in response to these broad classes of environmental stimuli.

One of these broad trait domains is Openness/Intellect. This dimension describes individual differences in cognitive exploration, or variation in the tendency to seek out, detect, appreciate, understand, and use sensory and abstract information (DeYoung, 2014; DeYoung et al., 2012). Individuals scoring high in Openness/Intellect are curious, imaginative, creative, and innovative, while people scoring low in Openness/Intellect are practical, conventional, traditional, and down-to-Earth. From a cybernetic perspective, Openness/Intellect represents individual variability in the ability to a) gather and interpret sensory feedback to influence interpretations of the world, b) detect discrepancies between the current state of reality and imagined states, and c) predict useful strategies in pursuing one's goals (DeYoung, 2015). This trait is vital in understanding how individuals generate and manage nuanced representations of reality and themselves.

Others have characterized Openness/Intellect as the trait describing variation in the capacity for optimal framing within the larger cognitive economy (Hovhannisyan & Vervaeke, 2021).

Continued psychometric research has revealed that personality has a relatively consistent structure, or regular patterns of covariation among traits. This evidence converges on the notion of personality as inherently hierarchical, with broader domains subsuming lower order aspects, and more specific facets beneath them. As the name implies, Openness/Intellect encompasses the shared variance of its two aspects, Openness and Intellect. The Openness aspect describes individual variation in sensitivity to sensory and perceptual information, and the Intellect aspect reflects variation in sensitivity to semantic or abstract information (DeYoung et al., 2007; DeYoung et al., 2012). Individuals scoring high in Openness are artistic, reflective, fantasy-prone, and perceptive. Individuals scoring high in Intellect are philosophically-minded, quick-witted, and perceived as intelligent. Like their larger domain, Intellect and Openness have unique hypothesized cybernetic functions, with Openness reflecting variation in the sensitivity to spatial and temporal correlational patterns, and Intellect reflecting variation in sensitivity to logical or causal patterns within environmental stimuli that can be construed abstractly (DeYoung, 2015).

Beneath the aspects are an indeterminate number of facets describing more nuanced patterns of personality variation. In the case of Openness/Intellect, some central facets include traits such as imagination and creativity (Saucier, 1992). At the extremes, other facets like intelligence and need for cognition are well described by Intellect, and facets like fantasy-proneness, perceptual aberration, magical ideation, and tendencies

toward paranormal beliefs are captured by Openness. This particular arrangement of facets has been dubbed a “paradoxical simplex” on account of the facets at opposite ends of spectrum being negatively correlated with each other, yet both loading positively on the same higher-order factor (DeYoung et al., 2012).

This hierarchical organization of personality extends above domain level traits like Openness/Intellect as well. At the apex of the personality hierarchy, the two metatraits, Stability (the shared variance of Conscientiousness, Agreeableness, and low Neuroticism) and Plasticity (the shared variance of Extraversion and Openness/Intellect), describe the most fundamental cybernetic functions underlying personality variation. Stability has been interpreted as reflecting individual differences in the ability to protect existing characteristic adaptations (i.e. relatively stable goals, strategies, and interpretations acquired through an individual’s life circumstances) from disruption by impulses, and Plasticity as reflecting variation in a general capacity for exploration, or the creation of new characteristic adaptations. In this manner, the metatraits exhibit a dynamic tension that reflects psychological responses to encounters with anomalous information, with Stability permitting the maintenance of a reliable repertoire of available of characteristic adaptations to meet the demands of the environment, and Plasticity allowing the assimilation of new characteristic adaptations when existing ones prove insufficient to cope with reality (DeYoung, 2015).

Together, these traits provide an important arrangement for understanding how individuals vary in their ability to explore and integrate information from their environment. Of course, other traits within the personality hierarchy provide useful information in understanding the human experience, but this dissertation focuses on traits

most proximal to Openness/Intellect for the purpose of understanding individual differences governing the complexity of interpretations of reality, or "the breadth, depth, and permeability of consciousness" (McCrae & Costa, 1997, p. 826). The hierarchical arrangement of traits that are investigated in this dissertation are illustrated in Figure 1.

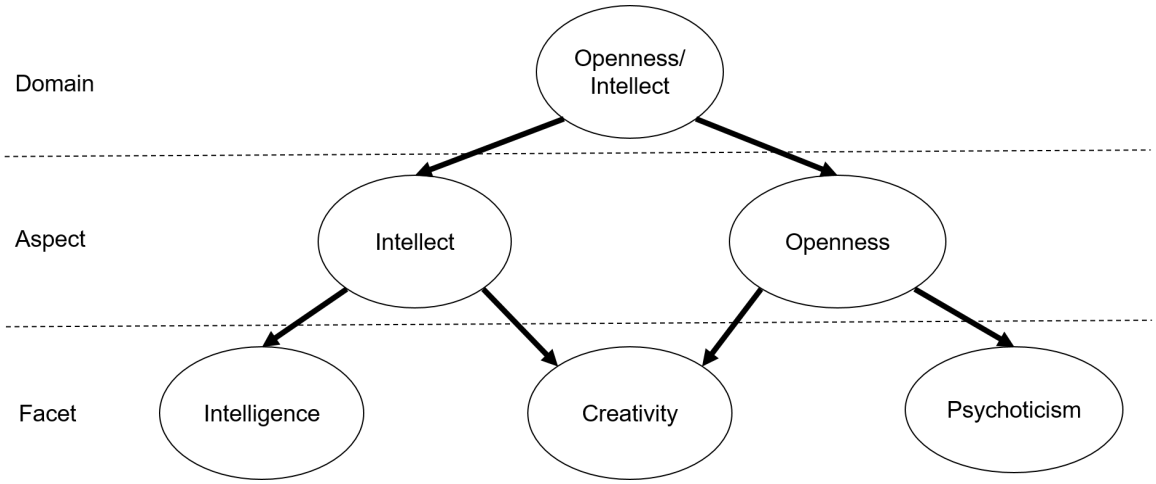

Figure 1. Personality traits related to Openness/Intellect studied in this dissertation and their hierarchical organization.

Aims and Methods of Personality Neuroscience

An understanding of the whole person would be incomplete without a proper recognition of each person as a biological organism. The confluence of genetic and evolutionary factors are important for understanding the emergence of personality, but equally important is the role of the brain. The brain is the most proximal explanation of patterns of behaviors that constitute personality traits, and understanding the role that the brain plays in shaping personality is the purview of personality neuroscience.

Understanding the biological basis of personality is a challenge on account of the sheer complexity of brain structure and function. However, growing technological advances have permitted a variety of different methods for assessing different properties of the brain itself or downstream consequences of brain activity. These methods include electroencephalography (EEG), functional magnetic resonance imaging (fMRI), positron emission tomography (PET), molecular genetics, assays of endogenous psychoactive substances, and psychopharmacological manipulation (DeYoung, 2010; DeYoung et al., 2022a). Although personality neuroscience encompasses a variety of techniques to understand associations of personality traits with individual differences in brain structure and function, fMRI remains the most common approach for investigating these associations. FMRI confers the advantages of being a noninvasive procedure, having high spatial resolution, and offering a degree of flexibility in the kinds of paradigms used to assess brain activity. One such paradigm is analysis of functional connectivity. Functional connectivity refers to temporal synchrony of particular voxels, vertices, or regions of interest across the brain. The identification of broad patterns of functional connectivity has led to growing interest in understanding large-scale brain networks and their associations with a variety of individual differences.

As part of the larger field tasked with understanding the nature of brain function, personality neuroscience also contends with the larger practical concerns of identifying and reporting patterns of brain connectivity. One of these concerns is the very definition of what constitutes a large-scale brain network. In graph theoretical terms, ‘network’ refers to the collection of fundamental units of a complex system (nodes) and their pairwise interactions (edges). This definition permits a relatively simple application of

nodes to graphical models of the brain, which can be defined as particular voxels in 4D volumetric representations, vertices in cortical surface meshes, or regions of interest defined through functional localizer tasks, functional atlases, or anatomical boundaries. Network edges can then be modeled as measures of covariation or waveform similarity between combinations of nodes. Through this perspective, networks are often described as reflecting spatially distributed components derived from multivariate analyses or large collections of pairwise edges. Despite this straightforward definition, controversy has stemmed from issues concerning the identification of a reliable set of macroscale networks across individuals, as well as inconsistencies in naming conventions. One recurring theme in the discussion of how particular networks are named is whether networks should be identified anatomically or their function, with examples including the cingulo-opercular network vs. salience/ventral attention network and the frontoparietal network vs. central executive or cognitive control network. Identifying a universal taxonomy of functional brain organization remains an ongoing challenge, but consensus on network criteria and naming conventions is growing in part due to concerted efforts to understand common limitations in network neuroscience literature (Uddin et al., 2023).

Despite these challenges, continued research on the global organization of functional connectivity has revealed a relatively consistent set of functional networks using different methodological approaches. The variety of network identification procedures are grouped into what are known as ‘soft’ vs. ‘hard’ parcellations. Soft parcellation refers to procedures in which network nodes can overlap spatially. One common soft parcellation procedure in personality neuroscience is independent components analysis (ICA; Hyvärinen & Oja, 2000). ICA is a procedure designed to

solve the blind source separation problem, which refers to the problem that the timeseries at any given voxel are the result of activation from multiple adjacent regions. ICA identifies larger functional networks by organizing the timeseries into statistically independent components in a manner similar to other multivariate procedures like factor analysis. These components can then be mapped onto particular voxels in the brain.

Soft parcellation approaches like ICA have a number of advantages and disadvantages. The fact that these components can be spatially overlapping is advantageous for identifying particular brain regions that participate in multiple functional networks. Researchers have also used a procedure known as dual regression in conjunction with ICA to deal with the challenge posed by the fact that the same functional networks can be in different places relative to anatomy. ICA can be useful for identifying components corresponding to potential sources of artifactual variance like cardiac or respiratory fluctuations, or head motion during the scan. However, two particularly noteworthy disadvantages of ICA-plus-dual-regression procedure are that 1) dual-regression is limited in that the more a participant's network deviates from the group-level component the more correction is required but the harder the correction is to accomplish because the farther from the desired time-series is the group time-series being used as the regressor, and 2) components derived using ICA are unique for each sample, which makes attempts in replicating particular associations with a given functional network across samples difficult.

Unlike soft parcellations, hard parcellations tile the cortex with nonoverlapping network nodes. Hard parcellations are often organized in cortical atlases, which attempt to identify relatively universal patterns of functional connectivity across large samples.

The growing popularity of cortical atlases in personality neuroscience is partly attributable to the ease of comparing functional regions across samples, since these atlases can be easily mapped onto neuroimages that conform to a common surface space. One atlas that has been particularly influential is the one derived by Yeo et al. (2011). This atlas divides the cortex into 7 non-overlapping functional networks (with another version identifying 17 networks). These networks, being identified and replicated across large samples, dominate the literature regarding network identification. At the time of writing, the article introducing these networks has been cited over six thousand times. These networks are useful for delineating concise anatomical boundaries and unique functional properties for each network. Additional efforts have also extended these networks to include the cerebellum (Buckner et al., 2011) and striatum (Choi et al., 2012).

This atlas is effective in describing broad patterns of functional connectivity but is not the only choice of atlas for measuring macroscale brain networks. Other atlases have incorporated local watershed gradients of connectivity or anatomical and cytoarchitectural information to estimate functional regions (Gordon et al., 2016; Glasser et al., 2016). Another particularly useful atlas in studying individual differences in functional connectivity is from Schaefer et al. (2018). This atlas is characterized as a local-global parcellation on account of its ability to model functional homogeneity within local functional regions as well as across global patterns of connectivity. This atlas has been argued to be the optimal choice for measuring functional connectivity on account of its ability to capture greater within-parcel homogeneity compared to other cortical atlases and its correspondence to the functional networks of the Yeo atlas (Schaefer et al., 2018;

Luppi et al., 2021). Additionally, variations of this atlas exist with multiple different parcel resolutions, which can be useful in addressing a variety of different research questions.

Despite the apparent benefits of hard parcellation approaches, there are also a number of limitations to consider. One assumption of many group-level atlases is that functional networks can be decomposed into smaller subnetworks. These subdivisions are identified statistically, but often lack clear theoretical justification. Given the previous discussion of the typical definition of what constitutes a network in neuroscience literature, there is some ambiguity in the distinction between the classification of a network and subnetwork and whether these two should be characterized as separate entities.

Further, all functional atlases assume that each brain has the same number of regions with the same shape and size. The rigidity of group-level atlases fails to account for individual variability in functional topology, and raises the challenge of creating a universal network taxonomy that simultaneously respects individual variation. The assumption that all individuals contain the same number of functional regions does not hold (Gordon et al., 2017), and the fact that certain individuals appear to be missing particular functional nodes raises the issue of how to specifically define a functional network. However, while this issue remains a challenge for network neuroscience, recent research has provided potential solutions to the separate issue of assuming uniform parcel boundaries. One solution is a class of procedures known as individualized parcellation. Two of these approaches, group prior individualized parcellation (GPIP; Chong et al., 2017) and multi-session hierarchical Bayesian modeling (MS-HBM; Kong et al., 2021)

apply iterative Bayesian algorithms to adjust boundaries of a group-level atlas to optimally reflect individual differences in functional localization, which can incorporate information across different tasks or scanning sessions. Already, these approaches have demonstrated their utility in predicting a wide assortment of individual differences (Anderson et al., 2021; Setton et al., 2022; Mwilambwe-Tshilobo et al., 2019), and they producing greater effect sizes in brain-behavior associations (Kong et al., 2021; Sassenberg et al., 2023) and more conservative patterns of functional-connectivity differences in case-control designs (Levi et al., 2023).

These methods of parceling the brain are useful approaches for precisely identifying functional networks in the brain that reflect both universal properties and individual variation. However, there is still debate in the field of network neuroscience as to the best way to effectively model connections within and between these networks for the prediction of individual differences. Depending on the resolution of a particular atlas, a researcher can still be dealing with multiple thousands of connections even after parceling the brain into discrete regions. Past research has relied on properties of individual components or parcels, using measures like the average correlation between voxels or vertices within these regions, or pairwise correlations between regions of interest. More sophisticated measures of network properties can be assessed using graph theoretical measures, which can identify specific properties of network configuration, including integration (e.g. global and local efficiency, path distance), segregation (e.g. modularity, clustering coefficient, transitivity), centrality, and degree configuration (Rubinov & Sporns, 2010).

Graph theory is a useful approach for summarizing connectivity patterns in line with how biological systems like the brain tend to organize, and past research has identified associations of particular properties of particular brain networks with Openness/Intellect and its facets, including efficiency (Beaty et al., 2016), and modularity (Hilger et al., 2020). The use of graph theory for the prediction of individual differences is growing in popularity in network neuroscience on account of its ability to summarize many kinds of systematic patterns of brain function across the network. However, with growing methodological advances in the field, other approaches have begun to emerge that promote stronger theoretical ties to the broader predictive processing framework. One of these methods is connectome harmonics, which posits that brain function is governed by fundamental principles of harmonic modes, or patterns of synchronous oscillations, that produce the reliable patterns of network organization across the cortex (Glomb et al., 2021; Margulies et al., 2016). Another method is assessing changes in network modularity over time to assess dynamic brain network flexibility, where different kinds of flexibility are hypothesized to relate to adaptive or maladaptive forms of cognition (Safron et al., 2022). Other research has discussed how the complexity of fMRI signals, as an index of the brain operating at a critical state, might relate to different trait dimensions, psychopathological measures, and developmental outcomes (Goekoop & de Kleijn, 2023). These emerging methods have demonstrated promise in predicting specific clinical outcomes and narrow dimensions of individual differences, but have yet to be applied to broad dimensions of personality like Openness/Intellect.

The goal of this dissertation is to explore associations of different functional properties of broad brain networks with Openness/Intellect and a number of its facets

across three different studies. These studies showcase a range of emerging techniques in network neuroscience, including individualized parcellation, graph theoretical approaches with dynamic functional connectivity, a form of connectome harmonic analysis known as diffusion map embedding to assess connectivity among broad macroscale brain networks, and the use of power-law scaling to assess self-organized criticality within the brain. Each study uses these analyses in well-powered samples to demonstrate best practices in personality neuroscience, and helps to situate the underlying cybernetic function of Openness/Intellect and its related facets in the larger predictive processing framework of brain organization.

Chapter II: Predicting Individual Differences in Creative Achievement and Openness/Intellect using Macroscale Cortical Gradients

The imagination has no limits

The physical world does

The work exists in both

-Rick Rubin, *The Creative Act: A Way of Being*, 2023

A growing body of research in network neuroscience is converging on the notion that brain function is characterized by patterns of connectivity represented through broad macroscale networks. Although progress has been made in understanding the behavioral correlates of these networks, other challenges persist in how to understand the interactions among these networks, and how the configuration of these cortical networks relates to other properties of brain architecture (Kong et al., 2023; Uddin et al., 2023). One perspective on the nature of brain function that helps to address these challenges is the idea of connectome harmonics. Connectome harmonics constitute a proposed underlying principle of macroscale cortical dynamics, using a broad mathematical framework for understanding wavelike oscillations that has been incorporated in theories of heat, light, sound, electricity, magnetism, gravitation, and fluid dynamics (Atasoy et al., 2016). By decomposing functional connectivity graphs using eigenfunctions, broad patterns of functional similarity across the cortex from high-dimensional data can be represented as eigenmodes, or functional gradients, in a lower dimensional manifold (Margulies et al., 2016; Bernhardt et al., 2022).

Functional gradients have been identified on the assumption that the topological configuration of the cortex affords a grounding framework for organizing patterns of cognition, and this type of gradient-based organization in the cortex has been observed across a variety of brain properties, including myelination (Huntenburg et al., 2017), anatomical structure (Park, Vos de Vael et al., 2021), white matter tract connectivity (Friedrich et al., 2020), evolutionary and ontogenetic expansion (Hill et al., 2010; Buckner & Krienen, 2013; Reardon et al., 2018), semantic processing (Shao et al., 2022), and physiologically coupled traveling waves (Pang et al., 2020). Many of the techniques used to derive macroscale cortical gradients are extensions of methods used to identify neuronal activity in highly specialized regions to generate dense maps of somatotopy, tonotopy, and retinotopy. Newer procedures extend the scale of this principle, and use cortical vertices or parcels that exhibit similar patterns of activity across the whole brain to generate gradients of functional similarity in latent space. In this manifold space, functional relations among voxels, vertices, or regions of interest are represented as geometric distance among points in the lower-dimensional space. Research using these kinds of approaches has consistently revealed the presence of two major gradients with identifiable functional properties (Setton et al., 2022; Knodt et al., 2023; Nenning et al., 2023; Paquola et al., 2019). The first of these gradients describes variation between functional regions characterized by unimodal and heteromodal processing, with highly specialized sensory cortex at one end and associative cortex implicated in higher-order cognition at the other end. The second gradient differentiates between somatomotor and visual processing within unimodal cortical regions. This gradient places unimodal regions at each end, and includes heteromodal regions in the middle. When plotted together, the

two gradients constitute a cortical hierarchy, distinguishing cortical regions with different functional properties.

The hierarchical connectivity pattern produced from these gradients maps well onto existing cortical network boundaries (Atasoy et al., 2016), and this correspondence is consistent with the tethering hypothesis, which describes how heteromodal cortex derives its properties from topological distance from primary sensory areas on the cortex (Huntenburg et al., 2017; Smallwood et al., 2021). This hypothesis provides a basis for distinguishing the abstract information processing of networks like the default, frontoparietal control network (FPCN), and salience/ventral attention networks (SVAN) from other networks responsible for more specialized forms of information processing. The utility of this approach is especially apparent when predicting individual differences implicated in widespread functional connectivity patterns across the cortex, since the complex functional profiles of multiple broad networks can be summarized through concise geometric associations between points in the manifold. Research using these gradients has been successful in identifying associations of functional gradient properties with a wide range of individual differences, including age (Setton et al., 2022), intelligence (Knodt et al., 2023), schizophrenia (Dong et al., 2023), and autism (Hong et al., 2019).

Another behavioral measure that has received considerable attention in network neuroscience research is creativity. Defined broadly, creativity describes the ability to generate new and appropriate ideas, and this trait is a core facet of the larger personality dimension Openness/Intellect, which describes individual differences in tendencies toward cognitive exploration (Saucier, 1992; Schwaba et al., 2020; DeYoung, 2015).

Much of the research exploring the functional correlates of creative cognition and related constructs like divergent thinking and cognitive flexibility has highlighted connectivity between heteromodal networks like the FPCN, SVAN, and default network (Beaty et al., 2016; Frith et al., 2021; Chen et al., 2014; Roberts et al., 2017; Patil et al., 2021). However, additional findings have implicated the involvement of other potentially relevant networks, including the somatomotor, limbic, and visual networks (Jiao et al., 2017; Wang et al., 2021; Zhuang et al., 2021). The involvement of multiple networks in creative cognition may not be too surprising, considering the complexity of the neural mechanisms needed to sustain the variety of cognitive capacities that play at least some small role in creative thought, including working memory, the flexible allocation of attention, and the simulation of various schemas, perceptual states, or kinesthetic actions.

Despite the growing body of research describing the functional correlates of creative cognition, assessing creativity using gradient approaches has been less common. Recent research has demonstrated an association of creativity with greater variability in the unimodal-heteromodal gradient (Huo et al., 2022). Considering the complex functional connectivity patterns associated with creativity described in previous research, this study aims to expand on these findings by testing associations between gradient topology and creative achievement. Unlike past research using task-based measures of creativity, this study tests associations of a self-report measure of creative achievement with the gradient properties and coupling among functional networks identified in previous literature. Beyond creativity, this study also explores how features of gradient topology contribute to the prediction of the larger personality domain Openness/Intellect and whether they are similar to those associated with creative achievement.

I hypothesize that creative achievement is related to individual differences in the functional architecture outlined by the tethering hypothesis. If creativity primarily involves adaptive and flexible reinterpretations of environmental stimuli or existing cognitive frameworks, where abstract thinking is not limited to conventional interpretations of reality informed by basic sensory processing, then this form of cognition might be reflected as greater functional dissimilarity between heteromodal and unimodal processing. Specifically, I hypothesize that creative achievement and Openness/Intellect, both tightly linked to complex cognition, are associated with greater range along the unimodal-heteromodal gradient. In other words, participants scoring higher in creative achievement and Openness/Intellect will exhibit greater differentiation between the functional properties of the heteromodal and unimodal networks. Additionally, in line with previous research on the functional correlates of higher-order cognition, I hypothesize that creative achievement and Openness/Intellect will be associated with reduced dispersion, or greater functional similarity, among points that characterize connectivity within and between the subnetworks of the FPCN, SVAN, and default network.

Methods

Sample 1

Participants

As part of a larger study, a total of 306 participants completed a single 5 minute resting-state fMRI session. These participants were recruited through online advertisements and fliers posted in the metro area surrounding Minneapolis and St. Paul, Minnesota. Participants were excluded on the basis of fMRI contraindications, a

diagnosis of neurological or severe psychiatric conditions, or substantial behavioral dysfunction attributable to drug or alcohol use. Following recruitment, additional participants were excluded from subsequent analysis on account of incomplete or poor quality fMRI data, excessive head motion identified during preprocessing and gradient analyses, or incomplete behavioral data. After these exclusions, a total of 236 participants were retained (121 female) ranging from 20 to 40 years old (M = 26, SD = 4.7). Protocols used in this study were approved by the University of Minnesota Twin Cities institutional review board, and all participants provided written informed consent.

Creative Achievement Questionnaire

The Creative Achievement Questionnaire CAQ (Carson et al., 2005) is a self-report measure that assesses achievements across 10 different creative domains: visual arts, music, dance, architectural design, creative writing, humor, inventions, scientific discovery, theater and film, and culinary arts. Participants were assigned points according to their achievements in each domain. For each domain there were seven levels of increasing achievement, and participants checked all levels that applied, receiving points for each corresponding to its level (e.g. in the domain of scientific discovery, 1 = "I often think about ways that scientific problems could be solved" and 7 = "My work has been cited by other scientists in national publications"). Recent meta-analytic research has demonstrated that CAQ scores exhibit good reliability across cultures, education levels, and ethnicities (Yörük & Sen, 2023). Following previous research, total creative achievement was computed as the sum of all domains of creative achievement. Similarly, creative achievement in the arts was computed as the sum of scores of visual arts, music, dance, creative writing, humor, and theater and film. Scores for scientific discovery and

inventions were summed to create a measure of creative achievement in the sciences (Kaufman et al., 2016).

Personality Measures

Analyses of Sample 1 used scores from two personality questionnaires. The Big Five Aspect Scales (BFAS; DeYoung et al., 2007), consists of 100 items rated on a 5-point Likert scale ranging from 1 (*strongly disagree*) to 5 (*strongly agree*). This questionnaire divides each of the Big Five into two subfactors called aspects, each measured through 10 items, which are averaged to create Big Five domain scores. In addition to the BFAS, participants also completed the Big Five Inventory (BFI; John et al., 2008), consisting of 44 items measuring the Big Five dimensions on a 5-point Likert scale ranging from 1 (*strongly disagree*) to 5 (*strongly agree*). This study used the domain level scores of Openness/Intellect, with the remaining Big Five included as covariates. In addition to self-report measures, peer-report measures were obtained by providing participants with 3 packets with instructions to have both questionnaires completed by individuals who knew the participant well. At least one peer report was available for 182 participants, and multiple peer-reports for a given subject were averaged to create a single peer-report score, when applicable. Self- and peer-report scores from the BFAS and BFI were averaged to create a composite measure of Openness/Intellect.

Intelligence

All participants included in the present study completed a subset of the Wechsler Adult Intelligence Scale – Fourth Edition (WAIS-IV; Wechsler, 2008), the Block Design, Matrix Reasoning, Vocabulary, and Similarities tests. Although the present study selected

these tests from the WAIS-IV, these four tests correspond to those used in the shorter alternative, the Wechsler Abbreviated Scale of Intelligence (WASI), and provide reliable estimates of full-scale IQ (Wechsler, 2011).

fMRI Data Acquisition and Preprocessing

fMRI data were acquired using a 3T Siemens Trio Scanner at the Center for Magnetic Resonance Research at the University of Minnesota Twin Cities. High-resolution T1-weighted MPRAGE images were acquired for anatomical surface registration for each participant, as well as functional echo-planar images with the following parameters: repetition time (TR) = 2 s; echo time (TE) = 28 ms; flip angle = 80°; voxel dimensions = 3.5 x 3.5 3.5 mm; pixel bandwidth = 2790 Hz.

Results included in this manuscript come from preprocessing performed using *fMRIPrep* version 20.2.1 (Esteban et al., 2018), a *Nipype* (Gorgolewski et al., 2011) based tool. Each T1w (T1-weighted) volume was corrected for INU (intensity non-uniformity) using N4BiasFieldCorrection v2.1.0 (Tustison et al., 2010) and skull-stripped using antsBrainExtraction.sh v2.1.0 (using the OASIS template). Spatial normalization to the ICBM 152 Nonlinear Asymmetrical template version 2009c (Fonov et al., 2009) was performed through nonlinear registration with the antsRegistration tool of ANTs v2.1.0 0 (Avants et al., 2008), using brain-extracted versions of both T1w volume and template. Brain tissue segmentation of cerebrospinal fluid (CSF), white-matter (WM) and gray-matter (GM) was performed on the brain-extracted T1w using fast (FSL v5.0.9; Zhang et al., 2001).

Functional data was slice time corrected using 3dTshift from AFNI v16.2.07 (Cox, 1996) and motion corrected using mcflirt (FSL v5.0.9; Jenkinson et al., 2002). This

was followed by co-registration to the corresponding T1w using boundary-based registration (Greve & Fischl, 2009) with nine degrees of freedom, using flirt (FSL). Motion correcting transformations, BOLD-to-T1w transformation and T1w-to-template (MNI) warp were concatenated and applied in a single step using antsApplyTransforms (ANTs v2.1.0) using Lanczos interpolation.

Physiological noise regressors were extracted applying CompCor (Behzadi et al., 2007). Principal components were estimated for the two CompCor variants: temporal (tCompCor) and anatomical (aCompCor). A mask to exclude signal with cortical origin was obtained by eroding the brain mask, ensuring it only contained subcortical structures. Six tCompCor components were then calculated including only the top 5% variable voxels within that subcortical mask. For aCompCor, six components were calculated within the intersection of the subcortical mask and the union of CSF and WM masks calculated in T1w space, after their projection to the native space of each functional run. Frame-wise displacement (Power et al., 2014) was calculated for each functional run using the implementation of *Nipype*. ICA-based Automatic Removal Of Motion Artifacts (AROMA) was used to generate aggressive noise regressors as well as to create a variant of the data that is non-aggressively denoised (Pruim et al., 2015). The non-aggressively denoised variant was used in the present study. Participants exhibiting a relative mean framewise displacement greater than 0.5 mm, a mean standardized derivative of RMS variance over voxels (DVARS) greater than 1.5, or any single occurrence of a coordinate displacement greater than 2.75 mm were excluded from subsequent analyses to avoid biased effects in associations with measures of functional connectivity (Power et al., 2012; Power et al., 2014).

Sample 2

Participants

A total of 260 participants either working or studying within science, technology, engineering, and mathematics (STEM) fields were recruited through postings throughout the University of New Mexico, nearby high schools, and various professional STEM businesses from communities surrounding Albuquerque, New Mexico. Participants were excluded on the basis of neurological and psychological disorders, fMRI contraindications, incomplete behavioral data, incidental fMRI findings, poor FreeSurfer surface registration, and excessive head motion identified through data preprocessing. A total of 234 participants were retained for the present study (115 females) ranging from 16 to 38 years old (*M* = 22**,** *SD* = 3.9**)**. All participants provided written informed consent, and all procedures in this study were approved by the University of New Mexico institutional review board.

Behavioral Measures

All participants in Sample 2 completed one of two personality questionnaires: the BFAS, or the NEO Five-Factor Inventory (FFI). The NEO-FFI represents a subset of the full NEO Personality Inventory, Revised (NEO PI-R; Costa & McCrae, 1992), consisting of 12 items per factor. Scale scores were calculated as item averages, using a five-point Likert scale ranging from 0 (*strongly disagree*) to 4 (*strongly agree*). A total of 57 participants completed the NEO-FFI, and 177 participants completed the BFAS. To account for differences in scale means, scores were centered by subtracting the sample mean of their respective scale. The present study utilized Openness/Intellect scores from all participants, with the remaining Big Five included as covariates. Participants also

completed the WASI, and the CAQ. Participants in this sample were also asked to denote the number of times a particular achievement occurred for items in each creative achievement domain, and the number of occurrences were multiplied by the item's point value before computing scores (Wertz et al., 2020).

fMRI Data Acquisition and Preprocessing

Using a 3T Siemens Prisma scanner, resting-state functional echo-planar images were acquired with the following parameters: 32 coronal slices; TR = 275 ms; TE = 30 ms; flip angle = 34°; multiband acceleration factor = 8; voxel dimensions = 3.5 x 3.5 x 3.5 mm, pixel bandwidth = 1736 Hz. High-resolution T1-weighted MPRAGE images were acquired for anatomical surface registration through a 5 echo sequence with the following parameters: TR = 25.3 s; TE = 1.64 ms, 3.5 ms, 5.36 ms, 7.22 ms, 9.08 ms; flip angle = 7°; voxel dimensions = 1 x 1 x 1 mm^3. Results included in this manuscript come from preprocessing performed using *fMRIPrep* version 20.2.1 using the same specifications described for Sample 1.

Diffusion Map Embedding

For each participant across both samples, denoised resting-state data were resampled to the fsaverage5 cortical surface mesh, and a functional connectivity matrix was defined using product-moment correlations between the timeseries of each vertex on the cortical surface, producing a 20,484 × 20,484 correlation matrix. I then applied the diffusion map embedding pipeline to each participant's functional connectivity matrix of Z-transformed correlations to derive individual gradients in manifold space. These gradients were computed using the BrainSpace toolbox in MATLAB (https://github.com/MICA-MNI/BrainSpace; Vos de Wael et al., 2020). In line with

previous research, each participant's functional connectivity matrix was thesholded row-wise to retain only the upper 10% of connections. Cosine similarity was computed on this filtered matrix to produce an affinity matrix that describes similarity in whole-brain connectivity patterns between vertices.

Using this matrix, I then applied a nonlinear dimensionality manifold learning technique from the family of graph Laplacians to identify gradient components for each participant (Coifman et al., 2005). Each gradient describes a low-dimensional eigenvector estimated from a high-dimensional similarity matrix. In the lower-dimensional manifold space, vertices that exhibit a greater degree of similarity in their functional connectivity patterns appear closer together, and functionally dissimilar vertices appear farther apart. This algorithm is modulated by the parameter α, which determines the density of points in the manifold (Margulies et al., 2016). In order to permit the modeling of both global and local patterns of connectivity in the manifold, I used $\alpha = 0.5$. Gradients derived from a group-average functional connectivity matrix were also specified for each sample. To ensure the comparability of individual manifold spaces, I applied an iterative Procrustes rotation to align participant-specific gradients to their respective group-average gradients. Although it is possible to rotate gradients to match a template specified in another sample, in a procedure known as joint alignment, I instead chose to rotate individual gradients to match the average connectivity matrix of their respective sample. This was done to avoid unnecessarily prioritizing one sample over the other, and to ensure complete independence of gradients between samples. Across both samples, the first two gradients were extracted for each participant and were visually inspected to ensure proper alignment with their respective group-average template.

Group Prior Individualized Parcellation

To determine the functional assignments of vertices within each gradient, I used an individualized cortical parcellation approach. For each participant, resampled cortical surface data were overlaid with a pre-defined group atlas with 400 functionally distinct regions (Schaefer et al. 2018) mapped to the 17-network atlas defined by Yeo et al. (2011). A Bayesian algorithm was applied to iteratively adjust parcel boundaries to maximize within-parcel homogeneity according to each participant's unique patterns of functional connectivity (Chong et al. 2017). To ensure stable modifications of parcel boundaries, this algorithm was applied across 20 iterations until participants had no more than one vertex on the cortical surface mesh changing its parcel identification on the final iteration. Through this process, each participant acquired a unique variant of a standard group-level atlas, such that the boundaries of the parcels of the initial atlas optimally reflected each individual's patterns of resting-state functional connectivity, while parcels maintained their identity across subjects. These modified parcel boundaries were then used to identify vertices belonging to each of 17 individualized functional networks for each participant across both samples. Code used to produce individualized parcels of the Schaefer atlas is available at https://neuroimageusc.github.io/GPIP.

Analysis

To determine associations of creative achievement and Openness/Intellect with functional connectivity, I assessed three different properties of spatial organization within these gradients. First, I calculated measures of overall gradient range for the unimodal-heteromodal gradient, as well as the range of vertices within each of the 17 individualized networks of the Schaefer atlas along this gradient. Higher ranges for a particular network

indicate greater variability among vertex connectivity profiles among unimodal and heteromodal cortex (Bethlehem et al., 2020**;** Park, Bethlehem et al., 2021). Next, to assess the potential functional influence of the visual-somatomotor gradient on connectivity profiles, I computed measures of gradient dispersion, defined as the sum of the squared Euclidean distance of each vertex from the centroid in gradient space. Measures of dispersion were also calculated for each network (Bethelehem et al., 2020; Setton et al., 2022). Greater dispersion values indicate greater variability in network connectivity among regions of visual, somatomotor, and heteromodal cortex. Lastly, I computed measures of network segregation, or between-network dispersion, defined as the Euclidean distance between network centroids (Bethlehem et al., 2020). I computed segregation measures for all combinations of subnetworks of the FPCN, SVAN, and default network. This was done to assess individual differences in functional similarity among networks that I hypothesized to be most likely related to Openness/Intellect and creative achievement, as well as to limit the number of tests.

I used multiple regression to predict creative achievement and Openness/Intellect from network range, dispersion, and segregation. For measures of range and dispersion, values for each network were included as simultaneous predictors. Since range values of individual networks were dependent on the range of the entire gradient, each network's range was residualized by regressing it on the overall range before entering it in the model. Similarly, regression was used to partial variance in overall dispersion from measures of network dispersion and network segregation before entering the model. Since distributions of creative achievement measures in both samples were right-skewed with many zeros, I used Poisson regression with the robust Huber-White sandwich

estimator in models predicting creative achievement to account for the overdispersion (Kaufman et al., 2016; Silvia & Kimbrel, 2010; Silvia et al., 2012). For all models, age, sex, intelligence, head motion and total brain volume were included as covariates. Models predicting Openness/Intellect also included Extraversion, Agreeableness, Neuroticism, and Conscientiousness as covariates. Considering the potentially influential effect of intelligence, each of the previous models were also fit without intelligence as a covariate. Additionally, models predicting Openness/Intellect were also fit without the remaining Big Five to assess the impact of covariates on prediction.

Results

Descriptive statistics for behavioral measures in both samples are reported in Table 1.

Table 1.

Descriptive statistics for Openness/Intellect and creative achievement measures.

	***M*(*SD*)**	**Range**	**Skew**
Sample 1			
CAQ Arts	6.71(4.75)	25.00	.82
CAQ Sciences	1.70(1.57)	11.00	1.77
CAQ Total	9.38(5.80)	33.00	.87
Self-report BFAS Openness/Intellect	4.02(.51)	2.60	-.44
Peer-report BFAS Openness/Intellect	3.86(.43)	2.95	-.40
Self-report BFI Openness/Intellect	3.82(.66)	3.40	-.52
Peer-report BFI Openness/Intellect	3.80(.57)	3.80	-.65
Sample 2			
CAQ Arts	11.37(11.99)	78.00	2.00
CAQ Sciences	6.88(10.95)	75.00	2.84
CAQ Total	19.50(18.61)	106.00	1.95
BFAS Openness/Intellect	3.93(.38)	2.25	-.21

NEO-FFI Openness/Intellect	3.09(.59)	2.42	-.75

Note. BFAS = Big Five Aspect Scales, BFI = Big Five Inventory, CAQ = Creative Achievement Questionnaire, NEO-FFI = NEO Five Factor Inventory. CAQ scores in Sample 2 were multiplied by the number of achievements in each domain.

Gradient Manifolds

Gradient organization was largely similar across samples. The functional network assignments and sample-average gradient values for each vertex in manifold space are illustrated in Figure 2.

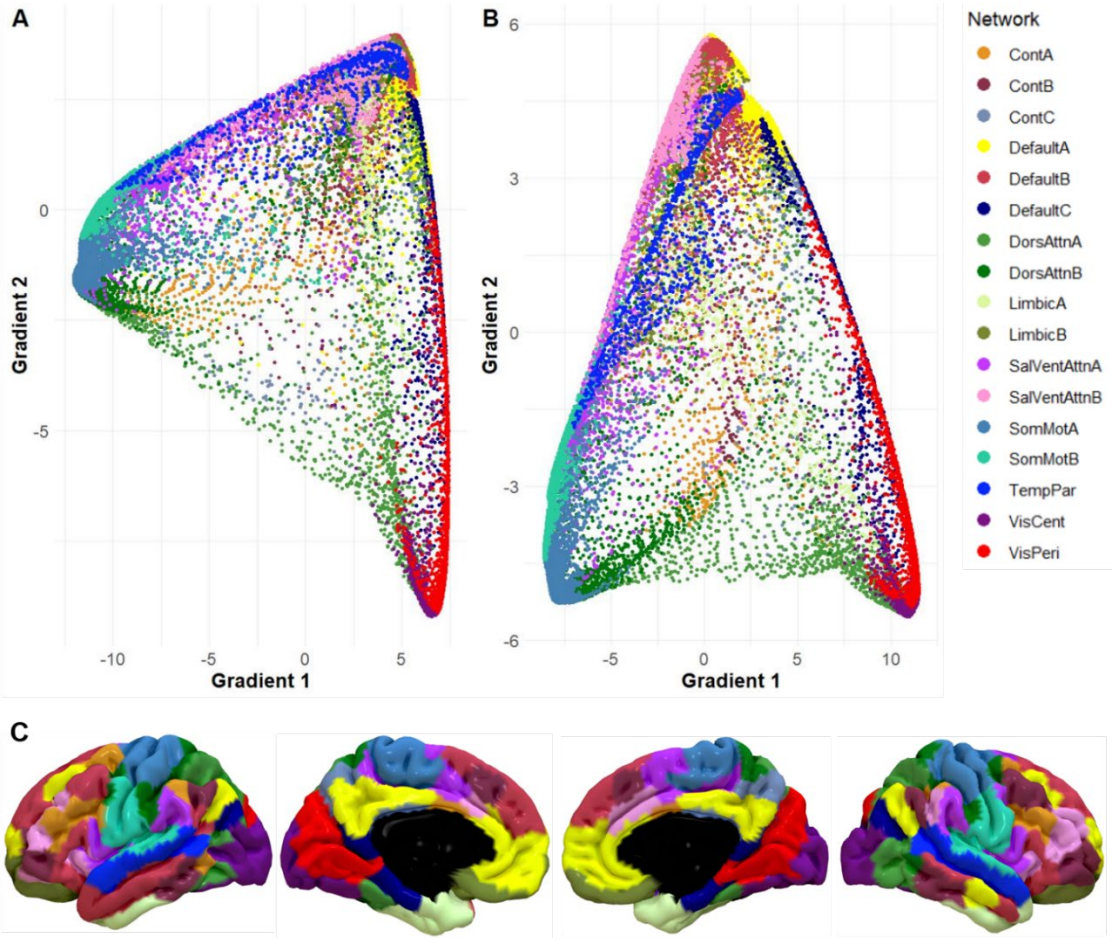

Figure 2. Values of the first two functional gradients in Sample 1 (**A**) and Sample 2 (**B**). 17 functional networks from Yeo et al. (2011) mapped to the Schaefer atlas are shown in

(**C**). Gradient values are arbitrary, but permit relative comparisons of functional similarity between vertices. Cont = frontoparietal control, DorsAttn = dorsal attention, SalVentAttn = salience/ventral attention, SomMot = somatomotor, TempPar = temporoparietal, VisCent = central visual, VisPeri = peripheral visual.

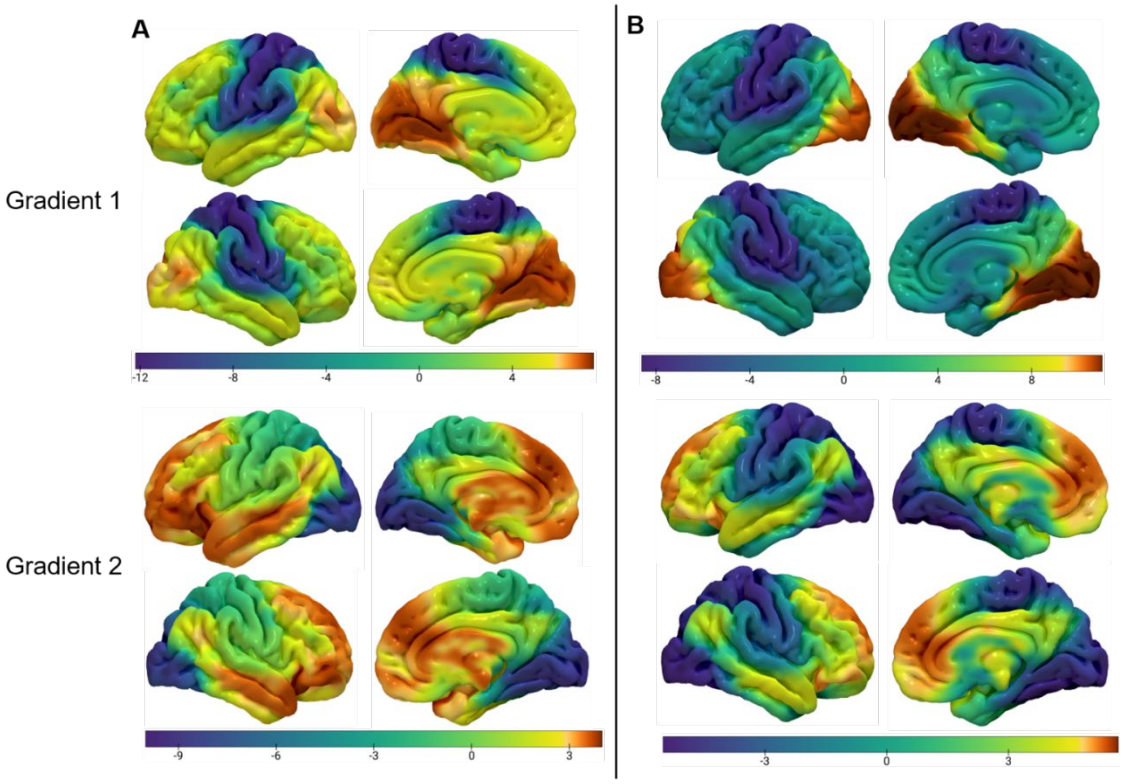

Figure 3. Sample average values for Sample 1 (**A**) and Sample 2 (**B**). Gradient values are not directly comparable across samples, but permit comparisons of relative functional similarity between regions within samples.

In both samples, the first gradient distinguished between regions of the visual and somatomotor networks (with heteromodal networks in the center), while the second

gradient distinguished regions in networks associated with higher-order cognition like the FPCN, SVAN, default, and limbic networks, from regions in the visual and somatomotor networks. This manifold configuration is consistent with descriptions of functional architecture in previous literature. Sample average values for the first two gradients mapped to the cortical surface are illustrated in Figure 3.

Predicting Creative Achievement from Gradient Properties

Gradient Range

In Sample 2, overall range of the unimodal-heteromodal gradient was significantly associated with overall creative achievement ($b = .14$, $p < .05$) and creative achievement in the sciences ($b = .23$, $p < .05$), but these associations were not replicated in Sample 1. At the network level, the range of the SVAN subnetwork A along the unimodal-heteromodal gradient was associated with overall creative achievement ($b = .20$, adjusted $p < .01$) and creative achievement in the arts ($b = .25$, adjusted $p < .01$) in Sample 1 after controlling for false discovery rate, but these associations were not replicated in Sample 2.

Gradient Dispersion

Similarly, overall dispersion across the first two gradients was significantly associated with overall creative achievement ($b = .15$, $p < .05$), creative achievement in the arts ($b = .11$, $p < .05$), and creative achievement in the sciences ($b = .19$, $p < .01$) in Sample 2, but these associations were not replicated in Sample 1. Additionally, dispersion of the dorsal attention subnetwork B was associated with overall creative achievement ($b = -.43$, adjusted $p < .01$) and creative achievement in the arts ($b = -.47$, adjusted $p < .01$) in Sample 2, but these associations were not replicated in Sample 1.

Gradient Segregation

Associations of creative achievement with network segregation are reported in Table 2. In Sample 1, creative achievement in the arts was significantly associated with segregation among three pairs of the core subnetworks of the SVAN, FPCN, and default network after controlling for false discovery rate. In Sample 2, creative achievement in the sciences was associated segregation among seven pairs of subnetworks. Across both samples, creative achievement was associated with increased segregation between the core FPCN and default subnetworks. (This association did not persist in Sample 1 after removing intelligence as a covariate; b = .22, adjusted p = .11.).

Table 2.

Associations of network segregation with creative achievement

	Sample 1 (Arts)			Sample 2 (Sciences)		
Predictor	*b*	Robust SE	Unadjusted p	*b*	Robust SE	Unadjusted p
SVANA_SVANB	.38	.29	.20	.05	.36	.89
SVANA_FPCNA	**-.63**	**.20**	**< .01**	-.50	1.11	.66
SVANA_FPCNB	.64	.27	.02	.68	.80	.40
SVANA_FPCNC	-.08	.05	.13	.13	.18	.47
SVANA_DNA	**.51**	**.19**	**.01**	-.02	.25	.94
SVANA_DNB	-.79	.43	.06	-.76	.46	.10
SVANA_DNC	-.20	.10	.05	.11	.22	.61
SVANB_FPCNA	.11	.10	.28	**-1.13**	**.40**	**.01**
SVANB_FPCNB	-.06	.09	.51	**.60**	**.17**	**< .01**
SVANB_FPCNC	-.20	.26	.46	**-1.05**	**.38**	**.01**
SVANB_DNA	-.03	.13	.81	-.30	.16	.06
SVANB_DNB	.02	.07	.72	-.20	.28	.46
SVANB_DNC	.00	.20	.99	.13	.20	.50
FPCNA_FPCNB	.08	.07	.27	**-1.10**	**.39**	**< .01**
FPCNA_FPCNC	-.18	.19	.33	.67	.81	.41

FPCNA_DNA	**.24**	**.09**	**.01**	**1.99**	**.44**	**< .01**
FPCNA_DNB	-.24	.10	.02	-.04	.22	.84
FPCNA_DNC	.11	.10	.27	.14	.49	.78
FPCNB_FPCNC	-.13	.19	.47	**-1.39**	**.47**	**< .01**
FPCNB_DNA	-.12	.09	.18	-.43	.22	.05
FPCNB_DNB	.20	.10	.05	.28	.15	.06
FPCNB_DNC	-.05	.14	.71	-.68	.29	.02
FPCNC_DNA	-.20	.25	.43	.86	.31	.01
FPCNC_DNB	.22	.30	.07	.82	.58	.15
FPCNC_DNC	.22	.09	.02	.02	.26	.94
DNA_DNB	.00	.14	.99	-.44	.32	.17
DNA_DNC	-.11	.09	.19	.11	.16	.48
DNB_DNC	.04	.23	.86	.66	.35	.06
Age	-.12	.06	.04	.02	.12	.87
Sex (M)	**.38**	**.10**	**< .01**	.36	.25	.15
Head Motion	.01	.06	.84	-.23	.12	.06
Brain Volume	-.07	.06	.24	.13	.13	.30
Intelligence	**.13**	**.05**	**.01**	.11	.11	.35

Note. SE = standard error. Robust standard errors were derived using the Huber-White Sandwich estimator to account for skewness in creative achievement scores. Sex was dummy coded: 0 = female, 1 = male. Estimates with adjusted p-values < .05 are shown in bold. SVANA = salience/ventral attention subnetwork A, SVANB = salience/ventral attention subnetwork B, FPCNA = frontoparietal control subnetwork A, FPCNB = frontoparietal control subnetwork B, FPCNC = frontoparietal control subnetwork C, DNA = default subnetwork A, DNB = default subnetwork B, DNC = default subnetwork C.

Predicting Openness/Intellect from Gradient Properties

Across both samples, Openness/Intellect was not significantly associated with either the overall range of the unimodal-heteromodal gradient or the overall dispersion of the first two gradients. In Sample 1, Openness/Intellect was negatively associated with the range of the temporoparietal network along the unimodal-heteromodal gradient after controlling for false discovery rate (β = -.21, adjusted p < .05), but this association was not replicated in Sample 2. Additionally, Openness/Intellect was not significantly

associated with segregation among the SVAN, FPCN, and default subnetworks across both samples after controlling for false discovery rate.

Discussion

Across two large samples, creative achievement was associated with greater functional dissimilarity between core subnetworks of the FPCN and default network. These findings are largely consistent with previous literature describing the functional networks associated with creative cognition, and provide an important extension of this research by investigating the connectivity correlates of a self-report measure of creative achievement using gradient analyses. Previous research exploring the connectivity correlates of creativity has emphasized the role of the FPCN and default network. Much of this research has reported increased connectivity between these networks, as well as unique patterns of coupling and uncoupling at different times during creative cognition (Beaty et al., 2016; 2019; Madore et al., 2017; Takeuchi et al., 2017). These results expand on this research, suggesting that creativity is not only associated with greater integration, but also greater functional distinctness between these networks. In other words, creative cognition might emerge from increased communication between networks that carry out different functional roles.

One potential explanation for this association is an interpretation of creative thought reflecting a cognitive process of variation and selection, or complementary generative and evaluative modes of thought, where greater functional distinctness between these two networks permits a dynamic interaction between two opposing modes of cognition (Ellamil et al., 2012; Beaty et al., 2014; Jung, 2014; Bendetowicz et al., 2018). The kind of cognition driven by the default network, especially the simulation of

novel ideas or interpretations of reality, may be less restrained through greater functional dissimilarity from the FPCN. In determining the appropriateness or application of these ideas, the FPCN may recruit the default network to meet specific creative task demands (Spreng et al., 2010), and the process of effectively meeting these demands may benefit from a greater number of simulated ideas. The functional distinctiveness of these two networks may afford greater cognitive flexibility when testing these ideas against the constraints imposed by the external environment. Further, the distinct functional properties of these networks are also consistent with research describing associations of creativity with a greater frequency of transitions between brain states (Sun et al., 2019; Li et al., 2017). Frequent switching between functionally dissimilar networks might permit creative individuals to access atypical cognitive states that contribute to the production of unconventional ideas.

This interpretation also accords with previous research reporting associations of divergent thinking with greater range of the SVAN (Huo et al., 2022). This network has been known to act as a mediator of the dynamic tension between the FPCN and default network (Menon & Uddin, 2010; Kucyi et al., 2017). Considering this role, a greater span of the SVAN in creative individuals is reasonably consistent with the FPCN and default network being farther apart in gradient space. Although past research has also implicated a greater range of the unimodal-heteromodal gradient in creativity, this association was not replicated in the present study. The present findings suggest that creativity is primarily associated with networks involved in the management of abstract higher-order cognition, and any association with more specialized functional processing through visual or somatomotor processing may be secondary.

In the present study, an important feature of the association between creative achievement and functional connectivity is that it appeared in creative achievement in the arts in Sample 1, but creative achievement in the sciences in Sample 2. This difference seems likely to be due to the differences in the participants' creative achievements between the samples. Sample 1 included participants across a range of educational and occupational statuses, while Sample 2 included individuals with STEM backgrounds. The absolute values of creative achievement across samples are influenced by the fact that that there are more domains in the arts. Additionally, participants in Sample 2 were asked to multiply creative item values by the number of achievements, resulting in a difference in scoring compared to Sample 1. However, scores of creative achievement in the sciences are considerably higher relative to creative achievement in the arts in Sample 2, and this difference may partly explain the association with different types of creative achievement. Creative achievement in the arts captures creative domains that may be more accessible to the general public, like visual arts or creative writing, while creative achievement in the sciences is measured through scientific discoveries and inventions, the kind of achievements that may be more exclusive to a sample of individuals with specific training in STEM backgrounds.

This study leveraged a number of methodological advantages in estimating the functional connectivity correlates of creativity. Beyond exploring multiple different properties of gradient organization, the use of individualized parcellation helps provide a more effective localization of network boundaries in determining features of gradient organization. The present findings are consistent with previous descriptions of the connectivity correlates of creativity, but future research using gradient approaches like

diffusion map embedding can make use of individualized parcellation to account for individual differences in functional organization.

Limitations

Despite these advantages, this study also included a number of limitations. Further, the lack of associations of gradient properties with Openness/Intellect may be due to differences in personality measurement across samples. Openness/Intellect was assessed using multiple self- and peer-report measures in Sample 1, but deviation scores across two different inventories in Sample 1. These measurement differences across samples may have contributed to differences in associations across samples.

Conclusion

This research presents associations of creative achievement with gradient properties describing functional connectivity patterns across the cortex. Creative achievement was associated with greater functional dissimilarity between the core FPCN and default network. These results provide additional evidence of the functional connectivity correlates of creative cognition by linking a self-report measure of creative achievement to relatively new techniques for assessing individual differences in functional connectivity profiles. This research also supports previous literature describing associations of creativity with connectivity patterns in broad macroscale networks associated with higher-order cognition.

Chapter III: Stable Individual Differences from Dynamic Patterns of Function: Brain Network Flexibility Predicts Openness/Intellect, Intelligence, and Psychoticism

Neuroscience research using techniques like functional magnetic resonance imaging (fMRI) to understand the structure and function of the brain has led to a growing consensus regarding the existence of broad macroscale brain networks. Instead of conceptualizing brain functions as localized in discrete regions, a network-based paradigm has emerged from the observation that blood-oxygen-level dependent (BOLD) signals across the brain tend to exhibit widespread reliable correlations that are notably similar in resting-state and task conditions (Eickhoff et al., 2011; Yeo et al., 2011; Smith et al., 2013). These functional connections between spatially distant regions allow identification of a canonical set of large-scale functional networks, each with unique behavioral correlates.

To capture the complexity of interactions within and between these brain networks, measures of functional connectivity are often derived using multivariate approaches like independent components analysis, which identifies patterns of intercorrelations among voxel timeseries and maps them to statistically independent components in the brain (Hyvärinen & Oja, 2000). Another common approach is the use of graph theory metrics to characterize regions of interest as nodes and their correlations as edges, which together can provide a variety of measures of network topology (Bullmore & Sporns, 2012; Rubinov & Sporns, 2010). One particularly useful graph theory metric is community structure, which describes the organization of broad networks

into smaller functional units called communities (also called cliques or modules), that tend to exhibit greater connectivity within their unit than with the rest of the network (Porter et al., 2009).

Much of the research seeking to identify patterns in brain organization has relied on timeseries across the duration of an entire fMRI scan to produce estimates of typical connectivity patterns in the brain, described as *static* functional connectivity. However, a growing emphasis on understanding the brain as a complex dynamical system has emphasized a form of connectivity reflecting variation in temporal dynamics, or *dynamic* functional connectivity. A variety of methods have been developed to estimate dynamic functional connectivity, including characterizing the most predictive aspects of BOLD timeseries (Karahanoğlu & Van De Ville, 2015; Tagliazucchi et al., 2012), constraining functional pathways by structural connections (Griffa et al., 2017; Vohryzek et al., 2020), describing connectivity through metastates or trajectories through attractor landscapes (Breakspear, 2017; Vidaurre et al., 2017), and using sliding-window approaches (Allen et al., 2014; Preti et al., 2017). An important advantage of dynamic functional connectivity analysis is the ability to capture the evolution of cortical topology measures like community structure over time as a potential index of moment-to-moment brain state transitions.

The variety of approaches for studying dynamic functional connectivity offers a framework for understanding the neural correlates of personality traits. Recent research has speculated that indices of network flexibility, or the tendency of brain regions to change from one community to another, may be reliable measures of adaptive functioning, and may demonstrate associations with the personality metatrait Plasticity

(Safron et al., 2022). Plasticity reflects the shared variance of the traits Extraversion and Openness/Intellect, and describes individual differences in exploration, adaptability, and the tendency to develop new goals, strategies, and interpretations (DeYoung, 2006; 2015). Safron et al. (2022) speculated that the patterns of cognition and behavior described by Plasticity may be a consequence of particular kinds of network flexibility. Specifically, they hypothesized that cohesive flexibility, describing the tendency for functional regions to change communities together, may be a good index of self-organizing criticality within the brain and may be positively associated with the general exploratory tendencies described by Plasticity.

However, much of the evidence used to support this hypothesis involves associations between network flexibility and a variety of lower-order facets specifically within the Openness/Intellect domain. Openness/Intellect is the Big Five dimension that describes individual differences in cognitive exploration, or variation in the tendency to seek out, detect, appreciate, understand, and use sensory and abstract information (DeYoung, 2015). Many features of complex cognition have been shown to be associated with network flexibility, including working memory capacity (Braun et al., 2015), cognitive fatigue (Betzel, Satterthwaite et al., 2017), need for cognition (an excellent marker of the Intellect aspect of Openness/Intellect), and creativity (He et al., 2019; Patil et al., 2021). These findings suggest the possibility that network flexibility may be more simply related to traits occupying positions in the personality hierarchy lower than Plasticity, such as Openness/Intellect or intelligence. This notion is also supported by evidence describing associations of facets of Openness/Intellect like creativity and intelligence with processing speed and the capacity for organizing brain functional

dynamics across broad networks (Lee & Chabris, 2013; Langer et al., 2011; Zhuang et al., 2021). Another potentially relevant facet of Openness/Intellect that might be related to flexibility is Psychoticism, which describes the tendency to identify perceptual or causal patterns where none exist (DeYoung et al., 2012). Finally, if the association were with Plasticity, network flexibility should be similarly related to Extraversion as it is to Openness/Intellect, and this seems unlikely because Extraversion has been most linked to reward sensitivity and more specific neural processes in reward networks that are not as broadly distributed throughout the cortex as networks supporting complex cognition (Wacker & Smillie, 2015; Smillie et al., 2019).

In the present research, therefore, I draw inspiration from the hypothesis of Safron et al. (2022) to test associations between flexibility in patterns of dynamic resting-state functional connectivity with personality, but I hypothesize that associations are more likely with Openness/Intellect, Psychoticism, and general intelligence than with Plasticity more generally. Using a machine learning approach with publicly available resting-state data from the Human Connectome Project, I perform what is, to the best of my knowledge, the first empirical test of associations of brain network flexibility with three influential constructs that occupy different strata of the personality hierarchy but share outcomes pertaining to engagement with new and complex information. (Because of my doubts about the relevance of Plasticity as a criterion personality trait, and because my analytic approach did not allow modeling Plasticity as a latent variable (which is the preferred method for measuring the metatraits), I focus my analyses on Openness/Intellect and its facets. (Analyses using metatrait Plasticity as a manifest variable are reported in the appendix and did not show any significant effects.)

Methods

Participants

A total of 994 participants (528 female) were selected from the WU-Minn Consortium of the Human Connectome Project (HCP) (Van Essen et al., 2012). Initial HCP exclusion criteria included a history of severe psychiatric, neurological, or medical disorders. Participants of the 1200 young adult sample were further excluded from subsequent analyses on the basis of missing personality and intelligence task data, and missing resting-state fMRI scan data. Participants' ages ranged from 22 to 37 years old (M = 28.7**,** SD = 3.7). All participants of the 1200 young adult sample provided informed consent. Further information regarding the informed consent procedure is described by Van Essen et al. (2013). All study protocols were approved by the Institutional Review Board of Washington University in St. Louis. Data are available from the HCP website: https://db.humanconnectome.org

Behavioral Measures

Big Five

Participants included in the present study completed the NEO Five-Factor Inventory (FFI). The NEO-FFI is a short form of the NEO Personality Inventory, Revised (NEO PI-R; Costa & McCrae, 1992), consisting of 12 items per factor. Scale scores were calculated as item averages, using a five-point Likert scale ranging from 0 (*strongly disagree*) to 4 (*strongly agree*). Openness/Intellect scores were used in subsequent analyses, and scores of the remaining Big Five were included as covariates.

Intelligence

In line with previous research assessing brain-behavior associations in HCP, a measure of general intelligence (*g*) was calculated by entering 10 cognitive tasks from the NIH Toolbox (Heaton et al., 2014) and Penn Computerized Neurocognitive Battery (Moore et al., 2015) into an exploratory bifactor model (Dubois et al. 2018a; Feilong et al. 2021). These tasks included the Oral Reading Recognition (*ReadEng_Unadj*), Picture Vocabulary (*PicVocab_Unadj*), Picture Sequence Memory (*PicSeq_Unadj*), Flanker Inhibitory Control and Attention (*Flanker_Unadj*), Dimensional Change Card Sort (*CardSort_Unadj*), Pattern Comparison Processing Speed (*ProcSpeed_Unadj*), Penn Progressive Matrices (*PMAT24_A_CR*), Penn Word Memory Test (*IWRD_TOT*), Variable Short Penn Line Orientation Test (*VSPLOT_TC*), and List Sorting Tasks (*ListSort_Unadj*). Consistent with previous literature, parallel analysis suggested a structure with four group factors (Dubois et al., 2018a), and this approach produced a well-fitting model with a general factor (*g*) explaining 56% percent of the variance among task scores (RMSEA = .03, CFI = .98, SRMR = .02). Factor scores for *g* were computed to be used in subsequent analyses.

Psychoticism

Participants also completed 123 items of the Achenbach self-report (ASR; Achenbach, 2009) to assess multiple dimensions of psychopathology. In the present study, I selected items corresponding to features of Psychoticism: “I hear sounds or voices that other people think aren’t there” (*ASR_040*), “I see things that other people think aren’t there” (*ASR_070*), “I do things that other people think are strange” (*ASR_084*), and “I have thoughts that other people would think are strange” (*ASR_085*).

Each item was scored on a three point Likert scale, and these items were averaged to create a composite Psychoticism score for each participant.

fMRI Data Acquisition and Preprocessing

fMRI data were acquired using a customized 3T Siemens Skyra scanner for all participants at Washington University in St. Louis. The present study used a single left-to-right phase encoded resting-state scan acquired using the following parameters: 72 axial slices; TR = 0.72 s; TE = 33 ms; flip angle = 52°; multiband acceleration factor = 8; voxel dimensions = 2 x 2 x 2 mm^3; pixel bandwidth = 2,290 Hz. Additionally, high-resolution T1-weigthed MPRAGE structural images were acquired for anatomical surface registration with the following parameters: TR = 24 s; TE = 2.14 ms; flip angle = 8°; voxel dimensions = 0.7 x 0.7 x 0.7 mm^3. Resting-state scans were preprocessed using the HCP minimal preprocessing pipeline and motion artifacts were removed using ICA-FIX (Burgess et al., 2016). Relative mean framewise displacement was also computed to be included as a covariate in subsequent analyses. Details of the HCP minimal preprocessing pipeline are described in greater depth in previous literature (Glasser et al., 2013; Ugurbil et al., 2013).

Group Prior Individualized Parcellation

Functional regions were identified using the same individualized cortical parcellation approach described in Chapter II.

Dynamic Network Construction

Dynamic functional connectivity matrices were identified using a sliding window approach. For each participant, the average timeseries of each of their individualized parcels were divided into a set of 16 windows of 75 TRs (approximately 54 seconds).

This division was motivated by previous research describing the susceptibility of windows shorter than 40 seconds to sampling variability and obscuring genuine patterns of network reconfiguration (Zalesky & Breakspear, 2015; Leonardi & Van De Ville, 2015). Additionally, this window size permitted windows of equal length across the duration of the scan. To assess functional connectivity between each pair of parcels, we constructed a low frequency wavelet coherence matrix describing the magnitude squared coherence of the scale two Daubechies wavelet (length 4) decomposition of the timeseries for each pair of parcels within the band-pass filtered range of .125-.25 Hz in each window using the WMTSA Wavelet Toolkit in MATLAB (https://www.atmos.washington.edu/wmtsa/). Magnitude squared coherence is a measure of functional connectivity that describes similarity in the signal waveform within a consistent frequency range. Using this metric ensures a stable index of functional connectivity across windows, while also conferring greater robustness to noise and signal outliers compared to product-moment correlation measures of dynamic functional connectivity (Andrew & Pfurtscheller, 1996; Zhang et al., 2016). Additionally, previous research has demonstrated that low frequency wavelet analyses are well-suited for measuring the properties of signals that typify resting-state activity in the cortex using fMRI (Maxim et al., 2005). These coherence matrices were concatenated across windows to create a single 400 × 400 × 16 array for each participant.

Community Identification

To quantify the temporal reconfiguration of communities of parcels, I utilized a greedy Louvain multi-layer modularity algorithm to assign all parcels in all layers to communities, where each participant's windowed 400 × 400 coherence matrix was used

as a single layer in a multi-layer network (Jutla et al., 2011; Mucha et al., 2010; Betzel et al., 2019). Multi-layer modularity is described by the maximization of the modularity quality function:

$$Q(\gamma, \omega) = \frac{1}{2\mu}\sum_{ijlr}\{(A_{ijl} - \gamma_l P_{ijl})\delta_{lr} + \delta_{ij}\omega_{jlr}\}\delta(g_{il}, g_{jr})$$

where A_{ijl} describes the coherence between nodes *i* and *j* in layer *l*. The quantity $\delta(g_{il}, g_{jr})$, known as the Kronecker delta, describes the community assignment of nodes across layers.

This algorithm defines communities as clusters of nodes characterized by stronger connections than would be expected by chance, and describes these communities by the density of these connections (Girvan & Newman, 2002; Newman, 2012). The function is modulated by two tuning parameters: the structural resolution of the communities, γ, and the temporal resolution of the communities, ω. Maximizing the function for small values of γ results in the identification of a few large communities, and maximizing the function for large values of γ results in the identification of many small communities. Similarly, maximizing the function for small values of ω results in greater variability in community structure over time, and large values of ω permit greater community homogeneity over time.

The use of the multi-layer modularity algorithm also relies on the specification of a suitable null model, P_{ijl}, with which to compare the configuration of observed connections. In the present analyses, I utilized the multi-layer modification of the common Newman-Girvan model (Porter et al. 2009). This model was chosen on account of its ability to test the hypothesis that the observed network's communities are a function

of the particular degree sequence, and for its utility when testing networks in which connections can occur between any pair of nodes (Betzel, Medaglia et al., 2017). (Code for identifying communities using multi-layer modularity maximization is available at https://www.brainnetworkslab.com/coderesources.)

I specified $\gamma = 1$ and $\omega = 1$ in the present analyses, in line with previous research (Bassett et al., 2013; Betzel, Satterthwaite et al., 2017). While there are more and less common approaches to setting these tuning parameters, there is no singular canonical method, and different parameter settings may be appropriate for different datasets, and potentially for capturing differing dynamics within a single experiment. Additionally, because I did not know how many communities would be identified using $\gamma = 1$, and to investigate associations of Openness/Intellect and intelligence with functional communities of different sizes, I also specified partitions using $\gamma = 1.1$ and 1.2. These partitions produced functionally recognizable communities, and exhibited sufficient variability across windows upon visual inspection. An example of each of these three community partitions mapped to the atlas by Schaefer et al. (2018) in one subject is illustrated in Figure 4. These patterns were similar across subjects.

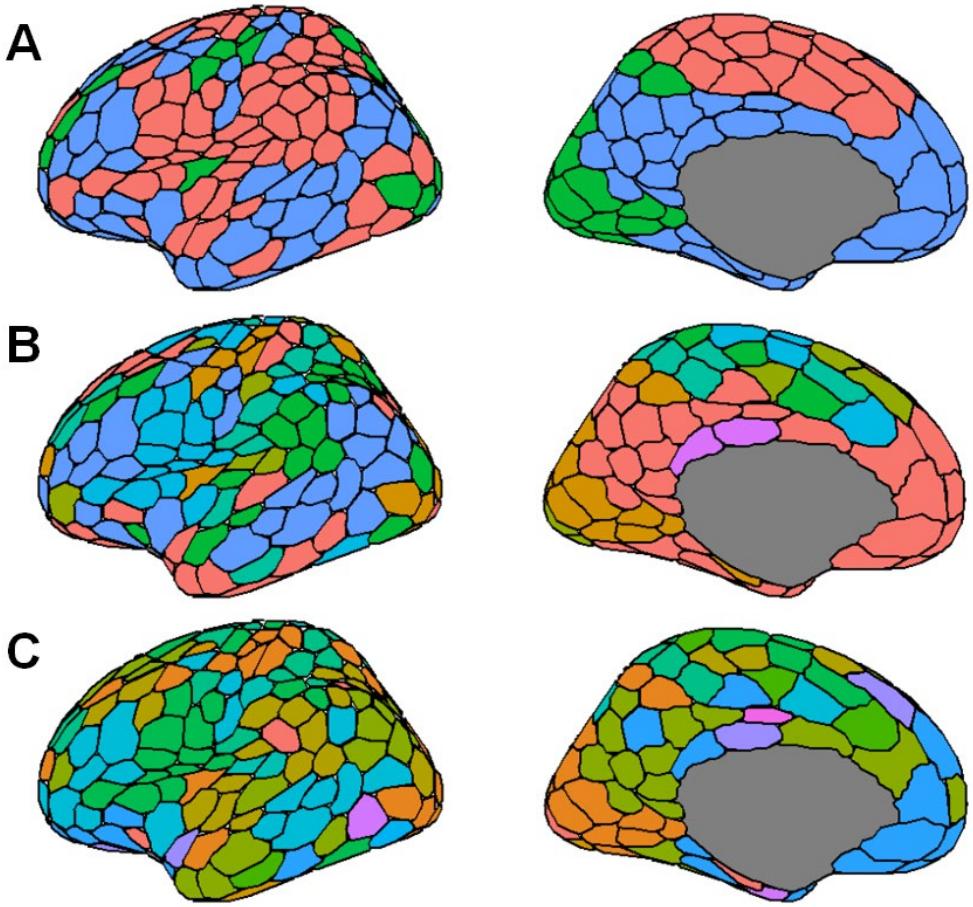

Figure 4. Three community structural partitions in subject 100206 at the first time window. Colors correspond to unique functional communities identified through multi-layer modularity maximization at γ = 1 (**A**), 1.1 (**B**), and 1.2 (**C**). Colors signify unique communities only within each partition, and do not represent equivalent communities across panels.

Network Flexibility

For each participant, I computed measures of overall node flexibility, cohesive flexibility, and disjoint flexibility using the Network Community Toolbox in MATLAB (http://commdetect.weebly.com). Overall flexibility is defined as the proportion of the

number of times a node changes communities to the number of times a node could change communities. Cohesive flexibility is defined as the proportion of the number of times a node moves *with other nodes* from one community to another, relative to the number of times it could change communities. Disjoint flexibility is defined as the proportion of the number of times a node changes communities *by itself* to the number of possible times it could change communities (Bassett et al., 2011; Telesfold et al., 2017). Since this multi-layer modularity optimization algorithm relies on randomized components, I repeated the community identification procedure 10 times for each participant and averaged the values for each type of flexibility measure across all iterations to produce a final value for each parcel.

Analysis

Predicting Openness/Intellect from Parcel Flexibility

I used elastic net regression to identify potential associations of Openness/Intellect with flexibility metrics of potentially influential parcels. To assess the predictive ability of the flexibility of these parcels, the original sample was divided into equally sized training and test samples (*N*'s = 497). Where multiple individuals from a single family were included in the sample, all individuals within a family were assigned to the same subsample, ensuring complete independence of the training and test samples.

Flexibility measures for each of the 400 individualized parcels were included as predictors in the model. Age, gender, mean relative RMS movement, Conscientiousness, Agreeableness, Neuroticism, Extraversion, and *g* were included as covariates. I also regressed out the effects of handedness, total brain volume (*FS_BrainSeg_Vol*), and the type of image reconstruction algorithm used in the HCP minimal preprocessing pipeline,

which changed during HCP data collection (*fMRI_3T_ReconVrs*). These covariates have previously been demonstrated to affect global functional connectivity patterns in resting-state fMRI (Pool et al., 2015**;** Li et al., 2015; Van Dijk et al., 2012; Elam, 2015). All covariates were regressed out of flexibility measures and Openness/Intellect using multiple linear regression.

Elastic net models were fit using the *glmnet* package in R (Friedman et al. 2010). Flexibility measures were log-transformed and standardized before entering the model. The mixing (α) and penalty parameters (λ) were optimized in the training sample with 10-fold cross validation for each model through a grid search using the *caret* package in R (Kuhn, 2021). The model with parameters producing the highest R^2 value across folds was selected for further analyses. Coefficients derived in the training sample were then applied to the predictors in the test sample. This procedure was then repeated using measures of cohesive and disjoint flexibility, across each community structural partition. Measures of root-mean squared error (RMSE), mean absolute error (MAE), and R^2 were calculated for both samples to assess model fit. In line with previous research, the R^2 values in the test sample were computed as the squared correlation between the observed scores and fitted values. Nonparametric permutation testing was used to determine the significance of model performance in the test set. A null distribution of R^2 values was created by shuffling the flexibility measures in the test set to break any dependence between the personality scores and flexibility measures. This was accomplished using Freedman-Lane permutation to properly account for the role of covariates (Freedman & Lane, 1983), and with exchangeability blocks to account for family structure within the

test set (Winkler et al., 2014). This null distribution was then used to determine whether the variance explained in the test set was significantly greater than expected by chance.

Predicting Intelligence from Parcel Flexibility

The same procedure was used to predict *g*. These models used age, gender, mean relative RMS movement, handedness, total brain volume, and the type of image reconstruction algorithm as covariates. Separate models were fit for each of the three types of flexibility across all community partitions.

Analytic Procedure and Influence of Covariates

To address the influence of particular analytic choices on the predictive ability of these models, models predicting Openness/Intellect were fit without the remaining Big Five, and again without the effect of intelligence to determine how much the choice of covariates had on the hypothesized results. Similarly, models predicting intelligence were also fit including the Big Five as covariates. To further test the specificity of the prediction, I also repeated these analyses using each of the Big Five as criterion variables, using the same sets of covariates described previously.

Predicting Psychoticism from Parcel Flexibility

To explore the possibility of associations of flexibility with a pathological facet of this domain, additional exploratory analyses were conducted predicting Psychoticism from flexibility. These models used age, gender, mean relative RMS movement, handedness, total brain volume, the type of image reconstruction algorithm, and *g* as covariates. These models also included Neuroticism, Extraversion, Conscientiousness, and Agreeableness as covariates to remove variance associated with general negative evaluation, but not variance specific to the larger domain associated with Psychoticism.

Separate models were fit for each of the three types of flexibility across all community partitions. Additional models were fit without intelligence, without the Big Five, and with Openness/Intellect to assess the influence of covariates.

Results

Descriptive statistics for personality and intelligence measures are reported in Table 3.

Table 3.

Descriptive statistics for personality and intelligence measures

	***M*(*SD*)**	**Range**	**Skew**
NEO-FFI Openness/Intellect	2.37(.52)	3.08	.22
NEO-FFI Extraversion	2.56(.50)	3.08	-.26
NEO-FFI Agreeableness	2.80(.48)	3.17	-.32
NEO-FFI Conscientiousness	2.87(.49)	3.08	-.36
NEO-FFI Neuroticism	1.37(.61)	3.58	.42
ASR Psychoticism	.11(.23)	1.5	2.52
NIH Picture Vocabulary	117.06(9.56)	62.40	.17
NIH Picture Sequence Memory	111.99(13.23)	59.13	.11
NIH List Sorting Task	111.41(11.39)	63.71	.20
NIH Oral Reading Recognition	117.13(10.57)	66.51	-.13
NIH Dimensional Change Card Sort	115.38(10.35)	62.67	.22
NIH Flanker Inhibitory Control and Attention	111.99(10.08)	56.37	.18
NIH Pattern Comparison Processing Speed	115.24(15.34)	103.07	.20
Variable Short Penn Line Orientation Test	14.99(4.40)	25.00	-.29
Penn Progressive Matrices	17.01(4.70)	20.00	-.61
Penn Word Memory Test	35.61(2.95)	18.00	-.88

Note. NEO-FFI = NEO Five Factor Inventory, ASR = Achenbach Self-Report, NIH = National Institutes of Health

Individual Parcel Flexibility

Before investigating associations of Openness/Intellect and intelligence with flexibility measures, I first evaluated the distribution of parcel flexibility measures across the cortex. Parcels' relative flexibility values remained largely consistent across partitions, with greater parcel flexibility observed in regions of the bilateral insula, medial frontal and parietal cortex, and reduced parcel flexibility in the lateral somatomotor and primary visual cortex, as well as regions of the inferior parietal lobule. Mean flexibility values were more variable across the cortex in the larger community partition, and more uniform in the partition with smaller communities. This pattern of parcel flexibility is similar to previous findings describing inter-subject functional connectivity variability patterns (Kong et al., 2019)**,** and is largely consistent with previous descriptions of regions of cortex constituting a "flexible club" (Betzel, Satterthwaite et al., 2017; Yin et al., 2020). Mean values of overall flexibility for each parcel across the three community partitions are illustrated in Figure 5.

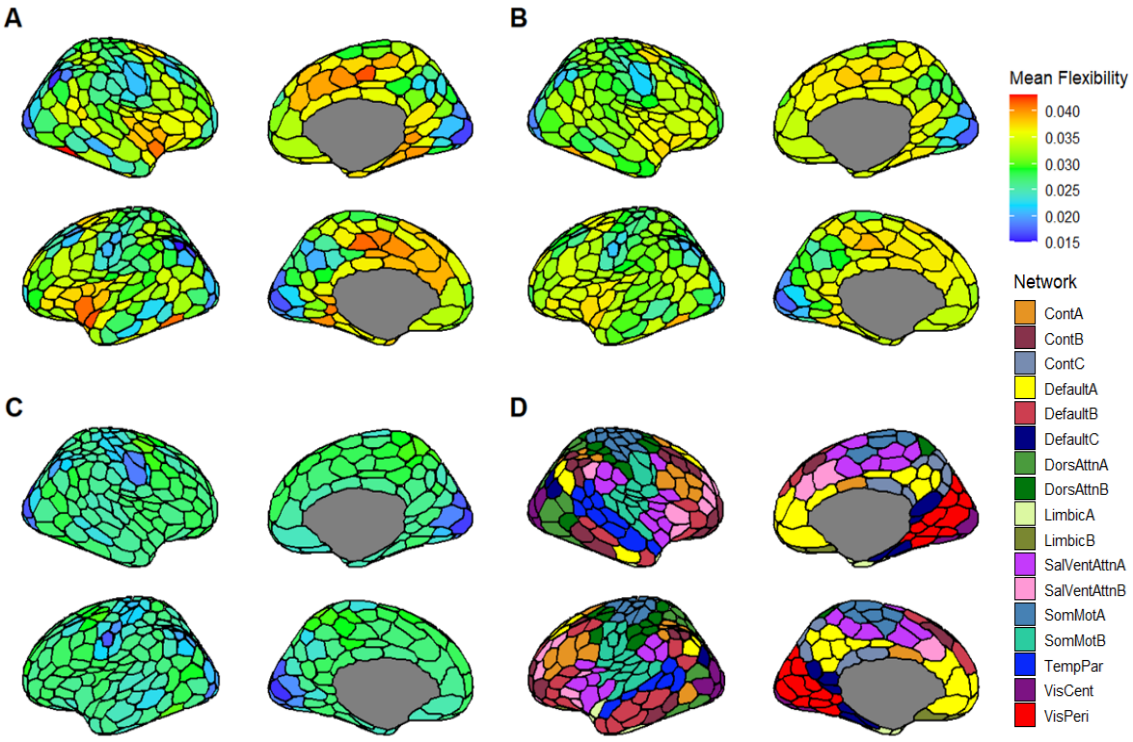

Figure 5. Mean overall flexibility across all participants derived from the communities optimized at $\gamma = 1$ (**A**), 1.1 (**B**), and 1.2 (**C**). Because each community partition reflects a different number of communities used to compute the flexibility of each parcel, mean flexibility values are not directly comparable across panels. Network assignments of parcels to 17 functional networks in the Schaefer et al. (2018) atlas are shown in panel **D**. Cont = frontoparietal control, DorsAttn = dorsal attention, SalVentAttn = salience/ventral attention, SomMot = somatomotor, TempPar = temporoparietal, VisCent = central visual, VisPeri = peripheral visual

Distributions of whole brain flexibility values for each community partition and flexibility type are illustrated in Figure 6. Cohesive and disjoint flexibility values differed across partitions as a result of the number and size of communities. At $\gamma = 1$, having only

a few large communities resulted in a small absolute number of changes, most of which were cohesive, thus yielding disjoint flexibility values near zero. Conversely, at $\gamma = 1.2$, multiple small communities increased the likelihood of parcels changing affiliation independently, resulting in greater disjoint flexibility. Considering the relatively few number of functional communities and low disjoint flexibility values at the $\gamma = 1$ partition, I limited my hypothesis testing to the $\gamma = 1.1$ and 1.2 partitions to explore the unique predictive ability of cohesive and disjoint flexibility. (For completeness, I report analyses using $\gamma = 1$ in the appendix.)

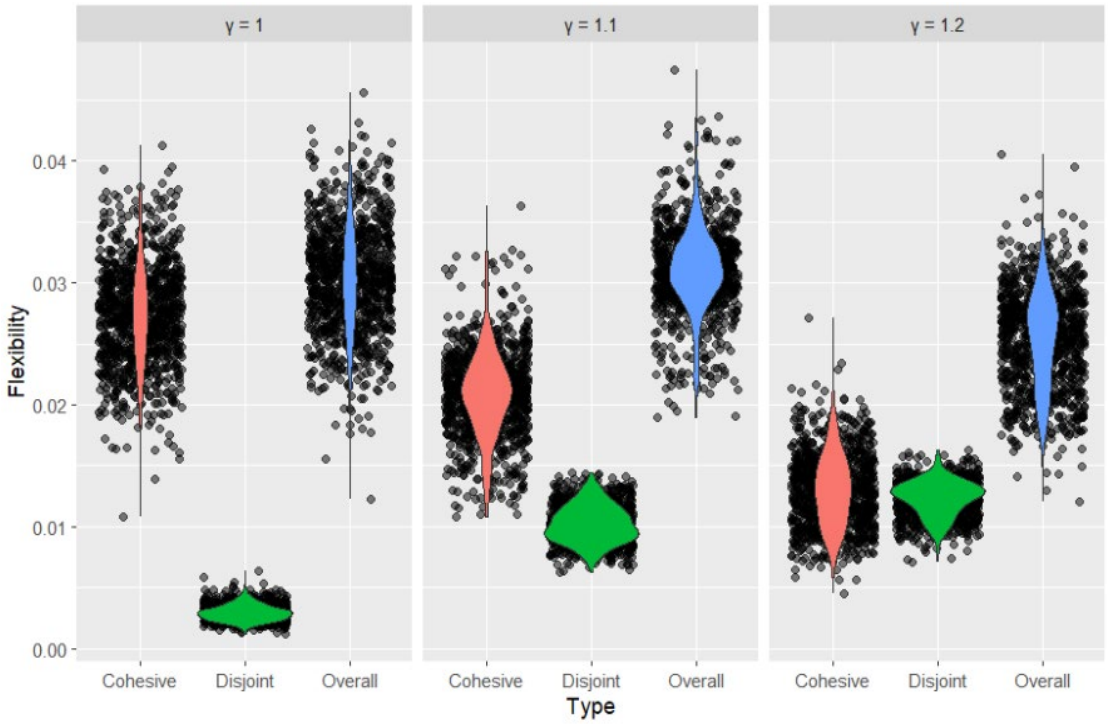

Figure 6. Distributions of whole brain flexibility values by flexibility type and community partition.

Model Performance

Model parameters and performance metrics in the training and test sets for models using all parcels are reported in Table 4. Coefficients for all significant models are reported in the appendix.

Table 4.

Performance metrics of models using flexibility of all parcels as predictors

	Community	Type	Training Sample					Test Sample		
			α	λ	RMSE	MAE	R^2	RMSE	MAE	R^2
O/I	γ = 1.1	Overall	0.8	.06517	.99	.78	.047	1.04	.83	.000
		Cohesive	0.2	.00006	2.58	2.10	.040	2.57	2.04	.001
		Disjoint	0.6	.13338	1.00	.78	.041	1.01	.81	.001
	γ = 1.2	Overall	0.7	.04620	1.00	.80	.060	1.04	.84	.010*
		Cohesive	0.4	.00078	2.58	2.05	.055	2.35	1.87	.002
		Disjoint	0.8	.02471	1.12	.89	.026	1.17	.93	.000
g	γ = 1.1	Overall	1	.10163	1.01	.79	.046	1.00	.81	.000
		Cohesive	0.1	.00006	3.00	2.40	.011	2.52	1.95	.016**
		Disjoint	0.9	.10501	1.01	.80	.059	.99	.81	.002
	γ = 1.2	Overall	0.4	.12726	1.01	.79	.032	1.01	.82	.004
		Cohesive	0.1	.00014	3.21	2.52	.037	2.29	1.81	.002
		Disjoint	1	.00036	2.37	1.91	.044	2.19	1.74	.000
P	γ = 1.1	Overall	0.7	.12255	.99	.69	.035	1.00	.69	.003
		Cohesive	1	.11925	.99	.70	.037	1.00	.69	.004
		Disjoint	0.9	.06539	.99	.69	.055	1.00	.71	.008
	γ = 1.2	Overall	0.5	.10638	1.06	.71	.047	1.01	.70	.000
		Cohesive	0.5	.12569	1.00	.70	.065	1.00	.70	.008
		Disjoint	1	.00366	1.74	1.38	.037	1.65	1.28	.009*

Note. *permutation $p < .05$, **permutation $p < .01$. *g* = general intelligence. O/I = Openness/Intellect. P = Psychoticism. α = mixing parameter, λ = penalty parameter, RMSE = root-mean-square error. MAE = mean absolute error

Openness/Intellect

Openness/Intellect was not significantly associated with any flexibility measures in the $\gamma = 1.1$ community partition. In the communities identified at $\gamma = 1.2$, overall flexibility significantly predicted 1% of the variance in Openness/Intellect in the independent test set (permutation $p = .03$). Prediction of Openness/Intellect increased only slightly when removing intelligence as a covariate ($R^2 = .015$, permutation $p < .01$), and remained unchanged when removing the rest of the Big Five ($R^2 = .01$, permutation $p = .03$). The model included 136 parcels as predictors, distributed across all 17 networks, with the greatest frequency of parcels in the somatomotor, dorsal attention B, and default B networks. Openness/Intellect was most strongly associated with increased flexibility in the bilateral extrastriate cortex, postcentral gyrus, and dorsal prefrontal cortex, and with reduced flexibility in regions of the somatomotor cortex, ventrolateral prefrontal cortex, and frontal operculum. However, results from a Kruskal-Wallis rank sum test indicated no significant differences in median parcel coefficient magnitude across networks ($H(16) = 9.8747$, $p = .87$). Model coefficients are illustrated in Figure 7.

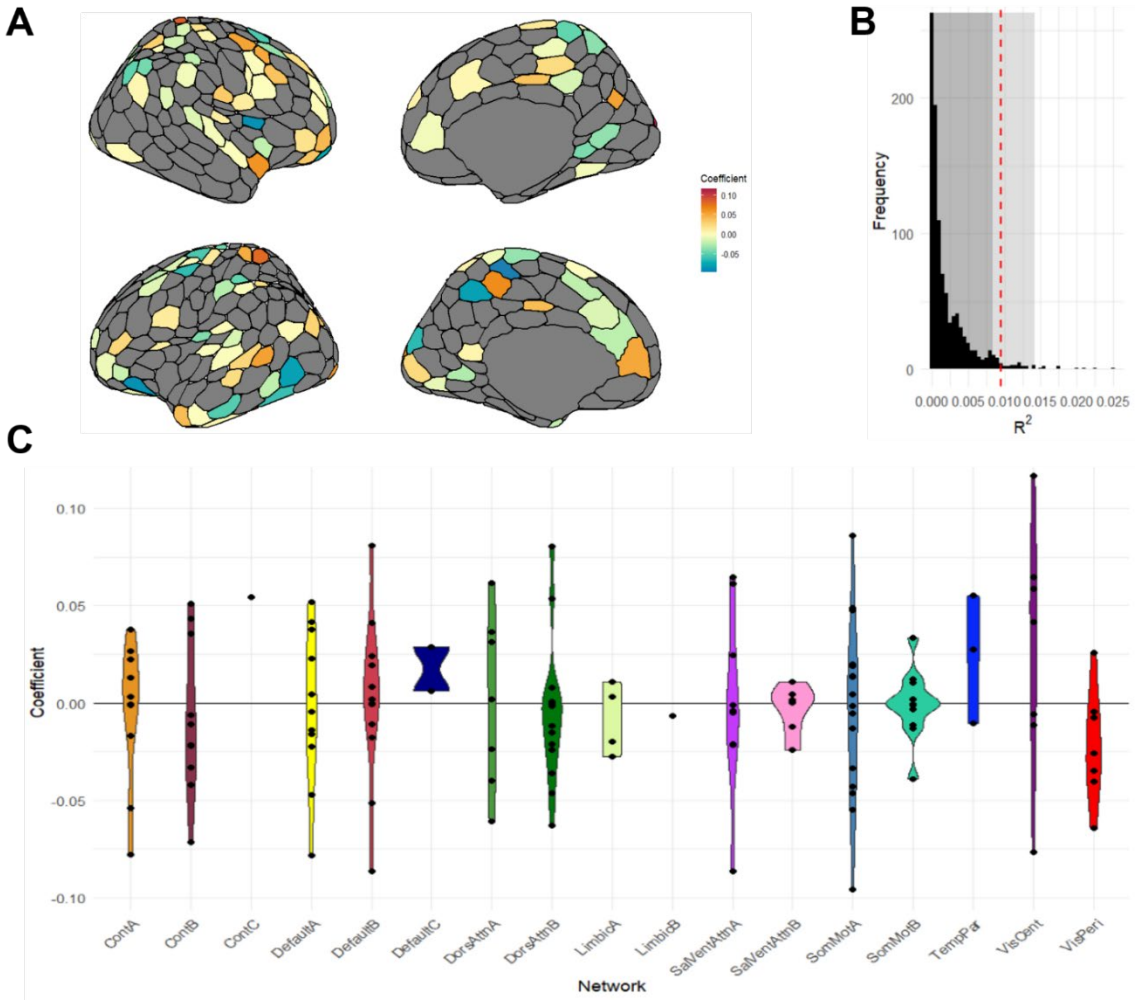

Figure 7. Model predicting Openness/Intellect from overall parcel flexibility. **A**: Model coefficients selected in the community partition optimized at γ = 1.2. Parcels not retained in the model are shown in gray. **B:** Null distribution of permuted R^2 values. The red dashed line indicates the observed R^2 value. The dark shaded region signifies values at $p \geq .05$. The light shaded region signifies values at $p \geq .01$. **C:** Violin plots of model coefficients sorted by 17 functional networks from the Schaefer et al. (2018) atlas

Intelligence

Intelligence was not significantly associated with any flexibility measures in the γ = 1.2 community partition. In the communities identified at γ = 1.1, cohesive flexibility significantly predicted 1.6% of the variance in intelligence in the independent test set (permutation $p < .01$). Cohesive flexibility also significantly predicted intelligence when including the Big Five as covariates ($R^2 = .009$, permutation $p = .03$). As with Openness/Intellect, this model included parcels from all networks, but in contrast included all 400 parcels as predictors. Intelligence was most strongly associated with increased cohesive flexibility of parcels in the bilateral extrastriate and somatomotor cortex, superior parietal lobule, frontal pole, and dorsolateral prefrontal cortex (dlPFC), as well as decreased flexibility in regions of the primary visual cortex, postcentral gyrus, and precuneus, but results from a Kruskal-Wallis rank sum test again indicated no significant differences in median parcel coefficient magnitude across networks ($H(16) = 7.3246$, $p = .97$). Parcels included in this model are illustrated in Figure 8.

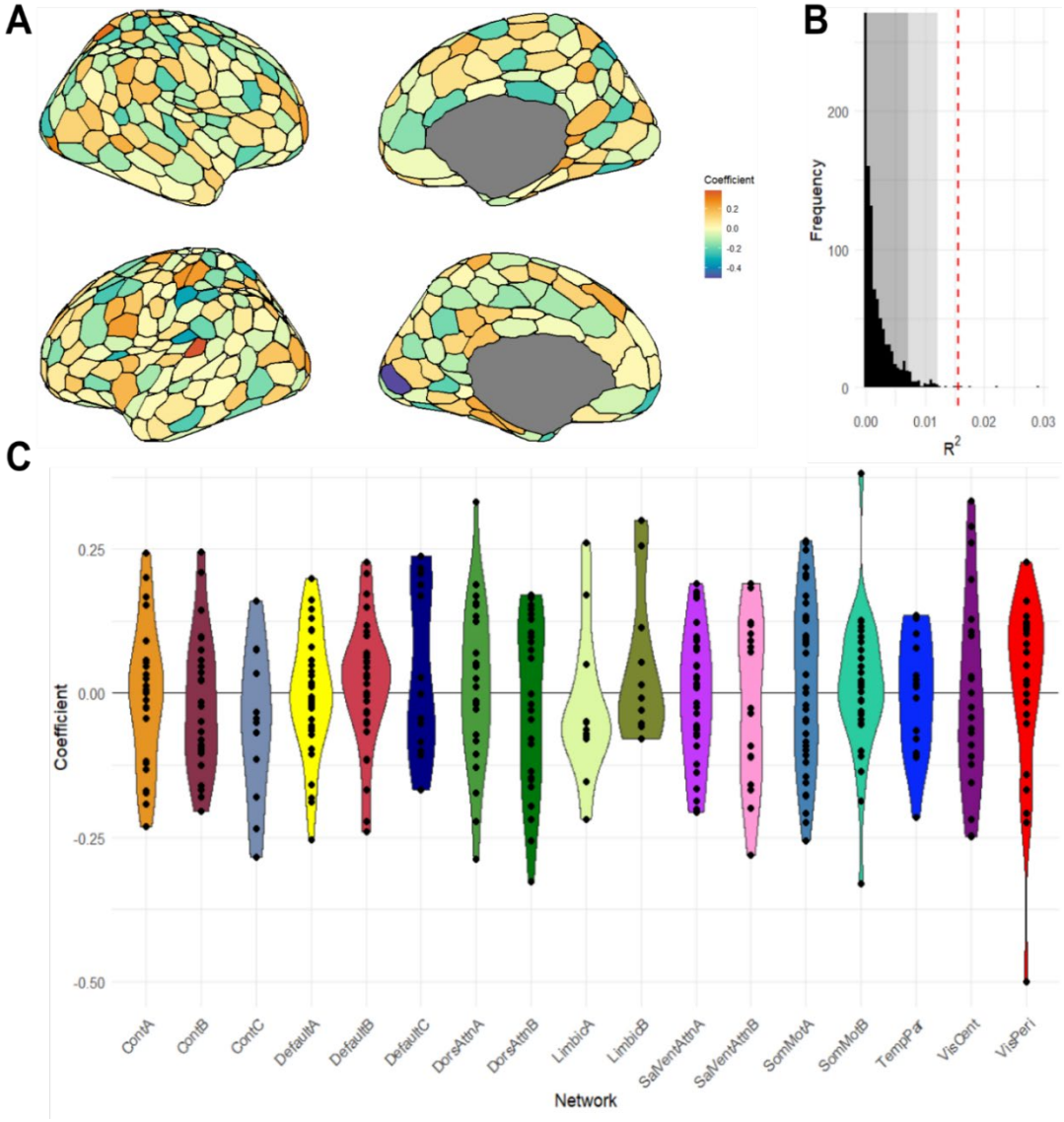

Figure 8. Model predicting intelligence from parcel cohesive flexibility. **A**: Model coefficients selected in the community partition optimized at γ = 1.1. **B:** Null distribution of permuted R^2 values. The red dashed line indicates the observed R^2 value. The dark shaded region signifies values at $p \geq .05$. The light shaded region signifies values at $p \geq .01$. **C:** Violin plots of model coefficients sorted by 17 functional networks from the Schaefer et al. (2018) atlas.

Psychoticism

In the communities identified at $\gamma = 1.2$, disjoint flexibility predicted 0.9% of the variance in Psychoticism (permutation $p = .03$). Similar to previous models, this model included parcels from all networks. Psychoticism was most strongly associated with increased disjoint flexibility of parcels in the bilateral insula and dlPFC, temporoparietal junction, and medial frontal gyrus, as well as decreased flexibility in regions of the primary visual cortex, middle temporal gyrus, and anterior temporal lobe, but results from a Kruskal-Wallis rank sum test indicated no significant differences in median parcel coefficient magnitude across networks ($H(16) = 22.03$, $p = .14$). Parcels included in this model are illustrated in Figure 9.

Discriminant Validity

Additional tests of discriminant validity revealed that all flexibility types were not significantly associated with any of the remaining Big Five across all community partitions. Performance metrics of models predicting the remaining Big Five are included in Table 5.

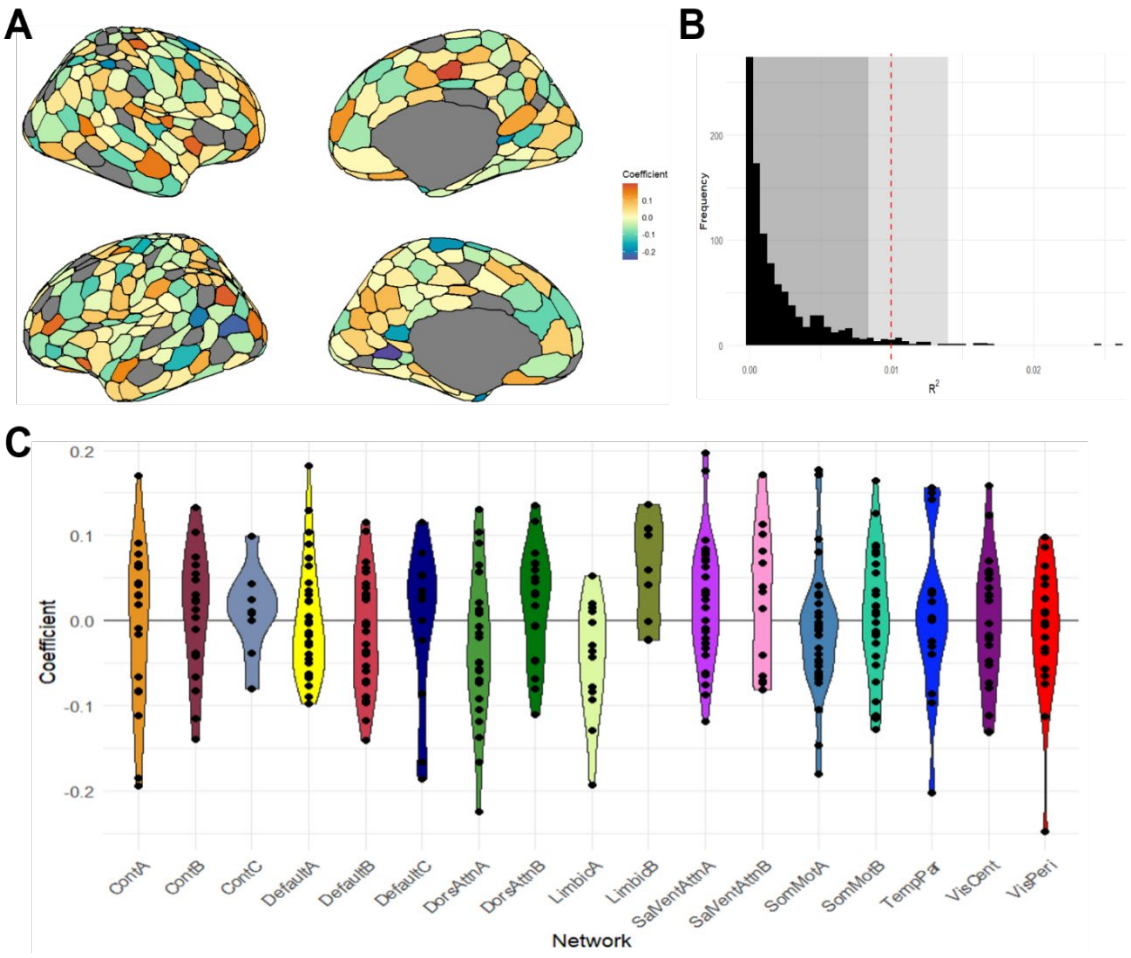

Figure 9. Model predicting Psychoticism from parcel disjoint flexibility. **A**: Model coefficients selected in the community partition optimized at γ = 1.2. **B:** Null distribution of permuted R^2 values. The red dashed line indicates the observed R^2 value. The dark shaded region signifies values at $p \geq .05$. The light shaded region signifies values at $p \geq .01$. **C:** Violin plots of model coefficients sorted by 17 functional networks from the Schaefer et al. (2018) atlas.

Table 5.

Performance metrics of models predicting the remaining Big Five from parcel flexibility

	Community	Type	Training Sample					Test Sample		
			α	λ	RMSE	MAE	R^2	RMSE	MAE	R^2
E	γ = 1.1	Overall	1	.00434	1.62	1.30	.033	1.52	1.22	.001
		Cohesive	1	.02429	1.16	.92	.040	1.10	.88	.000
		Disjoint	1	.13489	.99	.79	.026	1.00	.80	.001
	γ = 1.2	Overall	0.2	.10774	1.07	.85	.027	1.11	.90	.000
		Cohesive	0.4	.10233	1.07	.85	.039	1.03	.83	.000
		Disjoint	0.9	.15810	.99	.78	.051	1.00	.81	.002
A	γ = 1.1	Overall	0.5	.12486	.99	.77	.044	1.01	.80	.002
		Cohesive	1	.11197	1.00	.79	.034	1.00	.79	.001
		Disjoint	0.7	.12403	1.01	.78	.032	1.00	.79	.000
	γ = 1.2	Overall	0.3	.01037	1.46	1.15	.033	1.54	1.21	.000
		Cohesive	0.7	.00196	1.84	1.48	.021	1.88	1.49	.002
		Disjoint	0.2	.12022	1.08	.86	.028	1.13	.88	.002
N	γ = 1.1	Overall	0.9	.14585	.99	.77	.042	1.00	.79	.005
		Cohesive	0.2	.00935	1.51	1.23	.047	1.75	1.34	.001
		Disjoint	1	.11662	1.00	.78	.016	1.00	.79	.003
	γ = 1.2	Overall	0.9	.15162	.99	.77	.037	1.00	.79	.000
		Cohesive	0.2	.13718	1.07	.83	.022	1.05	.84	.001
		Disjoint	0.1	.00006	2.29	2.32	.025	2.38	1.92	.001
C	γ = 1.1	Overall	0.6	.07223	1.01	.79	.040	1.04	.82	.002
		Cohesive	1	.18706	1.00	.77	.059	1.00	.79	.001
		Disjoint	0.9	.14284	1.00	.77	.027	1.00	.79	.002
	γ = 1.2	Overall	0.4	.12244	1.02	.80	.025	1.03	.80	.001
		Cohesive	0.3	.05777	1.08	.86	.045	1.14	.91	.000
		Disjoint	0.4	.01007	1.31	1.06	.069	1.53	1.21	.000

Note. E = Extraversion, A = Agreeableness, N = Neuroticism, C = Conscientiousness. α = mixing parameter, λ = penalty parameter, RMSE = root-mean-square error. MAE = mean absolute error

Discussion

Openness/Intellect and Psychoticism, measured by questionnaire, and intelligence, measured by cognitive performance tests, were significantly associated with

brain network flexibility. The prediction accuracy metrics reported in this study are small, but they accord with previous research using machine learning approaches with common functional connectivity measures to predict traits like Plasticity and Openness/Intellect (Dubois et al., 2018b), psychotic-like experiences (Ma et al., 2022), and executive function (Heckner et al., 2023). These results suggest that measures of flexibility in a dynamic functional connectivity framework may provide a similar degree of information about personality as static resting-state functional connectivity, using cross-validation procedures, despite recent evidence suggesting that dynamic and static functional connectivity describe different properties of neural activity (Zhang et al., 2023; Zhu et al., 2021).

Although the amount of variance explained by functional community flexibility is small, this result is nonetheless an important step in a larger effort to understand the neural correlates of broad personality domains as dynamical systems. Previous research has described associations of a variety of influential behavioral phenotypes like need for cognition, working memory, and creativity with flexibility (Braun et al., 2015; He et al., 2019), and these different traits and abilities are all situated within the larger Openness/Intellect domain (DeYoung et al., 2012; Saucier, 1992). This research helps expand on these findings by demonstrating that brain network flexibility similarly predicts the broader Openness/Intellect domain beyond specific facets describing features of higher-order cognition.

Features of these results cohere with results of prior research predicting Openness/Intellect, intelligence, and Psychoticism from functional connectivity. For example, much research using static functional connectivity suggests that effect sizes for

intelligence are larger than those for Openness/Intellect and other questionnaire variables (Kong et al., 2019; Li et al., 2019; Kong et al., 2021; Chen et al., 2022). One simple explanation for this pattern may be the fact that intelligence was assessed using a variety of different task measures, while Openness/Intellect and Psychoticism were measured through single, short self-report questionnaires. However, better measurement may not be the only reason for better prediction; there may be a more substantive reason as well, reflected in the fact that Openness/Intellect also seems to be more readily predicted from functional connectivity in the cortex than the other Big Five traits (Dubois et al., 2018b; Kong et al., 2021). Considering the conceptual similarity of Openness/Intellect and its facets in describing variation in complex cognition, one might expect complex cognition to be reflected more widely across the cortex compared to the more specific affective and motivational functions underlying other traits.

I observed that the cohesive flexibility of all 400 parcels contributed to the best prediction of intelligence in the larger ($\gamma = 1.1$) community partition. This observation is consistent with the hypothesis by Safron et al. (2022) that cohesive flexibility indexes adaptive functioning. The fact that cohesive flexibility specifically predicts intelligence aligns with previous research suggesting that intelligence reflects a form of global network integrity (Langer et al., 2012; Barbey, 2018; Wang et al., 2021), with intelligence predicting a variety of positive life outcomes (Gottfredson, 1997; Brown et al., 2021). Although no significant differences were observed across networks, many of the parcels with the strongest effect sizes were located in cortical hubs nominated by the Parieto-Frontal Integration Theory (P-FIT; Jung & Haier, 2007; Gur et al., 2021), including the dlPFC and superior parietal lobule.

These findings reveal that intelligence is associated with the tendency for networks to reorganize themselves frequently, throughout the cortex. Previous research has demonstrated the utility of using static functional connectivity profiles across the entire cortex to predict intelligence (Feilong et al., 2021), and these results indicate that a similar pattern exists using dynamic functional connectivity. The association of intelligence with cohesive flexibility across the cortex provides further evidence to support the notion that intelligence can be understood through integrative functional dynamics across the whole brain, but may be orchestrated by certain regions most implicated in higher-order cognition (Alavash et al., 2015; Avery et al., 2020; Cole et al., 2012; Hilger et al., 2017).

In contrast to intelligence, Psychoticism was best predicted by disjoint flexibility throughout a smaller set of parcels across the cortex. Previous research on the neural correlates of Psychoticism and schizophrenia has revealed associations with connectivity across many different cortical networks, particularly the default network and FPCN (Blain et al., Baker et al., 2014; Xia et al., 2018). Notably, many of the strongest effects with Psychoticism in the present study occurred in cortical regions that are key hubs of these networks, including the dlPFC, insula, and temporoparietal junction. Safron et al. (2022) hypothesized that disjoint flexibility may be a marker of a general tendency toward neural entropy, and additional research has shown that this may be the case especially in regions involved in higher-order cognition (Telesford et al., 2017). These findings suggest that the kind of disorganized cognition expressed in Psychoticism might be a reflection of a general tendency toward fragmentation of functional communities in the brain.

Despite its empirical and conceptual relations to intelligence and Psychoticism, Openness/Intellect exhibited different patterns of associations with flexibility, and these remained significant even when controlling for intelligence. Rather than cohesive or disjoint flexibility, Openness/Intellect was best predicted by the overall flexibility of an even more limited set of parcels, in the smaller community partition ($\gamma = 1.2$), with the strongest effects observed in both somatosensory regions and areas implicated in abstract and self-referential thought like the dorsal prefrontal cortex and precuneus. Of note, Openness/Intellect was reliably predicted by overall flexibility specifically, rather than cohesive of disjoint flexibility individually. Overall flexibility reflects both cohesive and disjoint flexibility. Given that Openness/Intellect domain subsumes a variety of facets capturing elements of both adaptive and disorganized cognition (DeYoung et al., 2012), both cohesive and disjoint brain dynamics could be contributing unique variance to the prediction of this broad personality domain, especially when controlling for the effect of intelligence.

Previous research has implicated dopaminergic function in Openness/Intellect (DeYoung, 2013; Passamonti et al., 2015), and D2 receptor binding specifically has been linked to cognitive flexibility (Durstewitz & Seamans, 2008; Wacker et al., 2012). To connect these results with the hypothesized link between Openness/Intellect and dopamine, I conducted additional exploratory analyses using D2 receptor density positron emission tomography (PET) maps from Smith et al. (2019) and Sandiego et al. (2015), which were averaged and parcellated using the Schaefer atlas by Hansen et al. (2022). These receptor maps are available at https://github.com/netneurolab/hansen_receptors. I found that D2 receptor density was significantly positively associated with overall

flexibility across all parcels in the γ = 1.2 partition (r = .11, p < .05), the same partition associated with Openness/Intellect, but not with flexibility in the γ = 1.1 (r = .06, p = .20) or γ = 1 partitions (r = .02, p = .68).

This association might suggest a potential neurobiological mechanism underlying the kind of community reconfiguration that contributes to cognitive flexibility. D2 dopamine neurons projecting to prefrontal cortical regions from midbrain structures are described as salience coding neurons, and support cognitive processes relating to exploration of information (Bromberg-Martin et al., 2010). This engagement with complex information can involve multiple different cognitive operations, including the redirection of attentional resources, the manipulation of information in working memory, self-referential thought, and the management of different or conflicting goal states. Further, tasks involving complex cognition have been shown to recruit multiple cortical networks with hubs in prefrontal regions, often at different times during the task (Beaty et al., 2016; Patil et al., 2021). It may be that cortical regions with greater D2 receptor density participate in more frequent but relatively localized community changes as a means of flexibly managing the cognitive demand of identifying and exploring abstract or sensory information.

Flexibility and Individualized Parcellation

One particular strength of my method is the use of individualized parcellation. Previous research has described a variety of properties differing between group-level atlases and their individualized counterparts, with the latter yielding increased effect sizes in brain-behavior associations (Kong et al., 2021; Sassenberg et al., 2023) and more conservative patterns of functional connectivity in case-control designs (Levi et al.,

2023). To the best of my knowledge, no other research investigating brain-behavior associations with flexibility has made use of individualized parcellation. Other research using similar procedures to identify functional communities, but without individualized parcellation, has reported similar but slightly larger flexibility values (Yin et al., 2020). It may be that more accurate localization of parcel boundaries, using individualized parcellation, produces a more conservative but more accurate estimation of community dynamics over time. Parcel boundaries in group-level atlases do not respect the individual variation in functional topography on the cortical surface, and so canonical parcels without individualization may instead capture distinct functional regions within the same boundary, leading to estimates of greater flexibility than what actually occurs. For instance, a poorly estimated parcel boundary could erroneously group two functional regions belonging to networks with negatively correlated activation patterns like the FPCN and default network. That parcel might then exhibit greater flexibility as it appears to change affiliation with other communities containing FPCN or default network parcels, simply depending on the relative activation patterns of each network in a given window.

Limitations

The present study incorporated a number of cutting-edge analytic strategies beyond individualized parcellation, including calculation of functional connectivity through magnitude squared coherence and the use of the 400-parcel Schaefer atlas. Evidence suggests that magnitude squared coherence performs at least as well as product-moment correlations as a measure of functional connectivity (Betzel, Satterthwaite et al., 2017) and that the Schaefer atlas exhibits greater within-parcel homogeneity compared to its competitors (Schaefer et al., 2018). However, there are also important limitations to

consider. One limitation is that these analyses included flexibility metrics only for cortical parcels. Examination of subcortical structures involved in dopamine modulation might provide additional insight in relating Openness/Intellect and intelligence to brain network flexibility.

Additionally, the particular parameters of the multi-layer modularity algorithm in the present analyses were chosen to explore results across different spatial resolutions of the cortical communities, but I did not explore different temporal resolutions when calculating network flexibility. Fixing the ω parameter to 1 for all analyses was done to manage the computational intensity and number of analyses, but that means I do not know how results might be affected by employing different temporal windows in my analysis of flexibility.

Further, this study is limited by the use of a sliding-window approach to dynamic functional connectivity. Future research can explore whether these associations persist using more sophisticated measures of functional connectivity dynamics like dwell time. This measure of flexibility also may be limited by the features of the general Louvain community optimization algorithm, which categorizes parcels into discrete communities. Explorations into more nuanced measures of community partitioning like stochastic block modeling might also improve prediction accuracy (Lee & Wilkinson, 2019).

The relatively low prediction accuracies derived from the current findings also echo recent concerns of whether the explained variance is useful for identifying precise neural mechanisms underlying these traits, as well as whether these performance metrics would improve substantially through the use of task-based designs (Finn, 2021; DeYoung et al., 2022). Further research would benefit from examining model performance under

conditions where participants are engaged in tasks that elicit cognitive states corresponding to particular traits of interest, as it may be the case that dynamic reconfigurations of cortical topology are more pronounced (or importantly different in other ways) from dynamics observed at rest (Greene et al., 2018; Rzucidlo et al., 2013; Salehi et al., 2020).

Lastly, future research exploring associations of cortical flexibility with measures of personality would benefit from improved measurement of behavioral constructs. Although a measure of intelligence in the present research was constructed using a variety of different tasks, Openness/Intellect was limited to a single, relatively short questionnaire measure. Future research could use multiple self- and peer-report measures of personality and use latent variable analyses to model personality constructs.

Conclusion

This research presents the first empirical test of a hypothesis relating neural flexibility to broad personality traits describing cognitive and behavioral flexibility, inspired by the work of Safron et al. (2022). I describe reliable associations between intelligence and a pattern of cohesive flexibility across the entire cortex, Psychoticism and disjoint flexibility, as well as between Openness/Intellect and a more delimited pattern of general flexibility. These findings help to expand on previous research describing associations of neural flexibility with a variety of behavioral and cognitive traits relating to higher-order cognition within the broader framework of the personality hierarchy. This research also provides further support for previous research reporting associations between functional connectivity and these traits in the Human Connectome

Project, as well as helping to frame the neural correlates of these traits as dynamical systems.

Chapter IV: Individual Differences in Self-Organized Criticality: Associations of Psychoticism and Intelligence with Power-Law Dynamics in Resting-State fMRI

"Perhaps even the most complicated phenomena on Earth – humans with brains and personality – do reflect part of a world operating at the critical state."

-Per Bak, *How Nature Works*, 1996

Continued research in network neuroscience has contributed to a growing understanding of the way in which broad brain networks relate to a variety of individual differences. Methodological advances, including graph theoretical and other high-dimensional data reduction techniques, have permitted greater insights into how properties of brain organization relate to stable patterns of individual differences. Beyond prediction, an additional aim of this field is understanding how complex patterns of cognition and behavior might emerge from particular properties of brain function, and this line of thought has benefitted in recent years from theories explicating how complex system dynamics in the brain relate to universal features of human psychology (DeYoung, 2015; Friston et al., 2021; Safron & DeYoung, 2021; Seth, 2015).

An important property of dynamical systems that relates to their complexity is self-organized criticality. Systems in a critical state exhibit phase transitions, where multiple parts in the system collectively and abruptly reorganize. Self-organized criticality is a special case in which a system achieves a critical state without any external manipulation or tuning (Bak et al., 1987). Self-organized criticality has been shown to be related to a variety of other useful edge-of-chaos phenomena that characterize complex systems, including self-similarity, fractal dimensionality, and scale-invariant properties

(Eke et al., 2002). One popular approach for studying self-organized criticality is the use of power-law distributions. For a given system that changes in state over time, the magnitude and frequency of its behavior can be fit to a power-law function $O(f) \propto \frac{1}{f^{\alpha}}$, also referred to as 1/*f* noise. For systems exhibiting self-organized criticality, this function exhibits a polynomial decrease. In other words, the magnitude of the signal decreases exponentially in relation to the frequency according to some constant α.

Consequently, the constant α can be approximated as the linear slope when frequency and magnitude are plotted logarithmically. The value of the resulting slope coefficient can be used as an index of system complexity, where a slope near 0 indicates random noise, and a slope typically ranging between -1 and -3 indicates a system exhibiting criticality (Bak et al., 1997). Power-law distributions can be used to describe criticality in a variety of complex mathematical and natural phenomena across a wide range of scales, as well as patterns of human behavior like internet traffic and market fluctuations (Clegg et al., 2010; Lux & Alfarano, 2016).

Previous research has explored power-law distributions in the brain and found that both EEG and fMRI BOLD signals exhibit power-law distributions (Chiavlo, 2010; He et al., 2011; Hesse & Gross, 2014; Tagliazucchi et al., 2012; Fransson et al., 2013). Some of this research has explored associations of criticality with dysfunctional brain activity like epileptic seizures (Meisel et al., 2012), but comparatively little empirical research has explored how power-law distributions in the brain might relate to normative or pathological variation in dimensions of personality. Recent theoretical work has explicated how power-law distributions may relate to other, more thoroughly studied

properties in neuroscience like small-world networks, coupled frequency oscillations, and predictive processing accounts of brain function (Goekoop & de Kleijn, 2021; 2023). These accounts of how power-law dynamics relate to fundamental principles of brain organization provide a potential means of studying how they predict variation in trait dimensions.

Goekoop & de Kleijn (2023) hypothesize that the slope of power-law distributions reflects the depth of the generative models encoded by the brain regions producing the signals. They note that previous neuroimaging research using broad macroscale networks has identified a reliable nested hierarchical structure with small-world properties in the brain. Networks with this configuration tend to exhibit a hub structure, with a subset of high-degree nodes serving as information bottlenecks. In the active inference literature, this hierarchical hub configuration is described as an efficient mechanism for dissipating prediction error. Hierarchical processing suggests higher-order hub nodes encode derivations of the activity from downstream nodes. This integrative activity of hub nodes permits a vertical encoding of both timescales and part-whole relationships. Ascending the hierarchy, these hubs are thought to encode increasingly abstract priors that are used to quell lower-order prediction errors. In this account, the frequency decomposition from a brain network with a sophisticated generative model exhibits a preponderance of low-frequency oscillations from higher-order hubs that are effectively "explaining away" the prediction errors of lower-order nodes (Auksztulewicz et al., 2017; Bastos et al., 2020; Alamia & VanRullen, 2019; Mayer et al., 2016; Michalareas et al., 2016). This frequency distribution results in a steeper power-law slope. Conversely, a flatter slope results from a greater accumulation of higher

frequencies in the frequency spectra and suggests a greater accumulation of prediction error within higher-order nodes, as existing priors fail to predict the error signals coming from lower-order nodes.

Since this hierarchically organized small-world configuration exhibits scale-invariant properties, this pattern of organization extends more broadly to between-network communication as well. A large body of evidence using community detection and functional gradient analyses suggests that broad macroscale networks can be organized into a general cortical hierarchy (Margulies et al., 2016; Vidaurre et al., 2017; Nenning et al., 2023). At the apex of the hierarchy, studies consistently report networks involved in abstract processing integrating information from multiple sensory and cognitive modalities. These heteromodal networks include the default network, involved in abstract, internally-directed processing like self-referential thinking and mental time travel (Raichle et al., 2001; Andrews-Hanna et al., 2014; Spreng & Andrews-Hanna, 2015), the FPCN, involved in directing attention toward currently relevant information and managing information in working memory (Cole & Schneider, 2007; Niendam et al., 2012), the SVAN, implicated in the suppression of distractions and the prioritization of long-term goals (Corbetta & Shulman, 2002; Vossel et al., 2014; Rueter et al., 2019; Sassenberg et al., 2023), and the limbic network, involved in decision making, memory retrieval, emotion processing, and assessing the plausibility of counterfactuals (De Brigard et al., 2013; Sheldon et al., 2019; Reagh & Ranganath, 2023). Additional graph theoretical research has characterized many nodes in these networks as being key hubs in the brain (van den Heuvel & Sporns, 2011; Bertolero et al., 2017). Since these heteromodal networks exhibit activity during processes of abstract or self-oriented

cognition, assessing the criticality of these networks could be a suitable way to assess the sophistication of complex priors and how they relate to personality traits describing patterns of higher-order cognition.

The aim of this chapter is twofold. First, this study expands on previous research in resting-state fMRI by assessing individual differences in power-law dynamics across broad macroscale brain networks in multiple large samples. Second, this study relates power-law dynamics in key hub networks to different personality traits describing patterns of higher-order cognition. In the present study, I focus on intelligence and Psychoticism, based on previous neuroimaging evidence relating these traits to networks involved in heteromodal processing.

Current theories of the neural correlates of general intelligence emphasize the trait as reflecting a form of overall network integrity (Barbey, 2018; Wang et al., 2021), but likely coordinated by particular hubs described in theories like the Parieto-Frontal Integration Theory (P-FIT), which most strongly implicates the FPCN (Jung & Haier, 2007; Santarnecchi et al., 2017). Additional research has identified structural and functional correlates of intelligence within the default and SVAN (Gur et al., 2021; Feilong et al., 2021). Further, intelligence has been linked to faster processing specifically in the cognitive bottleneck of deciding on appropriate responses to stimulus representations (rather than to faster stimulus detection or faster motor output; Lee & Chabris, 2013), as well as to adaptive functioning in a wide variety of domains (Gottfredson, 1997). From this evidence, I hypothesize that intelligence reflects a greater depth and sophistication of higher-order generative models, reflected as steeper power-law slopes in heteromodal networks.

In addition to intelligence, Psychoticism also seems likely to show associations with power-law dynamics in the brain. Psychoticism reflects individual differences in the tendency to identify perceptual or causal patterns where none exist (DeYoung et al., 2016; DeYoung & Krueger, 2018; Krueger et al., 2012). Neuroimaging research on schizophrenia suggests psychoticism is likely to be related to reduced activation and connectivity in the FPCN (Baker et al., 2014), especially in the dorsolateral prefrontal cortex (Camchong et al., 2011; Barch et al., 2001). Other findings suggest that Psychoticism is related to reduced white matter integrity in prefrontal regions (Grazioplene et al., 2016), reduced FPCN-default network anticorrelations (Whitfield-Gabrieli et al., 2008; Woodward et al., 2011), and increased connectivity of the default network (Blain et al., 2020; Xia et al., 2018).

Traits related to Psychoticism are also predictive of a wide variety of interesting behaviors and outcomes that are conceptually related to the kind of higher-order cognitive processing carried out by the heteromodal networks, including odd speech, absorption in sensory stimuli and mental imagery (McConkey et al., 1999), greater immersion in virtual environments (Ling et al., 2013), as well as bizarre experiences like seeing auras (Zingrone et al., 2009), encounters with otherworldly entities (French et al., 2008), altered relationships with one's own body, and spiritual experiences (Lifshitz et al., 2019).

Together, these findings suggest that Psychoticism might reflect a tendency toward unusual or maladaptive predictions generated by models in higher-order hub networks (Andersen, 2022; Andersen et al., 2022). This interpretation is also consistent with theories describing Psychoticism as a sensitivity to Type I errors, or false positives

(DeYoung, 2015; DeYoung & Krueger, 2018). A maladaptive form of this sensitivity might be expressed as the emergence of faulty perceptions and beliefs in the context of more abstract representations of the self and broader social conventions. For example, suspicious tendencies, persecutory delusions, or hallucinations might emerge as a result of extremely imprecise predictions from dysfunctional higher-order generative models. I hypothesize, then, that Psychoticism is associated with flatter power-law slopes in hub networks in the brain. Recent evidence has provided initial support of the association of schizophrenia with reduced power-law slopes in heteromodal cortex compared to healthy controls (Lee et al., 2021), but the present study extends this hypothesis to subclinical personality measures.

Methods

Sample 1

Participants

Participants included in this sample are those described in Sample 1 of Chapter II. FMRI acquisition, preprocessing, and individualized parcellation procedures used in this study are also identical to those described in Chapter II.

Personality Measures

Participants completed the Personality Inventory for the DSM-5 (PID-5). The PID-5 (Krueger et al., 2012) questionnaire includes 220 items assessed on a 4-point Likert scale ranging from 0 (very false or often false) to 3 (very true or often true). This inventory was designed to measure maladaptive traits that are symptoms of personality disorder in the alternative model of personality disorder for the DSM-5. The PID-5 consists of 25 primary trait scales that are grouped into five broad dimensions: Negative

Affectivity, Detachment, Psychoticism, Antagonism, and Disinhibition. The present study used scores from the Psychoticism dimension.

Intelligence

Intelligence was assessed using the same tests described in Sample 1 in Chapter II.

Sample 2

Participants

Right-handed participants in this sample were selected from the Enrichment Study cohort from the Minnesota Center for Twin and Family Research, consisting of 998 monozygotic and same-sex dizygotic twins born between 1988 and 1994 (Keyes et al., 2009; Wilson et al., 2019), and the present analyses used data from when participants were assessed at 24 years old. Exclusion criteria for this sample were identical to those described for Sample 1. The final sample comprised 99 twin pairs and 101 unpaired participants (N = 298, 187 female).

fMRI Data Acquisition and Preprocessing

Resting-state fMRI data were collected using 3T Siemens Trio and Prisma scanners at the Center for Magnetic Resonance Research at the University of Minnesota Twin Cities. Functional echo-planar images were acquired with the Trio scanner with the following parameters: repetition time (TR) = 1.4 s; echo time (TE) = 25.4 ms; flip angle = 90°; voxel dimensions = 2 x 2 x 2 mm; pixel bandwidth = 1814 Hz. Images collected using the Prisma scanner used the following parameters: repetition time (TR) = 1.5 s; echo time (TE) = 30 ms; flip angle = 70°; voxel dimensions = 2 x 2 x 2 mm; pixel bandwidth = 1885 Hz. T1-weighted MPRAGE images were also acquired for anatomical

surface registration for each participant. Data for this sample were preprocessed using *fMRIprep* v. 21.0.1 using similar specifications described for Sample 1, in conjunction with an in-house preprocessing pipeline developed at the MCTFR. Details of this pipeline are available at https://github.com/sjburwell/fmriprep_denoising. Briefly, resting-state scans were corrected for field-map distortions, motion corrected, and normalized to standard MNI space. These data were denoised by regressing the mean CSF and WM signal, as well as through ICA-AROMA to generate a non-aggressively denoised variant of the data. This denoising pipeline balanced the tradeoff between reducing subject motion while maintaining functional connectivity similarity across twins. Denoised data were then transformed from MNI space to T1w native space using antsApplyTransforms, and functional network boundaries were computed using the individualized parcellation procedure described in Chapter II.

Behavioral Measures

Participants in this sample completed the Psychoticism scale from the PID-5. Participants also completed the Block Design and Vocabulary tests of the WAIS.

Sample 3

Participants

Participants included in this sample are those described in the HCP sample of Chapter III. FMRI acquisition, preprocessing, and individualized parcellation procedures used in this study are also identical to those described in Chapter III. One additional participant was excluded due to missing behavioral data.

Behavioral Measures

This study used the 4 items assessing Psychoticism from the Achenbach self-report described in Chapter III. Intelligence was assessed using tasks from the NIH Toolbox and the Penn Computerized Neurocognitive Battery described in Chapter III. Scores from the Picture Vocabulary, Matrix Reasoning, and List Sorting tasks were included in the present study.

Analysis

Power Law Dynamics

To assess individual differences the properties of functional brain networks, I computed power law distributions of the average BOLD signal within each network. First, I extracted and standardized the average timeseries for each individualized parcel. I then applied a fast Fourier transform to these timeseries to determine the power spectra. Since the three samples relied on different scanning parameters, I selected frequencies in the power spectra within a consistent range of .01 Hz and .15 Hz. This was done to mitigate the influence of scanner drift at the low end and aliasing effects near the Nyquist frequency (half of the sampling rate) at the high end, while retaining much of the signal frequencies for each parcel. This frequency range is consistent with previous recommendations for power spectra analysis in biophysical systems (Eke et al., 2000; 2002). Next, the power spectra and frequency data were transformed using a base 10 logarithm, and least squares regression was used to determine the slope coefficient predicting log-transformed power from log-transformed frequency. The slopes for each parcel within each network were then averaged to produce a network-level power-law slope. In the present study, I used the 400 parcel Schaefer atlas mapped to 7 networks by

Yeo et al. (2011). In this study, I used 7 networks to focus on the broad patterns of connectivity across the cortex.

Latent Variable Analyses

I used structural equation modeling to assess associations between network-level power law dynamics and personality trait variables. Across both samples, I assessed associations of power-law dynamics with a latent factor representing Psychoticism, as well as a latent factor of intelligence. Power-law slopes for the default, FPCN, SVAN, and limbic networks were allowed to load on a single factor to assess associations with signal complexity among key hub networks implicated in higher-order cognition.

In Sample 1, the three subscales of PID-5 Psychoticism (Unusual Beliefs and Experiences, Perceptual Dysregulation, and Eccentricity) were allowed to load on a single factor. I also included predictors of age, sex, and head motion. A latent factor of intelligence was created from the four tests of the WASI. I allowed the residuals of the vocabulary and similarities tests to correlate to improve model fit.

In Sample 2, the three subscales of PID-5 Psychoticism were allowed to load on a latent Psychoticism factor. Models in this sample included the same predictors as Sample 1. The latent intelligence factor was fit using the vocabulary and block design tests of the WASI, and these loadings were constrained to be equal. These models also included scanner type as a covariate to account for the change of scanner used during data collection, and its potential influence on fMRI data quality.

In Sample 3, items of the ASR were allowed to load on a latent Psychoticism factor. In line with previous research, the residuals of the ASR items “I do things that other people think are strange” and “I have thoughts that other people think are strange”

were allowed to correlate due to semantic similarity (Blain et al., 2020). Since these items were highly skewed and used as indicators, polychoric correlations were used in the model for this sample. This model included the same predictors as the previous samples. This sample used a latent factor of intelligence constituted by task performance variables on list sorting, picture vocabulary, and matrix reasoning tasks. For all models across all samples, maximum likelihood estimation was used, and common fit indices were reported. Models were fit using the Lavaan package in R (Rosseel, 2012).

Results

Descriptive statistics for personality and intelligence task variables are reported in Table 6.

Table 6.

Descriptive statistics for personality and intelligence task variables

	***M*(SD)**	**Range**	**Skew**
Sample 1			
PID-5 Unusual Beliefs and Experiences	1.78(.69)	3.0	1.01
PID-5 Eccentricity	2.26(.84)	3.0	.27
PID-5 Perceptual Dysregulation	1.63(.54)	2.5	1.06
WASI Block Design	11.61(3.01)	14	.07
WASI Matrix Reasoning	11.34(2.52)	15	-.25
WASI Vocabulary	13.07(3.25)	17	-.24
WASI Similarities	12.44(2.93)	15	-.19
Sample 2			
PID-5 Unusual Beliefs and Experiences	.43(.47)	2.50	1.56
PID-5 Eccentricity	.70(.65)	2.53	.82
PID-5 Perceptual Dysregulation	.38(.39)	1.75	1.21
WASI Block Design	39.96(8.07)	38	-.94
WASI Vocabulary	45.05(10.73)	52	-.43
Sample 3			

NIH List Sorting Task	111.44(11.37)	63.71	.20
NIH Picture Vocabulary	117.14(9.61)	62.40	.18
Penn Progressive Matrices	17.00(4.71)	20	-.61
Achenbach self-report item 40	.02(.16)	2	8.88
Achenbach self-report item 70	.02(.15)	2	9.01
Achenbach self-report item 84	.22(.49)	2	2.22
Achenbach self-report item 85	.19(.46)	2	2.50

Note. PID-5 = Personality Inventory for the DSM-5, WASI = Wechsler Abbreviated Scale of Intelligence, NIH = National Institutes of Health

Power Law Dynamics across Networks

Before investigating associations with personality variables, I first analyzed individual differences in power-law dynamics across the cortex. In Sample 1, the average slope across all parcels was near -1 (M = -.94, SD = .27), signifying individual differences in whole brain dynamics trending toward a critical state, and these values were largely similar in Sample 2 (M = -.82, SD = .20), and Sample 3 (M = -.97, SD = .25). A similar trend appeared across samples at the network level, with the majority of average network slopes near criticality. Distributions of slopes for the whole brain and each network across each sample are illustrated in Figure 10.

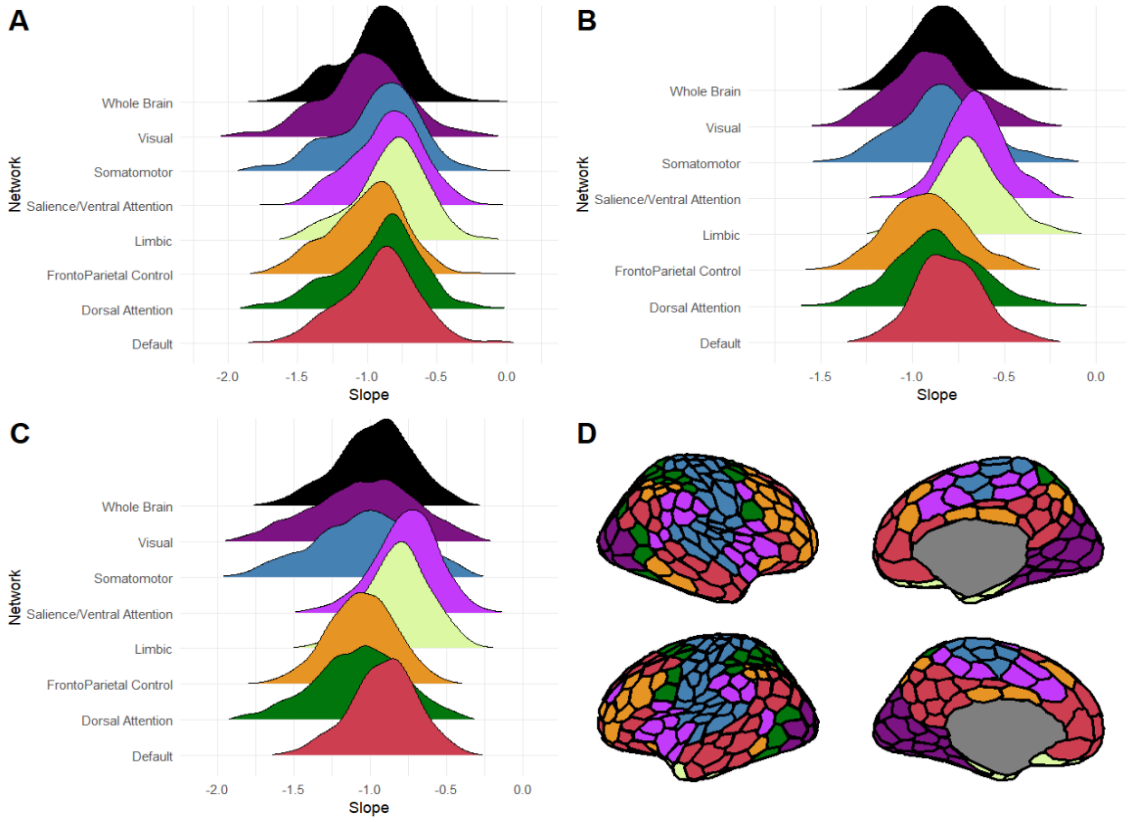

Figure 10. Distributions of power-law slopes by network. **A** = Sample 1, **B** = Sample 2, **C** = Sample 3. Parcels of the Schaefer atlas mapped to 7 networks from Yeo et al. (2011) are illustrated in **D**.

Additional results from repeated-measures one-way ANOVAs revealed significant differences in mean slope values across networks (Sample 1: $F(6,1434) = 117.5$, $p < .01$; Sample 2: $F(6,1782) = 515.1$, $p < .01$; Sample 3: $F(6,5952) = 1496$, $p < .01$). Mean differences between average slopes across networks are reported in Table 7.

Table 7.

Mean differences between power-law slopes by network

	Sample 1		Sample 2		Sample 3	
	Difference	Adjusted *p*	Difference	Adjusted *p*	Difference	Adjusted *p*
DAN-DN	-.01	.96	.07	<.01	-.16	<.01
FPCN-DN	-.09	<.01	-.13	<.01	-.14	<.01
Limbic-DN	.08	<.01	.10	<.01	.10	<.01
SVAN-DN	.05	<.01	.14	<.01	.15	<.01
SM-DN	-.02	.52	-.04	<.01	-.13	<.01
Visual-DN	-.11	<.01	-.09	<.01	-.13	<.01
FPCN-DAN	-.08	<.01	-.06	<.01	.02	<.01
Limbic-DAN	.09	<.01	.17	<.01	.26	<.01
SVAN-DAN	.06	<.01	.21	<.01	.31	<.01
SM-DAN	-.01	.98	.03	<.01	.03	<.01
Visual-DAN	-.10	<.01	-.02	.17	.04	<.01
Limbic-FPCN	.17	<.01	.23	<.01	.24	<.01
SVAN-FPCN	.14	<.01	.27	<.01	.29	<.01
SM-FPCN	.07	<.01	.09	<.01	.01	.27
Visual-FPCN	-.03	.07	.04	<.01	.02	.01
SVAN-Limbic	-.03	.02	.04	<.01	.05	<.01
SM-Limbic	-.10	<.01	-.14	<.01	-.23	<.01
Visual-Limbic	-.20	<.01	-.19	<.01	-.23	<.01
SM-SVAN	-.07	<.01	-.18	<.01	-.28	<.01
Visual-SVAN	-.17	<.01	-.23	<.01	-.28	<.01
Visual-SM	-.10	<.01	-.05	<.01	.01	.83

Note. DAN = dorsal attention network, DN = default network, FPCN = frontoparietal control network, SVAN = salience/ventral attention network, SM = somatomotor network. P-values were adjusted using Tukey's Honest Significant Difference test.

In addition to mean differences between network slopes, I also computed correlations of power law slopes between functional networks. I observed that slopes for all functional networks were strongly positively correlated, suggesting a brain-wide trend toward signal complexity. To assess the unique contribution of each network to this trend, I ipsatized participants' network-level slope values by subtracting each

participant's whole-brain slope estimate from each network-level slope. This procedure revealed a reliable pattern of correlations across samples, where ipsatized slope values of the FPCN, default, SVAN, and limbic networks were positively correlated, but were negatively correlated with slopes of the dorsal attention, visual, and somatomotor networks. This configuration is largely consistent with previous descriptions of the cortical hierarchy that distinguish unimodal from heteromodal cortex. Correlations between ipsatized network slopes across samples are reported in Table 8.

Table 8.

Correlations of ipsatized network power-law slopes across samples

		Network						
		1. Default	2. FPCN	3. Limbic	4. SVAN	5. Visual	6. SM	7. DAN
Sample 1	1.	1						
(*N* = 240)	2.	**.40**	1					
	3.	-.05	**.14**	1				
	4.	.13	.08	**.18**	1			
	5.	**-.39**	**-.27**	**-.36**	**-.50**	1		
	6.	**-.61**	**-.66**	**-.22**	**-.27**	.05	1	
	7.	**-.58**	**-.49**	.04	-.09	**-.15**	**.53**	1
Sample 2	1.	1						
(*N* = 298)	2.	**.24**	1					
	3.	**.14**	.02	1				
	4.	**.41**	.11	**.23**	1			
	5.	**-.42**	**-.27**	**-.30**	**-.51**	1		
	6.	**-.69**	**-.48**	**-.26**	**-.52**	.11	1	
	7.	**-.51**	**-.35**	**-.22**	**-.45**	-.03	**.50**	1
Sample 3	1.	1						
(*N* = 993)	2.	**.64**	1					
	3.	**.48**	**.59**	1				
	4.	**.47**	**.48**	**.44**	1			
	5.	**-.66**	**-.72**	**-.60**	**-.70**	1		
	6.	**-.79**	**-.76**	**-.66**	**-.59**	**.56**	1	
	7.	**-.56**	**-.45**	**-.30**	**-.30**	**.19**	**.45**	1

Note. Significant correlations at α = .05 are shown in bold. FPCN = frontoparietal control network, SVAN = salience/ventral attention network, SM = somatomotor, DAN = dorsal attention network

Predicting Hub Complexity from Psychoticism and Intelligence

Across all samples, I found no significant associations of whole-brain power-law slopes with either intelligence or Psychoticism. Turning to looking at the hub networks specifically, in Sample 1, I observed that the limbic network did not load significantly on the latent hub variable. Removing this indicator from the model significantly improved model fit (ΔChi-squared = 25.06, $p = .01$). Although the removal of this indicator as a hub network of interest limits the generalizability across samples, the limbic network is the smallest of the hypothesized hub networks, and estimated factor scores for the new latent variable remained highly correlated with scores estimated including the limbic network in this sample ($r = .98$, $p < .001$). Since the removal of this indicator has the potential to reduce the generalizability of the model, I refit the models in the other two samples without the limbic network to assess how this difference affected the association. Removing this indicator from the latent variables in the other samples did not alter associations with Psychoticism and intelligence.

I found that Psychoticism was significantly positively associated with the shared variance of the power-law slopes of hub networks in Sample 3, indicating a negative association with hub criticality, but this association was not replicated in Samples 1 and 2. Additionally, intelligence was negatively associated with the shared variance of the power-law slopes, but this association was not replicated in Samples 1 and 2. Model coefficients are reported in Table 9. Path diagrams for all models are illustrated in Figures 11, 12, and 13. Fit statistics for all models are reported in Table 10.

Table 9.

Coefficients of models predicting hub power-law slopes from intelligence and Psychoticism

	Sample 1			Sample 2			Sample 3		
	z	β	*p*	*z*	β	*p*	*z*	β	*p*
Hub Slopes									
Psychoticism	1.21	.11	.23	-1.25	-.08	.21	2.41	.17	.02
Intelligence	-1.28	-.14	.20	-.13	-.01	.90	-2.08	-.10	.04
Age	.81	.07	.42	-.08	-.01	.94	2.53	.10	.01
Gender	2.62	.23	.01	4.27	.44	<.01	5.01	.25	<.01
Head Motion	1.52	.13	.13	.97	.06	.33	6.38	.21	<.01
Scanner				1.94	.16	.05			

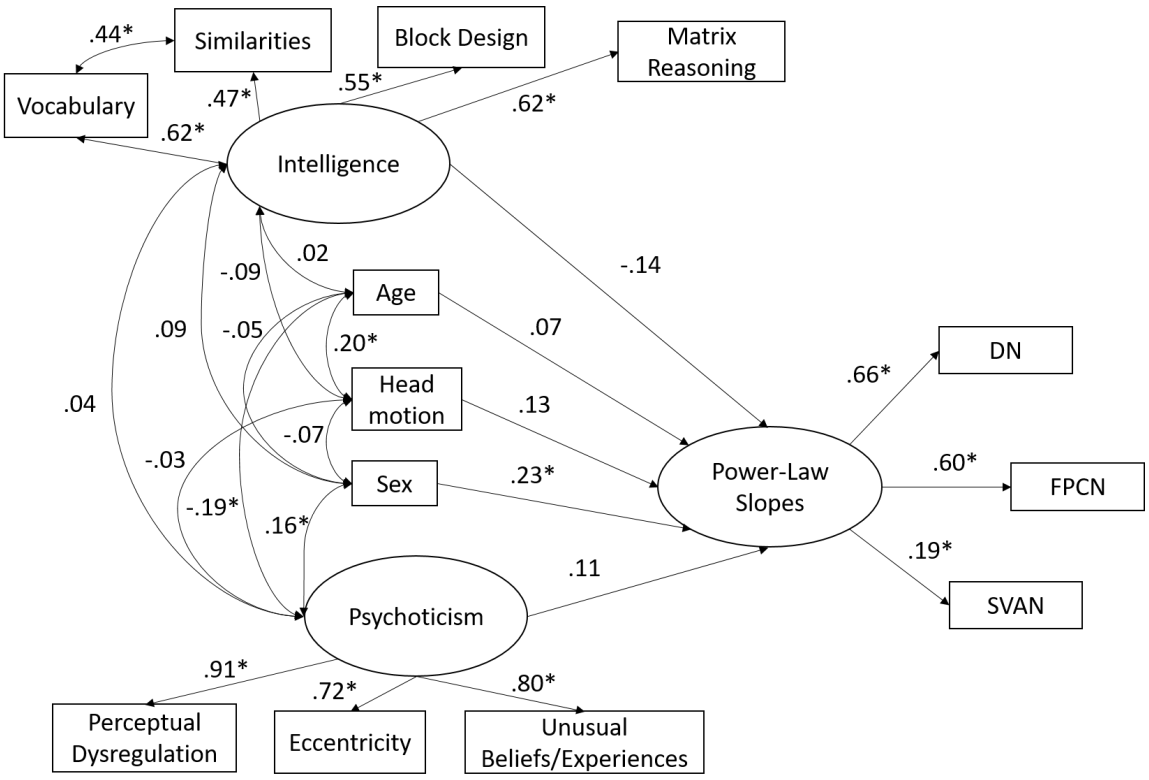

Figure 11. Structural equation model predicting power-law slopes in hub networks from Psychoticism and intelligence in Sample 1. DN = default network, FPCN = frontoparietal control network, SVAN = salience/ventral attention network.

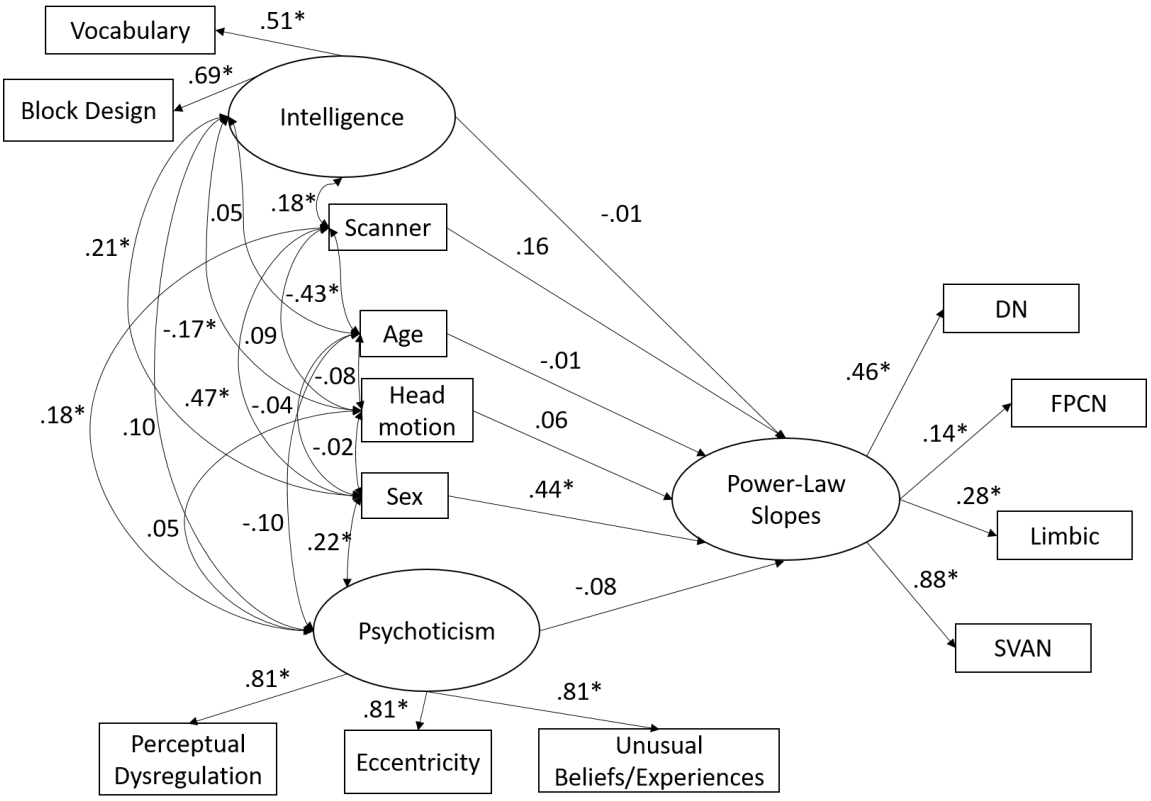

Figure 12. Structural equation model predicting power-law slopes in hub networks from Psychoticism and intelligence in Sample 2. DN = default network, FPCN = frontoparietal control network, SVAN = salience/ventral attention network.

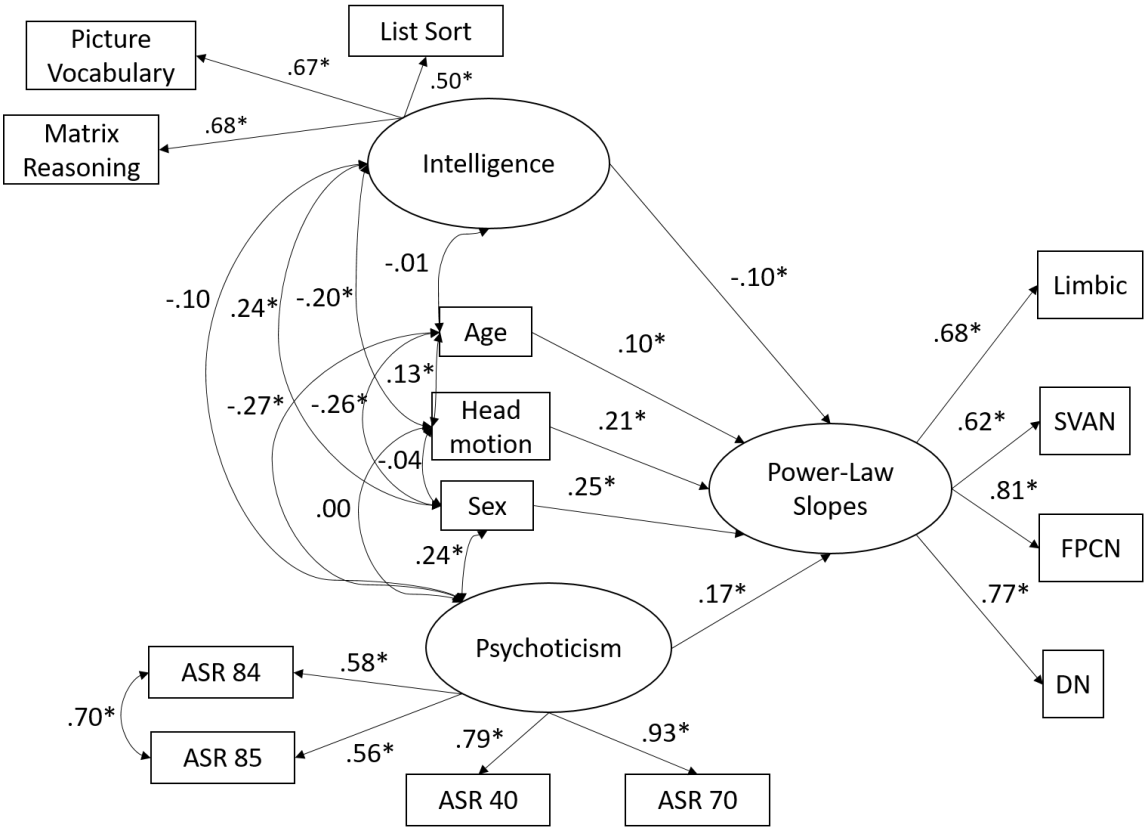

Figure 13. Structural equation model predicting power-law slopes in hub networks from Psychoticism and intelligence in Sample 3. DN = default network, FPCN = frontoparietal control network, SVAN = salience/ventral attention network, ASR = Achenbach Self-Report.

Table 10.

Fit statistics for structural equation models

Models	χ^2	*P*	RMSEA	95% C.I.	SRMR	TLI	CFI
Sample 1	113.61	<.001	.07	[.05, .09]	.06	.85	.91
Sample 2	83.88	<.01	.05	[.03, .07]	.05	.93	.95
Sample 3	98.89	<.01	.02	[.01, .03]	.05	.99	.99

Discussion

This study is the first to investigate power-law dynamics in resting-state fMRI across multiple different macroscale cortical networks, as well as their potential associations with broad personality dimensions. These findings provide a greater exploration on the nature of these underlying cortical dynamics, and how they might be used to predict important patterns of variation in cognition and behavior. Primarily, this work reveals an interesting trend of signal properties in the resting-state through a theoretical context of dynamically self-organized systems. Previous research has investigated associations of criticality using select nodes across different networks (He et al., 2011), but this study explores individual differences in these slopes across broad networks. I found evidence suggesting that power-law slopes across the entire cortex trended toward criticality across samples, but with substantial variability around this average. This observation is consistent with previous research reporting resting-state signal properties following quasi-critical or subcritical dynamics (Arviv et al., 2015; Bonachela & Muñoz, 2009; Fagerholm et al., 2015; Priesemann et al., 2014).

Further, network power-law slopes exhibited strong positive intercorrelations, suggesting a general global trend in signal complexity, which may be substantive,

artifactual, or some combination of both. However, ipsatizing these networks' slopes revealed a fairly consistent pattern of correlations across samples, despite differences in scanning parameters. The configuration among ipsatized networks is similar to patterns of functional organization shown in previous research through gradient or community estimation procedures (Margulies et al., 2016; Vidaurre et al., 2017). These results suggest possible links between more established methods of characterizing functional patterns across the cortex with properties of signal complexity.

Beyond investigating patterns of power-law dynamics across the cortex, I found initial evidence in the large HCP sample supporting a positive association of Psychoticism with power-law slopes in cortical hubs implicated in higher-order cognition (suggesting a negative association with criticality in these networks), as well as a negative association of intelligence with power-law slopes (suggesting a positive association with criticality in these networks). The direction of these effects is consistent with previous theoretical work describing links between both normative and pathological personality variation with power-law dynamics in the brain (Goekoop & de Kleijn, 2023), as well as previous empirical research relating these properties to schizophrenia and intelligence (Lee et al., 2021; Sokunbi et al., 2014; Xu et al., 2022). The specificity of these association with hub networks, rather than the whole brain, also coheres with previous research relating intelligence, Psychoticism, and schizophrenia to functional properties of networks like the default network, FPCN, and SVAN (Baker et al., 2014; Blain et al., 2020; Feilong et al., 2021; Grazioplene et al., 2016; Gur et al., 2021; Xia et al., 2018).

Further, this evidence also accords with more abstract interpretations of Psychoticism within a predictive processing framework, where features of psychosis are thought to reflect a tendency toward imprecise predictions in higher-order generative models (Andersen, 2022; Tarasi et al., 2023). A predictive processing interpretation of these findings helps support the conceptual associations between personality, psychopathology, and biologically based theories of information processing in the brain. Importantly, the associations of Psychoticism and intelligence with power-law slopes were only significant in the HCP sample, but these association are likely the most trustworthy among the three samples on account of greater statistical power, a longer scan length, and a short repetition time, so the estimation of both power-law slopes and associations with Psychoticism and intelligence are likely more precise.

These results suggest that the use of power-law dynamics in the cortex might be a useful framework for understanding associations with more fundamental, theoretically-grounded, signatures of brain organization. One unanticipated observation is that sex exhibited a strong positive association with power-law slopes in hub networks across all three samples, and these effects persisted even after refitting models with total brain volume as another potentially relevant covariate, suggesting that men exhibit reduced signal complexity in the hub networks compared to women. The associations of Psychoticism, intelligence, and sex, with power-law dynamics provide support for the potential value of using these metrics for the prediction of individual differences. Although this study sought to extend the scope of previous research to subclinical measures of personality, it may be the case that associations with power-law dynamics

are more apparent in more pathological variants of these traits, and could be more identifiable in a clinical sample.

Limitations

Despite the insights gleaned from this methodological approach, these findings have a number of important limitations. Participants in Sample 1 were only scanned for 5 minutes, but the associations of intelligence and Psychoticism with power-law slopes resemble those of the much larger HCP sample, suggesting that the lack of significance of these results may be influenced by statistical power. Another important limitation of this sample is that the limbic network did not load significantly on the latent hub network variable. In addition to the limitations of Sample 1, Sample 2 included data acquired from two different scanners, which may have affected estimation of power-law slopes. The type of scanner also exhibited unusually large effects with a number of covariates included the model, which may have influenced subsequent associations with Psychoticism and intelligence.

These limitations suggest further opportunities to explore these associations with patterns of personality variation in larger samples. Additionally, the measurement of criticality across broad networks using resting-state fMRI introduces the complicating influence of head motion. Across samples, but especially in the largest HCP sample, head motion was positively associated with power-law slopes in these networks. This influence invites a possibility to explore the sensitivity of these measures to different denoising pipelines. Further, although this study used individualized parcellation to improve the accuracy of functional localization, there were only seven functional networks included

in the present analyses to assess broad patterns of functional organization. Future research can use a greater number of functional networks to assess even more specific associations with personality dimensions or patterns of power-law dynamics across the cortex.

Another important conceptual limitation of this approach is the fact that power-law dynamics are a necessary, but not sufficient, condition for systems to be in a critical state. Although past research has made the case for criticality in the brain (Chiavlo et al., 2010; Hancock et al., 2022), assessing properties of broad macroscale cortical networks through power-law slopes may not be enough evidence to directly relate personality dimensions to individual differences in self-organized criticality in the brain. However, a more conservative interpretation of these results is that there is potential to explore patterns in fMRI signal complexity as its own unique predictor of personality variation.

Conclusion

This research describes patterns of power-law dynamics across the cortex, and helps to expand on past research relating indices of self-organized criticality to properties of fMRI signals. Additionally, this research provides some tentative initial evidence of an association of power-law dynamics in key hub networks in the brain with traits from the Openness/Intellect domain. Together, these findings provide at least a proof of concept for theories relating adaptive and maladaptive personality variation to complexity of functional properties in the brain.

Chapter V: General Discussion and Conclusions

This dissertation explores the neural correlates of Openness/Intellect and a variety of its influential facets using many different emerging methods for describing functional organization in the brain. Openness/Intellect is a complex trait domain, and a considerable amount of personality neuroscience research describing the functional connectivity correlates of Openness/Intellect report mixed findings. The studies in this dissertation help to push the boundaries of personality neuroscience by moving beyond network neuroscience paradigms emphasizing brain function as mere patterns of correlated signals, and instead focus on methods that have clearer theoretical links to why particular patterns of brain network connectivity exist. Together, these findings converge on a larger framework of Openness/Intellect as relating to patterns of individual differences in the functional properties of brain networks associated with abstract, higher-order cognition.

Chapter II provided evidence of associations of creative achievement with greater functional distinctiveness between the core default network and FPCN, and these findings accord with previous research describing the functional connectivity correlates of creativity. In lexical research, evidence supports the placement of creativity as a central facet of the Openness/Intellect domain, occupying a space between the Openness and Intellect aspects. Existing research on the neural correlates of these two aspects also helps cement creativity as a core feature of Openness/Intellect, with features of Openness predicted by the default network (Blain et al., 2020), and Intellect predicted by functional properties in the FPCN (DeYoung et al., 2009). Understanding creativity as a unique

cognitive state described by properties of these networks helps shed light on the kind of cognitive flexibility afforded by generative and evaluative modes of cognition acting in a complementary fashion.

Similarly, Chapters III and IV explore how broad cortical dynamics provide a clear framework for understanding how adaptive or maladaptive processes in the brain might predict adaptive or maladaptive processes at the behavioral level. Chapter III provides evidence of associations between intelligence with cohesive flexibility, Psychoticism with disjoint flexibility, and Openness/Intellect with overall flexibility. These findings help characterize personality dimensions like Openness/Intellect as products of variation in biologically grounded dynamical systems. In line with these findings, results from Chapter IV provided initial support for the notion that intelligence and Psychoticism were associated with patterns of criticality in these higher-order hub networks.

The associations reported in these studies are supported by past functional connectivity research, but provide greater theoretical support for the underlying cybernetic role of Openness/Intellect within a larger predictive processing framework. Much of the predictive processing research has investigated specific facets of this dimension and how they relate to variation in higher-order generative models, but few have explored these ideas in the context of broader personality dimensions. As described previously, Openness/Intellect can be characterized as the trait fundamentally reflecting variation in approaches to the cybernetic problem of optimal cognitive framing, and it incorporates facets describing dualities of associative vs. logical, correlative vs. causal,

and adaptive vs. disorganized cognition. The findings of this dissertation help to bridge the specific hypotheses from cybernetic theories of personality with the broader predictive processing framework. Approaches like connectome harmonics, brain network flexibility, and power-law dynamics all have strong theoretical ties to predictive processing, and the associations between Openness/Intellect and these functional properties lends support to the notion that this trait dimension fundamentally reflects variation in the appropriateness of generative models that influence interpretations of reality. Although this research describes associations of these particular functional properties with Openness/Intellect, future research can explore the discriminant validity of these results to determine whether these associations extend to other normative or pathological personality dimensions.

Some empirical links between these ideas have been revealed through these studies, but the connections extend to other more conceptual interpretations of these frameworks. The paradoxical nature of Openness/Intellect alludes to the seemingly fine line between adaptive and maladaptive patterns of cognition. This motif is seen throughout this research describing functional organization in the brain, with variation in balancing between cohesive and disjoint flexibility, integration and segregation, or critical and sub-critical signal dynamics. It may be the case that this fine line between adaptive and maladaptive cognition seen in Openness/Intellect is fundamentally a reflection of edge-of-chaos information processing in the brain, where the negatively correlated facets at either end of the Openness/Intellect simplex are behavioral manifestations of complementary forms of information processing. When working in

optimally calibrated dynamic tension, these forms of information processing allow individuals as complex systems to be creative, thoughtful, and adaptable, but variation in this tension can result in pathological forms of cognitive functioning.

General Limitations

Despite the application of a number of new and emerging practices in these studies, these findings also point to a number of general limitations of personality neuroscience research. The biggest of these limitations is the fact that this kind of research is correlational. Not only is this a limitation of larger resting-state fMRI research paradigms, but also the fact that personality research reflects patterns of behavior, cognition, emotion, and motivation across situations and time. How can researchers assess the causal associations between the brain and personality? For now, the answer to this question remains elusive. However, since these patterns of cognition and behavior are descriptions of underlying patterns of brain states, understanding the way that these states map on to psychologically grounded personality constructs is arguably the best approach. To this end, the most accessible and principled research must try to identify the most theoretically justified measures of brain function corresponding to trait measures of interest.

Beyond their correlational nature, these studies are limited by larger issues of measurement. Many of the samples used single questionnaire measures of personality variables, and had relatively short fMRI scan lengths. More broadly, these studies only used a single fMRI scan for each participant, and didn't explore associations with task-related activation or connectivity, so there are still questions regarding the reliability of

these associations across time and cognitive tasks. These issues of reliability also extend to the particular measures used in these studies. Many of the approaches reported here are in their infancy, and while results like these suggest new frontiers for exploring brain-behavior associations, there is still an important lack of evidence clarifying the specific limitations of these kinds of procedures.

What is the Future of Personality Neuroscience?

These issues are examples of many of the challenges of the larger field of network neuroscience. As methods in network neuroscience continue to grow more sophisticated, it is worth considering the kinds of challenges that personality neuroscience will face, and hopefully begin to overcome. Personality psychology is fundamentally integrative, and in order to fully understand the whole person, this field must synthesize the knowledge and perspectives from kindred disciplines like cognitive science, neuroscience, philosophy, and physics. I think personality neuroscience is the field that is uniquely positioned to pursue this integration to the fullest extent. Personality neuroscience has the ability to leverage the knowledge of the best ways to measure reliable patterns of human psychological variability, while also drawing upon the sophisticated theoretical background from other disciplines to properly contextualize personality variation as an emergent property of biophysical systems. As these other fields continue to evolve in the future, personality neuroscience must be attuned to their breakthroughs to understand how properties of the brain and dynamical systems in general can be used to carefully outline new hypotheses for their associations with personality variation.

Recent work is drawing attention to recurring issues of poor measurement and poor reliability in network neuroscience research reporting on brain-behavior associations (Haines et al., 2023; Hilger & Markett, 2021; Nebe et al., 2023). One potential remedy for these issues is to identify complex neural properties that more closely reflect variation in the biological source of the behavior. Exploring associations of personality with more fundamental principles of complex systems might be a way to improve the reliability of associations in future personality neuroscience research. Moving beyond simple patterns of brain function might also help to overcome many of the limitations discussed in Chapter I. However, even without this shift, researchers have a responsibility to handle more manageable pitfalls in personality neuroscience. Recent debates on best practices in personality neuroscience are encouraging in that researchers are moving toward a clearer consensus on remedies to the common issues like statistical power, poor measurement of psychological variables, and individualization of functional neuroimaging measures (Marek et al., 2022; Rosenberg & Finn, 2022; DeYoung et al., 2022b; Cecchetti & Handjaras, 2022; Spisak et al., 2022). The research in this dissertation is fundamentally an example of the application of theoretically grounded metrics of functional properties in the brain, as well as striving for best practices in the field of personality neuroscience, all within the context of predicting Openness/Intellect and its facets. Future research in personality neuroscience can continue to explore the application of these key ideas to further enhance our understanding of personality as whole.

References

Achenbach, T. M. (2009). *Achenbach System of Empirically Based Assessment (ASEBA): Development, Findings, Theory, and Applications.* Burlington, VT: University of Vermont, Research Center of Children, Youth & Families.

Alamia, A., & VanRullen, R. (2019). Alpha oscillations and traveling waves: Signatures of predictive coding? *PloS Biology, 17*(10), e3000487. https://doi.org/10.1371/journal.pbio.3000487

Alavash, M., Doebler, P., Holling, H., Thiel, C. M., & Gießing, C. (2015). Is functional integration of resting state brain networks an unspecific biomarker for working memory performance? *NeuroImage, 108*, 182-193. https://doi.org/10.1016/j.neuroimage.2014.12.046

Allen, E. A., Damaraju, E., Plis, S. M., Erhardt, E. B., Eichele, T., & Calhoun, V. D. (2014). Tracking whole-brain connectivity dynamics in the resting state. *Cerebral Cortex, 24*(3), 663-676. https://doi.org/10.1093/cercor/bhs352

Andersen, B. P. (2022). Autistic-like traits and positive schizotypy as diametric specializations of the predictive mind. *Perspectives on Psychological Science, 17*(6), 1653-1672. https://doi.org/10.1177/17456916221075252

Andersen, B. P., Miller, M., & Vervaeke, J. (2022). Predictive processing and relevance realization: Exploring convergent solutions to the frame problem. *Phenomenology and the Cognitive Sciences*. https://doi.org/10.1007/s11097-022-09850-6

Anderson, K. M., Ge, T., Kong, R., Patrick, L. M., Spreng, R. N., Subuncu, M. R., Yeo, B. T. T., & Holmes, A. J. (2021). Heritability of individualized cortical network

topography. *Proceedings of the National Academy of Sciences of the United States of America, 118*(9), e2016271118. https://doi.org/10.1073/pnas.2016271118

Andrew, C., & Pfurtscheller, G. (1996). Event-related coherence as a tool for studying dynamic interactions of brain regions. *Electroencephalography and Clinical Neurophysiology, 98*(2), 144-148. https://doi.org/10.1016/0013-4694(95)00228-6

Andrews-Hanna, J. R., Smallwood, J., & Spreng, R. N. (2014). The default network and self-generated thought: Component processes, dynamic control, and clinical relevance. *Annals of the New York Academy of Sciences, 1316,* 29–52. https://doi.org/10.1111/nyas.12360

Arviv, O., Goldstein, A., & Shriki, O. (2015). Near-critical dynamics in stimulus-evoked activity of the human brain and its relation to spontaneous resting-state activity. *Journal of Neuroscience, 35*(41), 13927-13942. https://doi.org/10.1523/JNEUROSCI.0477-15.2015

Atasoy, S., Donnelly, I., & Pearson, J. (2016). Human brain networks function in connectome-specific harmonic waves. *Nature Communications, 7*(1), 10340. https://doi.org/10.1038/ncomms10340

Auksztulewicz, R., Friston, K. J., & Nobre, A. C. (2017). Task relevance modulates the behavioural and neural effects of sensory predictions. *PloS Biology, 15*(12), e2003143. https://doi.org/10.1371/journal.pbio.2003143

Austin, J. T., & Vancouver, J. B. (1996). Goal constructs in psychology: Structure, process, and content. *Psychological Bulletin, 120*(3), 338-375. https://doi.org/10.1037/0033-2909.120.3.338

Avants, B. B., Epstein, C. L., Grossman, M., & Gee, J. C. (2008). Symmetric diffeomorphic image registration and cross-correlation: Evaluating automated labeling of elderly and neurodegenerative brain. *Medical Image Analysis, 12*(1), 26-41. https://doi.org/10.1016/j.media.2007.06.004

Avery, E. W., Yoo, K., Rosenberg, M. D., Greene, A. S., Gao, S., N, D. L., Scheinost, D., Constable, R. T., & Chun, M. M. (2020). Distributed patterns of functional connectivity predict working memory performance in novel healthy and memory-impaired individuals. *Journal of Cognitive Neuroscience, 32*(2), 241-255. https://doi.org/10.1162/jocn_a_01487

Bak, P. (1997). *How Nature Works*. Oxford University Press.

Bak, P., Tang, C., & Weisenfeld, K. (1987). Self-organized criticality: An explanation of 1/*f* noise. *Physical Review Letters, 59*(4), 381-384. https://doi.org/10.1103/PhysRevLett.59.381

Baker, J. T., Holmes, A. J., Masters, G. A., Yeo, B. T. T., Krienen, F., Buckner, R. L., & Öngür, D. (2014). Disruption of cortical association networks in schizophrenia and psychotic bipolar disorder. *JAMA Psychiatry*, *71*(2), 109-118. https://doi.org/10.1001/jamapsychiatry.2013.3469

Barbey, A. K. (2018). Network neuroscience theory of human intelligence. *Trends in Cognitive Sciences, 22*(1), 8-20. https://doi.org/10.1016/j.tics.2017.10.001

Barch, D. M., Carter, C. S., Braver, T. S., Sabb, F. W., MacDonald, A., Noll, D. C., & Cohen, J. D. (2001). Selective deficits in prefrontal cortex function in medication-naïve patients with schizophrenia. *Archives of General Psychiatry, 58*(3), 280-288. https://doi.org/10.1001/archpsyc.58.3.280

Bassett, D. S., Bullmore, E. T., Meyer-Lindenberg, A., Apud, J. A., Weinberger, D. R., & Coppola, R. (2009). Cognitive fitness of cost-efficient brain functional networks. *Proceedings of the National Academy of Sciences of the United States of America, 106*(28), 11747-11752. https://doi.org/10.1073/pnas.0903641106

Bassett, D. S., Porter, M. A., Wymbs, N. F., Grafton, S. T., Carlson, J. M., & Mucha, P. J. (2013). Robust detection of dynamic community structure in networks. *Chaos: An Interdisciplinary Journal of Nonlinear Science, 23*, 013142. https://doi.org/10.1063/1.4790830

Bastos, A. M., Lundqvist, M., Waite, A. S., Kopell, N., & Miller, E. K. (2020). Layer and rhythm specificity for predictive routing. *Proceedings of the National Academy of Sciences of the United States of America, 117*(49, 31459-31469. https://doi.org/10.1073/pnas.2014868117

Beaty, R. E., Benedek, M., Wilkins, R. W., Jauk, E., Fink, A., Silvia, P. J., Hodges, D. A., Koschutnig, K. & Neubauer, A. C. (2014). Creativity and the default network: A functional connectivity analysis of the creative brain at rest. *Neuropsychologia, 64*, 92-98. https://doi.org/10.1016/j.neuropsychologia.2014.09.019

Beaty, R. E., Seli, P., & Schacter, D. L. (2019). Network neuroscience of creative cognition: Mapping cognitive mechanisms and individual differences in the

creative brain. *Current Opinions in Behavioral Sciences, 27*, 22-30. https://doi.org/10.1016/j.cobeha.2018.08.013

Beaty, R. E., Benedek, M., Kaufman, S. B., & Silvia, P. J. (2016). Default and executive network coupling supports creative idea production. *Scientific Reports, 5*(1), 10964. https://doi.org/10.1038/srep10964

Behzadi, Y., Restom, K., Liau, J., & Liu, T. T. (2007). A component based noise correction method (CompCor) for BOLD and perfusion based fMRI. *NeuroImage, 37*(1), 90-101. https://doi.org/10.1016/j.neuroimage.2007.04.042

Bendetowicz, D., Urbanski, M., Garcin, B., Foulon, C., Levy, R., Bréchemier, M.-L., Rosso, C., de Shotten, M. T., & Volle, E. (2018). Two critical brain networks for generation and combination of remote associations. *Brain, 141*(1), 217-233. https://doi.org/10.1093/brain/awx294

Bernhardt, B. C., Smallwood, J., Keilholz, S., & Margulies, D. S. (2022). Gradients in brain organization. *NeuroImage, 251,* 118987. https://doi.org/10.1016/j.neuroimage.2022.118987

Bertolero, M. A., Yeo, B. T. T., & D'Esposito, M. (2017). The diverse club. *Nature Communications, 8*, 1277. https://doi.org/10.1038/s41467-017-01189-w

Bethlehem, R. A. I., Paquola, C., Seidlitz, J., Ronan, L., Bernhardt, B., Cam-CAN Consortium, & Tsvetanov, K. A. (2020). Dispersion of functional gradients across the adult lifespan. *NeuroImage, 222,* 117299. https://doi.org/10.1016/j.neuroimage.2020.117299

Betzel, R. F., Bertolero, M. A., Gordon, E. M., Gratton, C., Dosenbach, N. U. F., & Bassett, D. S. (2019). The community structure of functional brain networks exhibits scale-specific
patterns of inter- and intra-subject variability. *NeuroImage, 202*, 115990. https://doi.org/10.1016/j.neuroimage.2019.07.003

Betzel, R. F., Medaglia, J. D., Papadopoulos, L., Baum, G. L., Gur, R., Roalf, D., Satterthwaite, T. D., & Bassett, D. S. (2017). The modular organization of human anatomical brain networks: Accounting for the cost of wiring. *Network Neuroscience, 1*(1), 42-68. https://doi.org/10.1162/NETN_a_00002

Betzel, R. F., Satterthwaite, T. D., Gold, J. I., & Bassett, D. S. (2017). Positive affect, surprise, and fatigue are correlates of network flexibility. *Scientific Reports, 7*(520). https://doi.org/10.1038/s41598-017-00425-z

Blain, S. D., Grazioplene, R. G., Ma, Y., & DeYoung, C. G. (2020). Toward a neural model of the Openness-Psychoticism dimension: Functional connectivity in the default and frontoparietal control networks. *Schizophrenia Bulletin, 46*(3), 540-551.
https://doi.org/10.1093/schbul/sbz103

Bonachela, J. A., & Muñoz, M. A. (2009). Self-organization without conservation: True or just apparent scale-invariance? *Journal of Statistical Mechanics: Theory and Experiment, 2009,* P09009. https://doi.org/10.1088/1742-5468/2009/09/P09009

Braun, U., Schäfer, A., Walter, H., Erk, S., Romanczuk-Seiferth, N., Haddad, L., et al. (2015). Dynamic reconfiguration of frontal brain networks during executive

cognition in humans. *Proceedings of the National Academy of Sciences of the United States of America, 112,* 11678-11683. https://doi.org/10.1073/pnas.1422487112

Breakspear, M. (2017). Dynamic models of large-scale brain activity. *Nature Neuroscience, 20*(3), 340-352. https://doi.org/10.1038/nn.4497

Bromberg-Martin, E. S., Matsumoto, M., & Hikosaka, O. (2010). Dopamine in motivational control: Rewarding, aversive, and alerting. *Neuron, 68*, 815-834. https://doi.org/10.1016/j.neuron.2010.11.022

Brown, M. I., Wai, J., & Chabris, C. F. (2021). Can you ever be too smart for your own good? Comparing linear and nonlinear effects of cognitive ability on life outcomes. *Perspectives on Psychological Science, 16*(6), 1-23. https://doi.org/10.1177/1745691620964122

Buckner, R. L. & Krienen, F. M. (2013). The evolution of distributed networks in the human brain. *Trends in Cognitive Sciences, 17,* 648-665. https://doi.org/10.1016/j.tics.2013.09.017

Buckner, R. L., Krienen, F. M., Castellanos, A., Diaz, J. C., & Yeo, B. T. T. (2011). The organization of the human cerebellum estimated by intrinsic functional connectivity. *Journal of Neurophysiology, 106*(5), 2322-2345. https://doi.org/10.1152/jn.0039.2011

Bullmore, E., & Sporns, O. (2012). The economy of brain network organization. *Nature Reviews Neuroscience, 13*(5), 336-349. https://doi.org/10.1038/nrn3214

Burgess, G. C., Kandala, S., Nolan, D., Laumann, T. O., Power, J. D., Adeyemo, B., Harms, M. P., Petersen, S. E., & Barch, D. M. (2016). Evaluation of denoising strategies to address motion-correlated artifacts in resting-state functional magnetic resonance imaging data from the Human Connectome Project. *Brain Connectivity, 6*(9), 669-680. https://doi.org/10.1089/brain.2016.0435

Camchong, J., MacDonald III, A. W., Bell, C., Mueller, B. A., & Lim, K. O. (2009). Altered functional and anatomical connectivity in schizophrenia. *Schizophrenia Bulletin, 37*(3), 640-650. https://doi.org/10.1093/schbul/sbp131

Carson, S. H., Peterson, J. B., & Higgins, D. M. (2005). Reliability, validity, and factor structure of the Creative Achievement Questionnaire. *Creativity Research Journal, 17*(1), 37-50. https://doi.org/10.1207/s1532693crj1701_4

Cecchetti, L., & Handjaras, G. (2022). Reproducible brain-wide association studies do not necessarily require thousands of individuals. Online preprint: https://doi.org/10.31234/osf.io/c8xwe

Chen, J., Tam, A., Kebets, V., Orban, C., Ooi, L. Q. R., Asplund, C. L., Marek, S., Dosenbach, N. U. F., Eickhoff, S. B., Bzdok, D., Holmes, A. J., & Yeo, B. T. T. (2022). Shared and unique brain network features predict cognitive, personality, and mental health scores in the ABCD study. *Nature Communications, 13*(1), 2217. https://doi.org/10.1038/s41467-022-29766-8

Chen, Q., Yang, W., Li, W., Wei, D., Li, H., Lei, Q., Zhang, Q., & Qiu, J. (2014). Association of creative achievement with cognitive flexibility by a combined

voxel-based morphometry and resting-state functional connectivity study. *NeuroImage, 102*, 474-483. https://doi.org/10.1016/j.neuroimage.2014.08.008

Chiavlo, D. R. (2010). Emergent complex neural dynamics. *Nature Physics, 6*, 744-750. https://doi.org/10.1038/nphys1803

Choi, E. Y., Yeo, B. T. T., & Buckner, R. L. (2012). The organization of the human striatum estimated by intrinsic functional connectivity. *Journal of Neurophysiology, 108*, 2422-2263. https://doi.org/10.1152/jn.00270.2012

Chong, M., Bhushan, C., Joshi, A. A., Choi, S., Haldar, J. P., Shattuck, D. W., Spreng, R. N. & Leahy, R. M. (2017). Individual parcellation of resting fMRI with a group functional connectivity prior. *NeuroImage, 156*, 87-100. https://doi.org/10.1016/j.neuroimage.2017.04.054

Clegg, R. G., Di Cairano-Gilfedder, C., & Zhou, S. (2010). A critical look at power law modelling of the Internet. *Computer Communications, 33*(3), 259-268. https://doi.org/10.1016/j.comcom.2009.09.009

Coifman, R. R., Lafon, S., Lee, A. B., Maggioni, M., Nadler, B., Warner, F., Zucker, S. W. (2005). Geometric diffusions as a tool for harmonic analysis and structure definition of data: Diffusion maps. *Proceedings of the National Academy of Sciences of the United States of America, 102*(21), 7426-7431. https://doi.org/10.1073/pnas.0500334102

Cole, M. W., & Schneider, W. (2007). The cognitive control network: integrated cortical regions with dissociable functions. *NeuroImage, 37*(1), 343-360. https://doi.org/10.1016/j.neuroimage.2007.03.071

Cole, M. W., Yarkoni, T., Repovš, G., Anticevic, A., Braver, T. S. (2012). Global connectivity of prefrontal cortex predicts cognitive control and intelligence. *The Journal of Neuroscience, 32*(26), 8988-8999. https://doi.org/10.1523/JNEUROSCI.0536-12.2012

Corbetta, M., & Shulman, G. L. (2002). Control of goal-directed and stimulus-driven attention in the brain. *Nature Reviews, 3,* 201-215. https://doi.org/10.1038/nrn755

Costa, P. T., & McCrae, R. R. (1992). Revised NEO Personality Inventory (NEO PI-R) and NEO Five-Factor Inventory (NEO-FFI) Professional Manual. Psychological Assessment Resources.

Cox, R. W. (1996). AFNI: Software for analysis and visualization of functional magnetic resonance neuroimages. *Computers and Biomedical Research, 29*(3), 162-173. https://doi.org/10.1006/cbmr.1996.0014

De Brigard, R., Addis, D. R., Ford, J. H., Schacter, D. L., & Giovanello, K. S. (2013). Remembering what could have happened: Neural correlates of episodic counterfactual thinking. *Neuorpsychologia, 51*, 2401-2414. https://doi.org/10.1016/j.neuropsychologia.2013.01.015

DeYoung, C. G. (2006). Higher-order factors of the Big Five in a multi-informant sample. *Journal of Personality and Social Psychology, 91*(6), 1138-1151. https://doi.org/10.1037/0022-3514.91.6.1138

DeYoung, C. G. (2010). Personality neuroscience and the biology of traits. *Social and Personality Psychology Compass, 4*(12), 1165-1180. https://doi.org/10.1111/j.1751-9004.2010.00327.x

DeYoung, C. G. (2013). The neuromodulator of exploration: A unifying theory of the role of dopamine in personality. *Frontiers in Human Neuroscience, 7*, 762. https://doi.org/10.3389/fnhum.2013.00762

DeYoung, C. G. (2015). Cybernetic Big Five Theory. *Journal of Research in Personality, 56*, 33-58. https://doi.org/10.1016/j.jrp.2014.07.004

DeYoung, C. G., Beaty, R. E., Genç, E., Latzman, R. D., Passamonti, L., Servaas, M. N., Shackman, A. J., Smillie, L. D., Spreng, R. N., Viding, E., & Wacker, J. (2022). Personality neuroscience: An emerging field with bright prospects. *Personality Science, 3*, 1-21. https://doi.org/10.5964/ps.7269

DeYoung, C. G., Grazioplene, R. G., & Peterson, J. B. (2012). From madness to genius: The Openness/Intellect trait domain as a paradoxical simplex. *Journal of Research in Personality, 46*, 63-78. https://doi.org/10.1016/j.jrp.2011.12.003

DeYoung, C. G., & Krueger, R. F. (2018). A cybernetic theory of psychopathology. *Psychological Inquiry, 29*(3), 117-138. https://doi.org/10.1080/1047840X.2018.1513680

DeYoung, C. G., Shamosh, N. A., Green, A. E., Braver, T. S., & Gray, J. R. (2009). Intellect as distinct from Openness: Differences revealed by fMRI of working memory. *Journal of Personality and Social Psychology, 97*(5), 883-892. https://doi.org/10.1037/a0016615

DeYoung, G. C., Quilty, L. C., & Peterson, J. B. (2007). Between facets and domains: 10 aspects of the Big Five. *Journal of Personality and Social Psychology, 93,* 880-896. https://doi.org/10.1037/0022-3514.93.5.880

DeYoung, C. G., Quilty, L. C., Peterson, J. B., & Gray, J. R. (2014). Openness to experience, Intellect, and cognitive ability. *Journal of Personality Assessment, 96*, 46-52. https://doi.org/10.1080/00223891.2013.806327

DeYoung, C. G., Sassenberg, T. A., Abend, R., Allen, T. A., Beaty, R. E., … & Wacker, J. (2022b). Reproducible brain-behavior associations do not always require thousands of individuals. Online preprint: https://doi.org/10.31234/osf.io/sfnmk

Dong, D., Yao, D., Wang, Y., Hong, S.-J., Genon, S., Xin, F., Jung, K., He, H., Chang, X., Duan, M., Bernhardt, B. C., Margulies, D. S., Sepulcre, J., Eickhoff, S. B., & Luo, C. (2023). Compressed sensorimotor-to-transmodal hierarchical organization in schizophrenia. *Psychological Medicine, 53*(3), 771-784. https://doi.org/10.1017/S0033291721002129

Dubois, J., Galdi, P., Paul, L. K., & Adolphs, R. (2018a). A distributed brain network predicts general intelligence from resting-state human neuroimaging data. *Philosophical Transactions of the Royal Society B: Biological Sciences, 373*, 2017284. https://doi.org/10.1098/rstb.2017.0284

Dubois, J., Galdi, P., Han, Y., Paul, L. K., & Adolphs, R. (2018b). Resting-state functional brain connectivity best predicts the personality dimension of openness to experience. *Personality Neuroscience, 1*, e6. https://doi.org/10.1017/pen.2018.8

Durstewitz, D., & Seamans, J. K. (2008). The dual-state theory of prefrontal cortex dopamine function with relevance to catechol-O-methyltransferase genotypes and schizophrenia. *Biological Psychiatry, 64*, 739-749. https://doi.org/10.1016/j.biopsych.2008.05.015

Eickhoff, S. B., Bzdok, D., Laird, A. R., Roski, C., Caspers, S., Zilles, K., & Fox, P. T. (2011). Co-activation patterns distinguish cortical modules, their connectivity and functional differentiation. *NeuroImage, 57*(3), 938-949. https://doi.org/10.1016/j.neuroimage.2011.05.021

Eke, A., Hermán, P., Bassingthwaighte, J. B., Raymond, G. M., Percival, D. B., Cannon, M., Balla, I., & Ikrényi, C. (2000). Physiological time series: Distinguishing fractal noises from motions. *European Journal of Physiology, 439*, 403-415.

Eke, A., Herman, P., Kocsis, L., & Kozak, L. R. (2002). Fractal characterization of complexity in temporal physiological signals. *Physiological Measurement, 23*, 1-38. https://doi.org/10.1088/0967-3334/23/1/201

Elam, J. (2015). Ramifications of image reconstruction version differences. *HCP Data Release Updates: Known Issues and Planned Fixes.* https://wiki.humanconnectome.org/display/PublicData/

Ellamil, M., Dobson, C., Beeman, M., & Christoff, K. (2012). Evaluative and generative modes of thought during the creative process. *NeuroImage, 59*(2), 1783-1794. https://doi.org/10.1016/j.neuroimage.2011.08.008

Esteban, O. Markiewicz, C., Blair, R. W., Moodie, C., Isik, A. I., Aliaga, A. E., Kent, J., et al. (2018). fMRIPrep: A robust preprocessing pipeline for functional MRI. *Nature Methods, 16*(1), 111-116. https://doi.org/10.1038/s41592-018-0235-4

Fagerholm, E. D., Lorenz, R., Scott, G., Dinov, M., Hellyer, P. J., Mirzaei, N., Leeson, C., Carmichael, D. W., Sharp, D. J., Shew, W. L., & Leech, R. (2015). Cascades and cognitive state: Focused attention incurs subcritical dynamics. *The Journal of*

Neuroscience, 35(11), 4626-4634. https://doi.org/10.1523/JNEUROSCI.3694-14.2015

Feeley, T. H. (2002). Comment on halo effects in rating and evaluation research. *Human Communication Research, 28*(4), 578-586. https://doi.org/10.1111/j.1468-2958.2002.tb00825.x

Feilong, M., Guntupalli, J. S., & Haxby, J. V. (2021). The neural basis of intelligence in fine-grained cortical topographies. *eLife, 10,* e64058. https://doi.org/10.7554/eLife.64058

Finn, E. S. (2021). Is it time to put rest to rest? *Trends in Cognitive Sciences, 25*(12), 1021-1032. https://doi.org/10.1016/j.tics.2021.09.005

Fonov, V. S., Evans, A. C., McKinstry, R. C., Almli, C. R., & Collins, D. L. (2009). Unbiased nonlinear average age-appropriate brain templates from birth to adulthood. *NeuroImage, 47*, Supplement 1: S102. https://doi.org/10.1016/S1053-8119(09)70884-5

Fransson, P., Metsäranta, M., Blennow, M., Aden, U., Lagercrantz, H., & Vanhatalo, S. Early development of spatial patterns of power-law frequency scaling in fMRI resting-state and EEG data in the newborn brain. *Cerebral Cortex, 23*(3), 638-646. https://doi.org/10.1093/cercor/bhs047

Freedman, D., & Lane, D. (1983). A nonstochastic interpretation of reported significance levels. *Journal of Business & Economic Statistics, 1*(4), 292-298. https://doi.org/10.2307/1391660

French, C. C. Santomauro, J., Hamilton, V., Fox, R., & Thalbourne, M. A. (2008). Psychological aspects of the alien contact experience. *Cortex, 44*(10), 1387-1395. https://doi.org/10.1016/j.cortex.2007.11.011

Friedman, J., Hastie, T., & Tibshirani, R. (2010). Regularization paths for generalized linear models via coordinate descent. *Journal of Statistical Software, 33*(1), 1-22. https://doi.org/10.18637/jss.v033.i01

Friedrich, P., Forkel, S. J., & Thiebaut de Schotten, M. (2020). Mapping the principal gradient onto the corpus callosum. *NeuroImage, 223,* 117317. https://doi.org/10.1016/j.neuroimage.2020.117317

Friston, K. J., Fagerholm, E. D., Zarghami, T. S., Parr, T., Hipólito, I., Magrou, L., & Razi, A. (2021). Parcels and particles: Markov blankets in the brain. *Network Neuroscience, 5*(1), 211-251. https://doi.org/10.1162/netn_a_00175

Frith, E., Elbich, D. B., Christensen, A. P., Rosenberg, M. D., Chen, Q., Kane, M. J., Silvia, P. J., Seli, P., & Beaty, R. E. (2021). Intelligence and creativity share a common cognitive and neural basis. *Journal of Experimental Psychology: General, 150*(4), 609-632. https://doi.org/10.1037/xge0000958

Girvan, M., & Newman, M. E. J. (2002). Community structure in social and biological networks. *Proceedings of the National Academy of Sciences of the United States of America, 99*(12), 7821-7826. https://doi.org/10.1073/pnas.122653799

Glasser, M. F., Coalson, T. S., Robinson, E. C., Hacker, C. D., Harwell, J., Yacoub, E., Ugurbil, K., Andersson, J., Beckmann, C. F., Jenkinson, M., Smith, S. M., & Van Essen, D. C. (2016). A multi-modal parcellation of the human cerebral cortex.

Nature, 536(7615), 171-178. https://doi.org/10.1038/nature18933

Glasser, M. F., Sotiropoulos, S. N., Wilson, J. A., Coalson, T. S., Fischl, B., Andersson, J. L., Xu, J., Jbabdi, S., Webster, M., Polimeni, J. R., Van Essen, D. C., Jenkinson, M., … WU-Minn HCP Consortium. (2013). The minimal preprocessing pipelines for the Human Connectome Project. *NeuroImage, 80,* 105-124. https://doi.org/10.1016/j.neuroimage.2013.04.127

Glomb, K., Kringelbach, M. L., Deco, G., Hagmann, P., Pearson, J., & Atasoy, S. (2021). Functional harmonics reveal multi-dimensional basis functions underlying cortical organization. *Cell Reports, 36*(8), 109554. https://doi.org/10.1016/j.celrep.2021.109554

Goekoop, R., & De Kleijn, R. (2021). Permutation entropy as a universal disorder criterion: How disorders at different scale levels are manifestations of the same underlying principle. *Entropy, 23*(12), 1701. https://doi.org/10.3390/e23121701

Goekoop, R., & De Kleijn, R. (2023). Hierarchical network structure as the source of hierarchical dynamics (power-law frequency spectra) in living and non-living systems: How state-trait continua (body plans, personalities) emerge from first principles in biophysics. *Neuroscience & Biobehavioral Reviews, 33*(3), 259-268. https://doi.org/10.1016/j.neurobiorev.2023.105402

Gordon, E. M., Laumann, T. O., Adeyemo, B., Huckins, J. F., Kelley, W. M., Petersen, S. E. (2016). Generation and evaluation of a cortical area parcellation from resting-state correlations. *Cerebral Cortex, 26*, 288-303. https://doi.org/10.1093/cercor/bhu239

Gordon, E. M., Laumann, T. O., Adeyemo, B., Gilmore, A. W., Nelson, S. M., Dosenbach, N. U. F., & Petersen, S. E. (2017). Individual-specific features of brain systems identified with resting state functional correlations. *NeuroImage, 146,* 918-939. https://doi.org/10.1016/j.neuroimage.2016.08.032

Gorgolewski, K., Burns, C. D., Madison, C., Clark, D., Halchenko, Y. O., Waskom, M. L., & Ghosh, S. (2011). Nipype: A flexible, lightweight and extensible neuroimaging data processing framework in Python. *Frontiers in Neuroinformatics, 5*(13), 1-15. https://doi.org/10.3389/fninf.2011.00013.

Gottfredson, L. S. (1997). Why g matters: The complexity of everyday life. *Intelligence, 24*(1), 79-132. https://doi.org/10.1016/S0160-2896(97)90014-3

Grazioplene, R. G., Chavez, R. S., Rustichini, A., & DeYoung, C. G. (2016). White matter correlates of psychosis-linked traits support continuity between personality and psychopathology. *Journal of Abnormal Psychology, 125*(8), 1135-1145. https://doi.org/10.1037/abn0000176

Greene, A. S., Gao, S., Scheinost, D., & Constable, R. T. (2018). Task-induced brain state manipulation improves prediction of individual traits. *Nature Communications, 9*(1), 2807. https://doi.org/10.1038/s41467-018-04920-3

Greve, D. N., & Fischl, B. (2009). Accurate and robust brain image alignment using boundary-based registration. *NeuroImage, 48*(1), 63-72. https://doi.org/10.1016/j.neuroimage.2009.06.060

Griffa, A., Ricaud, B., Benzi, K., Bresson, X., Daducci, A., Vandergheynst, P., Thiran, J.-P., & Hagmann, P. (2017). Transient networks of spatio-temporal connectivity

map communication pathways in brain functional systems. *NeuroImage, 155*, 490-502. https://doi.org/10.1016/j.neuroimage.2017.04.015

Gur, R. C., Butler, E. R., Moore, T. M., Rosen, A. F. G., Ruparel, K., Satterthwaite, T. D., Roalf, D. R., Gennatas, E. D., Bilker, W. B., Shinohara, R. T., Port, A., Elliott, M. A., Verma, R., Davatzikos, C., Wolf, D. H., Detre, J. A., & Gur, R. E. (2021). Structural and functional brain parameters related to cognitive performance across development: Replication and extension of the Parieto-Frontal Integration Theory in a single sample. *Cerebral Cortex, 31*(3), 1444-1463. https://doi.org/10.1093/cercor/bhaa282

Haines, N., Sullivan-Toole, H., & Olino, T. (2023). From classical methods to generative models: Tackling the unreliability of neuroscientific measures in mental health research. *Biological Psychiatry: Cognitive Neuroscience and Neuroimaging, 8*(8), 822-831. https://doi.org/10.1016/j.bpsc.2023.01.001

Hancock, F., Rosas, F. E., Mediano, P. A. M., Luppi, A. I., Cabral, J., Dipasquale, O., & Turkheimer, F. E. (2023). May the 4C's be with you: An overview of complexity-inspired frameworks for analysing resting-state neuroimaging data. *Journal of the Royal Society Interface, 19*(191), 20220214. https://doi.org/10.1098/rsif.2022.0214

Hansen, J. Y., Shafiei, G., Markello, R. D., Smart, K., Cox, S. M. L., Nørgaard, M., Beliveau, V., Wu, Y., Gallezot, J.-D., Aumont, É., Servaes, S., Scala, S., DuBois, J. M., Wainstein, G., Bezgin, G., Funck, T., Schmitz, T. W., Spreng, R. N., Galovic, M., … Misic, B. (2022). Mapping neurotransmitter systems to the

structural and functional organization of the human neocortex. *Nature Neuroscience, 25*(11), 1569-1581. https://doi.org/10.1038/s41593-022-01186-3

He, B. J. (2011). Scale-free properties of the functional magnetic resonance imaging signal during rest and task. *Journal of Neuroscience, 31*(39), 13786-13795. https://doi.org/10.1523/JNEUROSCI.2111-11.2011

He, L., Zhuang, K., Li, Y., Sun, J., Meng, J., Zhu, W., et al. (2019). Brain flexibility associated with need for cognition contributes to creative achievement. *Psychophysiology, 56*(12), e13464. https://doi.org/10.1111/psyp.134464

Heaton, R. K., Akshoomoff, N., Tulsky, D., Mungas, D., Weintraub, S., Dikmen, S., Beaumont, J., Casaletto, K. B., Conway, K., Slotkin, J., & Gershon, R. (2014). Reliability and validity of composite scores from the NIH Toolbox Cognitive Battery in adults. *Journal of the International Neuropsychological Society, 20*(6), 588-598. https://doi.org/10.1017/S1355617714000241

Heckner, M. K., Cieslik, E. C., Patil, K. R., Gell, M., Eickhoff, S. B., Hoffstäder, F., & Langner, R. (2023). Predicting executive functioning from functional brain connectivity: Network specificity and age effects. *Cerebral Cortex, 33*(11), 6495-6507. https://doi.org/10.1093/cercor/bhac520

Hesse, J., & Gross, T. (2014). Self-organized criticality as a fundamental property of neural systems. *Frontiers in Systems Neuroscience, 8*, 166. https://doi.org/10.3389/fnsys.2014.00166

Hilger, K., Ekman, M., Fiebach, C. J., & Basten, U. (2017). Intelligence is associated with the modular structure of intrinsic brain networks. *Scientific Reports, 7*, 16088. https://doi.org/10.1038/s41598-017-15795-7

Hilger, K., Fukushima, M., Sporns, O., & Fiebach, C. J. (2020). Temporal stability of functional brain modules associated with human intelligence. *Human Brain Mapping, 41*, 362-372. https://doi.org/10.1002/hbm.24807

Hilger, K., & Markett, S. (2021). Personality network neuroscience: Promises and challenges on the way toward a unifying framework of individual variability. *Network Neuroscience, 5*(3), 631-645. https://doi.org/10.1162/netn_a_00198

Hill, J., Inder, T., Neil, J., Dierker, D., Harwell, J., & Van Essen, D. (2010). Similar patterns of cortical expansion during human development and evolution. *Proceedings of the National Academy of Sciences of the United States of America, 107*(29), 13135-13140. https://doi.org/10.1073/pnas.1001299107

Hodgson, K., Poldrack, R., A., Curran, J. E., Knowles, E. E., Mathias, S., Göring, H. H. H., Yao, N., Olvera, R. L., Fox, P. T., Almasy, L., Duggirala, R., Barch, D. M., Blangero, J., & Glahn, D. C. (2017). Shared genetic factors influence head motion during MRI and body mass index. *Cerebral Cortex, 27*(12), 5539-5546. https://doi.org/10.1093/cercor/bhw321

Hong, S.-J., Vos de Wael, R., Bethlehem, R. A. I., Lariviere, S., Paquola, C., Valk, S. L., Milham, M. P., Di Martino, A., Margulies, D. S., Smallwood, J., & Bernhardt, B. C. (2019). Atypical functional connectome hierarchy in autism. *Nature Communications, 10,* 1-13. https://doi.org/10.1038/s41467-019--8944-1

Hovhannisyan, G., & Vervaeke, J. (2021). Enactivist Big Five Theory. *Phenomenology and the Cognitive Sciences, 21*(2), 341-375. https://doi.org/10.1007/s11097-021-09768-5

Huntenburg, J. M., Bazin, P.-L., Goulas, A., Tardif, C. L., Villringer, A., & Margulies, D. S. (2017). A systematic relationship between functional connectivity and intracortical myelin in the human cerebral cortex. *Cerebral Cortex, 27*(2), 981-997. https://doi.org/10.1093/cercor/bhx030

Huo, T., Xia, Y., Zhuang, K., Chen, Q., Sun, J., Yang, W., & Qiu, J. (2022). Linking functional connectome gradient to individual creativity. *Cerebral Cortex, 32*(23), 5273-5284. https://doi.org/10.1093/cercor/bhac013

Hyvärinen, A., & Oja, E. (2000). Independent components analysis: algorithms and applications. *Neural Networks, 13*(4), 411-430. https://doi.org/10.1016/S0893-6080(00)00026-5

Jenkinson, M., Bannister, P., Brady, M., & Smith, S. (2002). Improved optimization for the robust and accurate linear registration and motion correction of brain images. *NeuroImage, 17*(2), 825-841. https://doi.org/10.1006/nimg.2002.1132

Jiao, B., Zhang, D., Liang, A., Liang, B., Wang, Z., Li, J., Cai, Y., Gao, M., Gao, Z., Chang, S., Hunag, R., & Liu, M. (2017). Association between resting-state brain network topological organization and creative ability: Evidence from a multiple linear regression model. *Biological Psychology, 129*, 165-177. https://doi.org/10.1016/j.biopsycho.2017.09.003

John, O. P., Naumann, L. P., & Soto, C. J. (2008). Paradigm shift to the integrative big-five trait taxonomy: History, measurement, and conceptual issues. In O. P. John, R. W. Robins, & L. A. Pervin (Eds.), *Handbook of personality: Theory and research* (pp. 114-158). New York, NY: Guilford Press.

Jung, R. E. (2014). Evolution, creativity, intelligence, and madness: "Here be dragons." *Frontiers in Psychology, 5,* 784. https://doi.org/10.3389/fpsyg.2014.00784

Jung, R. E., & Haier, R. J. (2007). The parieto-frontal integration theory (P-FIT) of intelligence: Converging neuroimaging evidence. *Behavioral and Brain Sciences, 30*(2), 135-154. https://doi.org/10.1017/S0140525X07001185

Jutla, I. S., Jeub, L. G., & Mucha, P. J. (2011). A generalized Louvain method for community detection implemented in MATLAB. https://netwiki.amath.unc.edu/GenLouvain

Karahanoğlu, F. I., & Van De Ville, D. (2015). Transient brain activity disentangles fMRI resting-state dynamics in terms of spatially and temporally overlapping networks. *Nature Communications, 6*(1), 7751. https://doi.org/10.1038/ncomms8751

Kaufman, S. B., Quilty, L. C., Grazioplene, R. G., Hirsh, J. B., Gray, J. R., Peterson, J. B., & DeYoung, C. G. (2016). Openness to experience and intellect differentially predict creative achievement in the arts and sciences. *Journal of Personality, 84,* 248-258. https://doi.org/10.1111/jopy.12156

Keyes, M. A., Malone, S. M., Elkins, I. J., Legrand, L. N., McGue, M., & Iacono, W. G. (2009). The enrichment study of the Minnesota twin family study: Increasing the

yield of twin families at high risk for externalizing psychopathology. *Twin Research and Human Genetics: The Official Journal of the International Society for Twin Studies, 12*(5), 489-501. https://doi.org/10.1375/twin.12.5.489

Knodt, A. R., Elliott, M. L., Whitman, E. T., Winn, A., Addae, A., Ireland, D., Poulton, R., Ramrakha, S., Caspi, A., Moffitt, T. E., & Hariri, A. R. Test-retest reliability and predictive utility of a macroscale principal functional connectivity gradient. *Human Brain Mapping,* https://doi.org/10.1002/hbm.26517

Kong, R., Li, J., Orban, C., Sabuncu, M. R., Liu, H., Schaefer, A., Sun, N., Zuo, X.-N., Holmes, A. J., Eickhoff, S. B., & Yeo, B. T. T. (2019). Spatial topography of individual-specific cortical networks predicts human cognition, personality, and emotion. *Cerebral Cortex, 29*(6), 2533-2551. https://doi.org/10.1093/cercor/bhy123

Kong, R., Tan, Y. R., Wulan, N., Ooi, L. Q. R., Farahibozorg, S.-R., Harrison, S., Bijsterbosch, J. D., Bernhardt, B. C., Eickhoff, S., & Yeo, B. T. T. (2023). Comparison between gradients and parcellations for functional connectivity prediction of behavior. *NeuroImage, 273,* 120044. https://doi.org/10.1016/j.neuroimage.2023.120044

Kong, R. Yang, Q., Gordon, E., Xue, A., Yan, X., Orban, C., Zuo, X., Spreng, R. N. Ge, T., Holmes, A., Eickhoff, S., & Yeo, B. T. T. (2021). Individual-specific areal-level parcellations improve functional connectivity prediction of behavior. *Cerebral Cortex, 31*(10), 4477-4500. https://doi.org/10.1093/cercor/bhab101

Krueger, R. F., Derringer, J., Markon, K. E., Watson, D., & Skodol, A. E. (2012). Initial construction of a maladaptive personality trait model and inventory for DSM-5. *Psychological Medicine, 42*, 1879-1890. https://doi.org/10.1017/S0033291711002674

Kucyi, A., Hove, M. J., Esterman, M., Hutchinson, R. M., & Valera, E. M. (2017). Dynamic brain network correlates of spontaneous fluctuations in attention. *Cerebral Cortex, 27*(3), 1831-1840. https://doi.org/10.1093/cercor/bhw029

Kuhn, M. (2021). Caret: Classification and regression training. R package version 6.0-90. https://CRAN.R-project.org/package=caret

Langer, N., Pedroni, A., Gianotti, L. R. R., Hänggi, J., Knoch, D., & Jäncke, L. (2012). Functional brain network efficiency predicts intelligence. *Human Brain Mapping, 33*(6), 1393-1406. https://doi.org/10.1002/hbm.21297

Lee, J. J., & Chabris, C. F. (2013). General cognitive ability and the psychological refractory period: Individual differences in the mind's bottleneck. *Psychological Science, 24*(7), 1226-1233. https://doi.org/10.1177/0956797612471540

Lee, Y.-J., Huang, S.-Y., Lin, C.-P., Tsai, S.-J., & Yang, A. C. (2021). Alteration of power-law scaling of spontaneous brain activity in schizophrenia. *Schizophrenia Research, 238*, 10-19. https://doi.org/10.1016/j.schres.2021.08.026

Lee, C., & Wilkinson, D. J. (2019). A review of stochastic block models and extensions for graph clustering. *Applied Network Science, 4*(1), 122-172. https://doi.org/10.1007/s41109-019-0232-2

Leonardi, N., & Van De Ville, D. (2015). On spurious and real fluctuations of dynamic functional connectivity during rest. *NeuroImage, 104*, 430-436. https://doi.org/10.1016/j.neuroimage.2014.09.007

Levi, P. T., Chopra, S., Pang, J. C., Holmes, A., Gajwani, M., Sassenberg, T. A., DeYoung, C. G., & Fornito, A. (2023). The effect of using group-averaged or individualized brain parcellations when investigating connectome dysfunction in psychosis. *Network Neuroscience, 7*(4), 1228-1247. https://doi.org/10.1162/netn_a_00329

Li, M., Chen, H., Wang, J., Liu, F., Wang, Y., Lu, F., et al. (2015). Increased cortical thickness and altered functional connectivity of the right superior temporal gyrus in left-handers. *Neuropsychologia, 67,* 27-34. https://doi.org/10.1016/j.neuropsychologia.2014.11.033

Li, J., Zhang, D., Liang, A., Liang, B., Wang, Z., Cai, Y., Gao, M., Gao, Z., Chang, S., Jiao, B., Huang, R., & Liu, M. (2017). High transition frequencies of dynamic functional connectivity states in the creative brain. *Scientific Reports, 7*, 46072. https://doi.org/10.1038/srep46072

Lifshitz, M., van Elk, M., & Luhrmann, T. M. (2019). Absorption and spiritual experience: A review of evidence and potential mechanisms. *Consciousness and Cognition, 73*, 102760. https://doi.org/10.1016/j.concog.2019.05.008

Ling, Y., Nefs, H. T., Brinkman, W. P., Qu, C., & Heynderickx, I. (2013). The relationship between individual characteristics and experienced presence.

Computers in Human Behavior, 29(4), 1519-1530. https://doi.org/10.1016/j.chb.2012.12.010

Luppi, A. I., Gellersen, H. M., Peattie, A. R. D., Manktelow, A. E., Menon, D. K., Dimitriadis, S. I., & Stamatakis, E. A. (2021). Searching for consistent brain network topologies across the garden of (shortest) forking paths. https://doi.org/10.1101/2021.07.13.452257

Lux, T. A., & Alfarano, S. (2016). Financial power laws: Empirical evidence, models, and mechanisms. *Chaos, Solitons, & Fractals, 88*, 3-18. https://doi.org/10.1016/j.chaos.2016.01.020

Ma, Y., Hendrickson, T., Ramsay, I., Shen, A., Sponheim, S. R., & MacDonald, A. W., III. (2022). Resting-state functional connectivity explained psychotic-like experiences in the general population and partially generalized to patients and relatives. *Biological Psychiatry Global Open Science.* https://doi.org/10.1016/j.bpsgos.2022.08.011

Madore, K. P., Thakral, P. P., Beaty, R. E., Addis, D. R., & Schacter, D. L. (2017). Neural mechanisms of episodic retrieval support creative thinking. *Cerebral Cortex, 29*(1), 150-166. https://doi.org/10.1093/cercor/bhx312

Marek, S., Tervo-Clemmens, B., Calabro, F. J., Montez, D. F., Kay, B. P., … & Dosenbach, N. U. F. (2022). Reproducible brain-wide association studies require thousands of individuals. *Nature, 603*, 654-660. https://doi.org/10.1038/s41586-022-04492-9

Margulies, D. S., Ghosh, S. S., Goulas, A., Falkiewicz, M., Huntenburg, J. M., Langs, G., Bezgin, G., Eickhoff, S. B., Castellanos, F. X., Petrides, M., Jefferies, E., & Smallwood, J. (2016). Situating the default-mode network along a principal gradient of macroscale cortical organization. *Proceedings of the National Academy of Sciences of the United States of America, 113*(44), 12574-12579. https://doi.org/10.1073/pnas.1608282113

Maxim, V., Sendur, L., Fadili, J., Suckling, J., Gould, R., Howard, R., & Bullmore, E. (2005). Fractional Gaussian noise, functional MRI and Alzheimer's disease. *NeuroImage, 25*(1), 141-158. https://doi.org/10.1016/j.neuroimage.2004.10.044

Mayer, A., Schwiedrzik, C. M., Wibral, M., Singer, W., & Melloni, L. (2016). Expecting to see a letter: Alpha oscillations as carriers of top-down sensory predictions. *Cerebral Cortex, 26*, 3146-3160. https://doi.org/10.1093/cercor/bhv146

McAdams, D. P., & Pals, J. L. (2006). A new big five: Fundamental principles for an integrative science of personality. *American Psychologist, 61*(3), 204-217. https://doi.org/10.1037/0003-066X.61.3.204

McCrae , R. R. & Costa, P. J. (1997). Conceptions and correlates of openness to experience. In R. Hogan, J. A. Johnson, & S. R. Briggs (Eds.), *Handbook of personality psychology* (pp. 825-847). San Diego: Academic. https://doi.org/10.1016/B978-012134645-4/50032-9

McConkey, K. M., Wende, V., Barnier, A. J. (1999). Measuring change in the subjective experience of hypnosis. *Int. J. Clin. Exp. Hypn., 47*(1), 23-39. https://doi.org/10.1080/00207149908410020

Meisel, C., Storch, A., Hallmeyer-Elgner, S., Bullmore, E., & Gross, T. (2012). Failure of adaptive self-organized criticality during epileptic seizure attacks. *PLoS Computational Biology, 8*, e1002312. https://doi.org/10.1371/journal.pcbi.1002312

Menon, V., & Uddin, L. Q. (2010). Saliency, switching, attention and control: A network model of insula function. *Brain Structure and Function, 214*(5), 655-667. https://doi.org/10.1007/s00429-010-0262-0

Michalareas, G., Vezoli, J., van Pelt, S., Schoffelen, J.-M., Kennedy, H., & Fries, P. (2016). Alpha-beta and gamma rhythms subserve feedback and feedforward influences among human visual cortical areas. *Neuron, 89*, 384-397. https://doi.org/10.1016/j.neuron.2015.12.018

Moore, T. M., Reise, S. P., Gur, R. E., Hakonarson, H., & Gur, R. C. (2015). Psychometric properties of the Penn Computerized Neurocognitive Battery. *Neuropsychology, 29*(2), 235-246. https://doi.org/10.1037/neu0000093

Moorman, E. L., & Samuel, D. B. (2018). Representing schizotypal thinking with dimensional traits: A case for the Five Factor Schizotypal Inventory. *Psychological Assessment, 30*(1), 19-30. https://doi.org/10.1037/pas0000497

Mucha, P. J., Richardson, T., Macon, K., Porter, M. A., & Onnela, J.-P. (2010). Community structure in time-dependent, multiscale, and multiplex networks. *Science, 328*(5980), 876-878. https://doi.org/10.1126/science.1184819

Mwilambwe-Tshilobo, L., Ge, T., Chong, M., Ferguson, M. A., Misic, B., Burrow, A. L., Leahy, R. M., & Spreng, R. N. (2019). Loneliness and meaning in life are

reflected in the intrinsic network architecture of the brain. *Social Cognitive and Affective Neuroscience, 14*(4), 423-433. https://doi.org/10.1093/scan/nsz021

Nebe, S., Reutter, M., Baker, D. H., Bölte, J., Domes, G., Gamer, M., Gärtner, A., Gießing, C., Gurr, C., Hilger, K., Jawinski, P., Kulke, L., Lischke, A., Markett, S., Meier, M., Merz, C. J., Popov, T., Puhlmann, L. M. C., Quintana, D. S., Schäfer, T., Schubert, A.-L., Sperl, M. F. J., Vehlen, A., Lonsdorf, T. B., Feld, G. B. (2023). Enhancing precision in human neuroscience. *eLife, 12*, e85980. https://doi.org/10.7554/eLife.85980

Nenning, K.-H., Xu, T., Franco, A. R., Swallow, K. M., Tambini, A., Margulies, D. S., Smallwood, J., Colcombe, S. J., & Milham, M. P. (2023). Omnipresence of the sensorimotor-association axis topography in the human connectome. *NeuroImage, 272*, 120059. https://doi.org/10.1016/j.neuroimage.2023.120059

Newman, M. E. J. (2012). Communities, modules and large-scale structure in networks. *Nature Physics, 8*(1), 25-31. https://doi.org/10.1038/nphys2162

Niendam, T. A., Laird, A. R., Ray, K. L., Dean, Y. M., Glahn, D. C., & Carter, C. S. (2012). Meta-analytic evidence for a superordinate cognitive control network subserving diverse executive functions. *Cognitive, Affective, & Behavioral Neuroscience, 12*(2), 241-268. https://doi.org/10.3758/s13415-011-0083-5

Pang, Z., Alamia, A., & VanRullen, R. (2020). Turning the stimulus on and off changes the direction of α traveling waves. *eNeuro, 7*(6), 1-11. https://doi.org/10.1523/ENEURO.0218-20.2020

Paquola, C., Vos De Wael, R., Wagstyl, K., Bethlehem, R. A. I., Hong, S.-J., Seidlitz, J., Bullmore, E. T., Evans, A. C., Misic, B., Margulies, D. S., Smallwood, J., Bernhardt, B. C. (2019). Microstructural and functional gradients are increasingly dissociated in transmodal cortices. *PLoS Biology, 17*(5), e3000284. https://doi.org/10.1371/journal.pbio.3000284

Park, B., Bethlehem, R. A., Paquola, C., Larivière, S., Rodrí-guez-Cruces, R., Vos de Wael, R., Bullmore, E. T., & Bernhardt, B. C. (2021). An expanding manifold in transmodal regions characterizes adolescent reconfiguration of structural connectome organization. *eLife, 10*, e64694. https://doi.org/10.7554/eLife.64694

Park, B.-Y., Vos de Vael, R., Paquola, C., Lariviére, S., Benkarim, O., Royer, J., Tavakol, S., Curces, R. R., Li, Q., Valk, S. L., Margulies, D. S., Mišić, B., Bzdok, D., Smallwood, J., & Bernhardt, B. C. (2021). Signal diffusion along connectome gradients and inter-hub routing differentially contribute to dynamic human brain function. *NeuroImage, 224*, 117429. https://doi.org/10.1016/j.neuroimag.2020.117429

Passamonti, L., Terraciano, A., Riccelli, R., Donzuso, G., Cerasa, A., Vaccaro, M. G., Novellino, F., Fera, F., & Quattrone, A. (2015). Increased functional connectivity within mesocortical networks in open people. *NeuroImage, 104,* 301-309. https://doi.org/10.1016/j.neuroimage.2014.09.017

Patil, A. U., Ghate, S., Madathil, D., Tzeng, O. J. L., Huang, H.-W., & Huang, C.-M. (2021). Static and dynamic functional connectivity supports the configuration of

brain networks associated with creative cognition. *Scientific Reports, 11*(1), 165. https://doi.org/10.1038/s41598-020-80293-2

Pool, E-M., Rehme, A. K., Eickhoff, S. B., Fink, G. R., & Grefkes, C. (2015). Functional resting-state connectivity of the human motor network: Differences between right- and left-handers. *NeuroImage, 109*, 298-306. https://doi.org/10.1016/j.neuroimage.2015.01.034

Porter, M. A., Onnela, J.-P., & Mucha, P. J. (2009). Communities in networks. *Notices of the AMS, 56*(9), 1082-1166. https://arxiv.org/abs/0902.3788

Power, J. D., Barnes, K. A., Snyder, A. Z., Schlaggar, B. L., & Petersen, S. E. (2012). Spurious but systematic correlations in functional connectivity MRI networks arise from subject motion. *NeuroImage, 59*(3), 2142-2154. https://doi.org/10.1016/j.neuroimage.2011.10.018

Power, J. D., Mitra, A., Laumann, T. O., Snyder, A. Z., Schlaggar, B. L., & Petersen, S. E. (2014). Methods to detect, characterize, and remove motion artifacts in resting state fMRI. *NeuroImage, 84*(Supplement C), 320-341. https://doi.org/10.1016/j.neuroimage.2013.08.048

Preti, M. G., Bolton, T. A. W., & Van De Ville, D. (2017). The dynamic functional connectome: State-of-the-art and perspectives. *NeuroImage, 160*, 41-54. https://doi.org/10.1016/j.neuroimage.2016.12.061

Priesemann, V., Wibral, M., Valderrama, M., Pröpper, R., Le Van Quyen, M., Geisel, T., Triesch, J., Nikolić, D., Munk, M. H. J. (2014). Spike avalanches in vivo suggest

a driven, slightly subcritical brain state. *Frontiers in Systems Neuroscience, 8*, 108. https://doi.org/10.3389/fnsys.2014.00108

Pruim, R. H. R., Mennes, M., van Rooij, D., Llera, A., Buitelaar, J. K., & Beckmann, C. F. (2015). ICA-AROMA: A robust ICA-based strategy for removing motion artifacts from fMRI data. *NeuroImage, 112*(Supplement C), 267-277. https://doi.org/10.1016/j.neuroimage.2015.02.064

Raichle, M. E., MacLeod, A. M., Snyder, A. Z., Powers, W. J., Gusnard, D. A., & Shulman, G. L. (2001). A default mode of brain function. *Proceedings of the National Academy of Sciences of the United States of America, 98,* 676-682. https://doi.org/10.1073/pnas.98.2.676

Reagh, Z. M., & Ranganath, C. (2023). Flexible reuse of cortico-hippocampal representations during encoding and recall of naturalistic events. *Nature Communications, 14*(1), 1-15. https://doi.org/10.1038/s41467-023-36805-5

Reardon, P. K., Seidlitz, J., Vandekar, S., Liu, S., Patel, R., Park, M. T. M., Alexander-Bloch, A., Clasen, L. S., Blumenthal, J. D., Lalonde, F. M., Giedd, J. N., Gur, R. C., Gur, R. E., Lurch, J. P., Chakravarty, M. M., Satterthwaite, T. D., Shinohara, R. T., & Raznahan, A. (2018). Normative brain size variation and brain shape diversity in humans. *Science, 360*(6394), 1222-1227. https://doi.org/10.1126/science.aar2578

Roberts, R. P., Wiebels, K., Sumner, R. L., van Mulukom, V., Grady, C. L., Schacter, D. L., & Addis, D. R. (2017). An fMRI investigation of the relationship between

future imagination and cognitive flexibility. *Neuropsychologia, 95*, 156-172. https://doi.org/10.1016/j.neuropsychologia.2016.11.019

Rosenberg, M. D., & Finn, E. S. (2022). How to establish robust brain-behavior relationships without thousands of individuals. *Nature Neuroscience, 25*, 835-837. https://doi.org/10.1038/s41593-022-01110-9

Rosseel, Y. (2012). Lavaan: An R package for structural equation modeling. *Journal of Statistical Software, 48*(2), 1-36. https://doi.org/10.18637/jss.v048.i02

Rubinov, M., & Sporns, O. (2010). Complex network measures of brain connectivity: Uses and interpretations. *NeuroImage, 52,* 1059-1069. https://doi.org/10.1016/j.neuroimage.2009.10.003

Rueter, A. R., Abram, S. V., MacDonald III, A. W., Rustichini, A., & DeYoung, C. G. (2019). The goal priority network as a neural substrate of Conscientiousness. *Human Brain Mapping, 39*(9), 3574-3585. https://doi.org/10.1002/hbm.24195

Rzucidlo, J. K., Roseman, P. L., Laurienti, P. J., & Dagenbach, D. (2013). Stability of whole brain and regional network topology within and between resting and cognitive states. *PloS ONE, 8*(8), e70275. https://doi.org/10.1371/journal.pone.0070275

Safron, A., & DeYoung, C. G. (2021). Integrating Cybernetic Big Five Theory with the free energy principle: A new strategy for modeling personalities as complex systems. In D. Wood, S. J. Read, P. D. Harms, & A. J. Slaughter (Eds.), *Measuring and Modeling Persons and Situations* (pp. 617-649). https://doi.org/10.1016/B978-0-12-819200-9.00010-7

Safron, A., Klimaj, V., & Hipólito, I. (2022). On the importance of being flexible: Dynamic brain networks and their potential significances. *Frontiers in Systems Neuroscience, 15*, 688424. https://doi.org/10.3389/fnsys.2021.688424

Salehi, M., Greene, A. S., Karbasi, A., Shen, X., Scheinost, D., & Constable, R. T. (2020). There is no single functional atlas even for a single individual: Functional parcel definitions change with task. *NeuroImage, 208,* 116366. https://doi.org/10.1016/j.neuroimage.2019.116366

Sandiego, C. M., Gallezot, J.-D., Lim, K., Ropchan, J., Lin, S.-F., Gao, H., Morris, E. D., & Cosgrove, K. P. (2015). Reference region modeling approaches for amphetamine challenge studies with [^{11}C]FLB 457 and PET. *Journal of Cerebral Blood Flow and Metabolism, 35*(4), 623-629. https://doi.org/10.1038/jcbfm.2014.237

Santarnecchi, E., Emmendorfer, A., & Pascual-Leone, A. (2017). Dissecting the parieto-frontal correlates of fluid intelligence: A comprehensive ALE meta-analysis study. *Intelligence, 63,* 9-28. https://doi.org/10.1016/j.intell.2017.04.008

Saucier, G. (1992). Openness versus intellect: Much ado about nothing? *European Journal of Personality, 6*(5), 381-386. https://doi.org/10.1002/per.2410060506

Sassenberg, T. A., Burton, P. C., Mwilambwe-Tshilobo, L., Jung, R. E., Rustichini, A., Spreng, R. N., & DeYoung, C. G. (2023). Conscientiousness associated with efficiency of the salience/ventral attention network: Replication in three samples using individualized parcellation. *NeuroImage, 272*, 120081. https://doi.org/10.1016/j.neuroimage.2023.120081

Schaefer, A., Kong, R., Gordon, E. M., Laumann, T. O., Zuo, X.-N., Holmes, A. J., Eickhoff, S. B., & Yeo, B. T. T. (2018). Local-global parcellation of the human cerebral cortex from intrinsic functional connectivity MRI. *Cerebral Cortex, 28*, 3095-3114. https://doi.org/10.1093/cercor/bhx179

Schwaba, T., Rhemtulla, M., Hopwood, C. J., & Bleidorn, W. (2020). A facet atlas: Visualizing networks that describe the blends, cores, and peripheries of personality structure. *PLoS ONE, 15*(7), e0236893. https://doi.org/10.1371/journal.pone.0236893

Seth, A. K. (2015). The cybernetic Bayesian brain – from interoceptive inference to sensorimotor contingencies. In T. Metzinger & J. M. Windt (Eds.) *Open MIND*. Frankfurt am Main: MIND Group. https://doi.org/10.15502/9783958570108

Setton, R., Mwilambwe-Tshilobo, L., Girn, M., Lockrow, A. W., Baracchini, G., Hughes, C., Lowe, A. J., Cassidy, B. N., Li, J., Luh, W., Bzdok, D., Leahy, R. M., Ge, T., Margulies, D. S., Misic, B., Bernhardt, B. C., Stevens, W. D., De Brigard, F., Kundu, P., Turner, G. R., & Spreng, R. N. (2022). Age differences in the functional architecture of the human brain. *Cerebral Cortex, bhac056,* 1-21. https://doi.org/10.1093/cercor/bhac056

Shao, X., Mckeown, B., Karapanagiotidis, T., Vos de Wael, R., Margulies, D. S., Bernhardt, B., Smallwood, J., Krieger-Redwood, K., & Jefferies, E. (2022). Individual differences in gradients of intrinsic connectivity within the semantic network relate to distinct aspects of semantic cognition. *Cortex, 150,* 48-60. https://doi.org/10.1016/j.cortex.2022.01.019

Sheldon, S., Fenerci, C., & Gurguryan, L. (2019). A neurocognitive perspective on the forms and functions of autobiographical memory retrieval. *Frontiers in Systems Neuroscience, 13*, 4. https://doi.org/10.3389/fnsys.2019.00004

Siegel, J. S., Mitra, A., Laumann, T. O., Seitzman, B. A., Raichle, M., Corbetta, M., & Snyder, A. Z. (2017). Data quality influences observed links between functional connectivity and behavior. *Cerebral Cortex, 27*(9), 4492-4502. https://doi.org/10.1093/cercor/bhw253

Silvia, P. J., & Kimbrel, N. A. (2010). A dimensional analysis of creativity and mental illness: Do anxiety and depression symptoms predict creative cognition, creative accomplishments, and creative self-concepts? *Psychology of Aesthetics, Creativity, and the Arts*, *4*, 2-10. https://doi.org/10.1037/a0016494

Silvia, P. J., Wigert, B., Reiter-Palmon, R., & Kaufman, J. C. (2012). Assessing creativity with self-report scales: A review and empirical evaluation. *Psychology of Aesthetics, Creativity, and the Arts, 6*, 19-34. https://doi.org/10.1037/a0024071

Sokunbi, M. O., Gradin, V. B., Waiter, G. D., Cameron, G. G., Ahearn, T. S., Murray, A. D., Steele, D. J., & Staff, R. T. (2014). Nonlinear complexity analysis of brain fMRI signals in schizophrenia. *PloS ONE, 9*(5), e95146. https://doi.org/10.1371/journal.pone.0095146

Spreng, R. N., & Andrews-Hanna, J. R. (2015). The default network and social cognition. *Brain Mapping: An Encyclopedic Reference, 3,* 165-169. https://doi.org/10.1016/8978-0-12-397025-1.00173-1

Spreng, R. N., Stevens, W. D., Chamberlain, J. P., Gilmore, A. W., Schacter, D. L. (2010). Default network activity, coupled with the frontoparietal control network, supports goal-directed cognition. *NeuroImage, 53*, 303-317. https://doi.org/10.1016/j.neuroimage.2010.06.016

Spisak, T., Bingel, U., & Wager, T. (2022). Replicable multivariate BWAS with moderate sample sizes. Online preprint: https://doi.org/10.1038/s41586-022-04492-9.

Smallwood, J., Bernhardt, B. C., Leech, R., Bzdok, D., Jefferies, E., & Margulies, D. S. (2021). The default mode network in cognition: A topographical perspective. *Nature Reviews Neuroscience, 22*(8), 503-513. https://doi.org/10.1038/s41583-021-00474-4

Smillie, L. D., Hayley, K. J., Hughes, D. M., Wacker, J., Cooper, A. J., & Pickering, A. D. (2019). Extraversion and reward-processing: Consolidating evidence from an electroencephalographic index of reward-prediction-error. *Biological Psychology, 146,* 107735. https://doi.org/10.1016/j.biopsycho.2019.107735

Smith, C. T., Crawford, J. L., Dang, L. C., Seaman, K. L., Danica San Juan, M., Vijay, A., Katz, D. T., Matuskey, D., Cowan, R. L., Morris, E. D., Zald, D. H., & Samanez-Larkin, G. R. (2019). Partial-volume correction increases estimated dopamine D2-like receptor binding potential and reduces adult age differences. *Journal of Cerebral Blood Flow and Metabolism, 39*(5), 822-833. https://doi.org/10.1177/0271678X17737693

Smith, S. M., Vidaurre, D., Beckmann, C. F., Glasser, M. F., Jenkinson, M., Miller, K. L., Nichols, T. E., Robinson, E. C., Salimi-Khorshidi, G., Woolrich, M. W., Barch, D. M., Uğurbil, K., & Van Essen, D. C. (2013). Functional connectomics from resting-state fMRI. *Trends in Cognitive Sciences, 17*(12), 666-682. https://doi.org/10.1016/j.tics.2013.09.016

Straub, K. T., & Kerns, J. G. (2021). Positive schizotypy, maladaptive openness, and openness facets. *Personality Disorders: Theory, Research, and Treatment, 12*(1), 51-58. https://doi.org/10.1037/per0000407

Sun, J., Liu, Z., Rolls, E. T., Chen, Q., Yao, Y., Yang, W., Wei, D., Zhang, Q., Zhang, J., Feng, J., & Qiu, J. (2019). Verbal creativity correlates with the temporal variability of brain networks during the resting state. *Cerebral Cortex, 29*(3), 1047-1058. https://doi.org/10.1093/cercor/bhy010

Tagliazucchi, E., Balenzuela, P., Fraiman, D., & Chialvo, D. R. (2012). Criticality in large-scale brain fMRI dynamics unveiled by a novel point process analysis. *Frontiers in Physiology, 3*(15), 1-12. https://doi.org/10.3389/fphys.2012.00015

Takeuchi, H., Taki, Y., Nouchi, R., Yokoyama, R., Kotozaki, Y., Nakagawa, S., Sekiguchi, A., Iizuka, K., Yamamoto, Y., Hanawa, S., Araki, T., Miyauchi, C. M., Shinada, T., Sakaki, K., Nozawa, T., Ikeda, S., Yokata, S., Daniele, M., Sassa, Y., & Kawashima, R. (2017). Regional homogeneity, resting-state functional connectivity and amplitude of low frequency fluctuation associated with creativity measured by divergent thinking in a sex-specific manner. *NeuroImage, 152,* 258-269. https://doi.org/10.1016/j.neuroimage.2017.02.079

Tarasi, L., Martelli, M. E., Bortoletto, M., di Pellegrino, G., & Romei, V. (2023). Neurla signatures of predictive strategies track individuals along the autism-schizophrenia continuum. *Schizophrenia Bulletin, 49*(5), 1294-1304. https://doi.org/10.1093/schbul/sbad105

Telesford, Q. K., Ashourvan, A., Wymbs, N. F., Grafton, S. T., Vettel, J. M., & Bassett, D. S. (2017). Cohesive network reconfiguration accompanies extended training. *Human Brain Mapping, 38*, 4744-4759. https://doi.org/10.1002/hbm.23699

Tustison, N. J., Avants, B. B., Cook, P. A., Zheng, Y., Egan, A., Yushkevich, P. A., & Gee, J. C. (2010). N4ITK: Improved N3 bias correction. *IEEE Transactions on Medical Imaging, 29*(6), 1310-1320. https://doi.org/10.1109/TMI.2010.2046908

Uddin, L. Q., Betzel, R. F., Cohen, J. R., Damoiseaux, J. S., De Brigard, F., Eickhoff, S. B., Fornito, A., Gratton, C., Gordon, E. M., Laird, A. R., Larson-Prior, L., McIntosh, A. R., Nickerson, L. D., Pessoa, L., Pinho, A. L., Poldrack, R. A., Razi, A., Sadaghiani, S., Shine, J. M., Yendiki, A., Yeo, B. T. T., & Spreng, R. N. (2023). Controversies and progress on standardization of large-scale brain network nomenclature. *Network Neuroscience, 7*(3), 864-905. https://doi.org/10.1162/netn_a_00323

Ugurbil, K., Xu, J., Auerbach, E. J., Moeller, S., Vu, A. T., Duarte-Carvajalino, J. M., Lenglet, C., Wu, X., Schmitter, S., Van de Moortele, P. F., Strupp, J., Sapiro, G., De Martino, F., Wang, D., Harel, N., Garwood, M., Chen, L., Feinberg, D. A., … Yacoub, E. (2013). Pushing spatial and temporal resolution for functional and

diffusion MRI in the Human Connectome Project. *NeuroImage, 80*, 80-104. https://doi.org/10.1016/j.neuroimage.2013.05.012

Van den Heuvel, M., & Sporns, O. (2011). Rich-club organization of the human connectome. *The Journal of Neuroscience, 31*(44), 15775-15786. https://doi.org/10.1523/JNEUROSCI.3539-11.2011

Van Dijk, K. R. A., Sabuncu, M. R., & Buckner, R. L. (2012). The influence of head motion on intrinsic functional connectivity MRI. *NeuroImage, 59*, 431-438. https://doi.org/10.1016/j.neuroimage.2011.07.044

Van Essen, D., C., Smith, S. M., Barch, D. M., Behrens, T. E. J., Yacoub, E., Ugurbil, K., & WU-Minn HCP Consortium. (2013). The WU-Minn human connectome project: An overview. *NeuroImage, 80,* 62-79. https://doi.org/10.1016/j.neuroimage.2013.05.041

Van Essen, D., Ugurbil, K., Auerbach, E., Barch, D., Behrens, T., Bucholz, R., Chang, A., Chen, L., Corbetta, M., Curtiss, S, Penna, D., Feinberg, D., Glasser, M. F., Harel, N., Heath, A. C., Larson-Prior, L., Marcus, D., Michalareas, G., Moeller, S., Oostenveld, R., … WU-Minn Consortium. (2012). The Human Connectome Project: A data acquisition perspective. *NeuroImage, 62*(4), 2222-2231. https://doi.org/10.1016/j.neuroimage.2012.02.018

Vidaurre, D., Smith, S. M., & Woolrich, M. W. (2017). Brain network dynamics are hierarchically organized in time. *Proceedings of the National Academy of Sciences of the United States of America, 114*(48), 12827-12832. https://doi.org/10.1073/pnas.1705120114

Vohryzek, J., Griffa, A., Mullier, E., Friedrichs-Maeder, C., Sandini, C., Schaer, M., Eliez, S., & Hagmann, P. (2020). Dynamic spatio-temporal patterns of brain connectivity reorganize across development. *Network Neuroscience, 4*(1), 115-133. https://doi.org/10.1162/netn_a_00111

Vos de Wael, R., Benkarim, O., Paquola, C., Lariviere, S., Royer, J., Tavakol, S., Xu, T., Hong, S.-J., Langs, G., Valk, S., Misic, B., Milham, M., Margulies, D., Smallwood, J., & Bernhardt, B. C. (2020). BrainSpace: A toolbox for the analysis of macroscale gradients in neuroimaging and connectomics datasets. *Communications Biology, 3*, 103. https://doi.org/10.1038/s43003-020-0794-7

Vossel, S., Geng, J. J., & Fink, G. R. (2014). Dorsal and ventral attention systems: Distinct neural circuits but collaborate roles. *The Neuroscientist, 20*(2), 150-159. https://doi.org/10.1177/1073858413494269

Wacker, J., Mueller, E. M., Hennig, J., & Stemmler, G. (2012). How to consistently link Extraversion and intelligence to the catechol-o-methyltransferase (COMT) gene: On defining and measuring psychological phenotypes in neurogenetic research. *Journal of Personality and Social Psychology, 102*, 427-444. https://doi.org/10.1037/a0026544

Wacker, J., & Smillie, L. D. (2015). Trait extraversion and dopamine function. *Social and Personality Psychology Compass, 9*(6), 225-238. https://doi.org/10.1111/spc3.12175

Wang, X., Zhuang, K., Li, Z., & Qiu, J. (2021). The functional connectivity basis of creative achievement linked with openness to experience and divergent thinking.

Biological Psychology, 168, 108260. https://doi.org/10.1016/j.biopsycho.2021.108260

Wechsler, D. (2008). *WAIS-IV administration and scoring manual.* Pearson.

Wechsler, D. (2011). *WASI-II: Wechsler abbreviated scale of intelligence.* PsychCorp.

Wertz, C. J., Chohan, M. O., Flores, R. A., & Jung, R. E. (2020). Neuroanatomy of creative achievement. *NeuroImage, 209*, 116487. https://doi.org/10.1016/j.neuroimage.2019.116487

Whitfield-Gabrieli, S., Thermenos, H. W., Milanovic, S., Tsuang, M. T., Faraone, S. V., McCarley, R. W., Shenton, M. E., Green, A. I., Nieto-Castanon, A., LaViolette, P., Wojcik, J., Gabrieli, J. D. E., & Seidman, L. J. (2008). Hyperactivity and hyperconnectivity of the default network in schizophrenia and in first-degree relatives of persons with schizophrenia. *Proceedings of the National Academy of Sciences of the United States of America, 106*(4), 1279-1284. https://doi.org/10.1073/pnas.0809141106

Wilson, S., Haroian, K., Iacono, W. G., Krueger, R. F., Lee, J. L., Luciana, M., Malone, S. M., McGue, M., Roisman, G. I., & Vrieze, S. (2019). Minnesota Center for Twin and Family Research. *Twin Research and Human Genetics, 22*(6), 746-752. https://doi.org/10.1017/thg.2019.107

Winkler, A. M., Ridgway, G. R., Webster, M. A., Smith, S. M., & Nichols, T. E. (2014). Permutation inference for the general linear model. *NeuroImage, 92,* 381-397. https://doi.org/10.1016/j.neuroimage.2014.01.060

Woodward, N. D., Rogers, B., & Heckers, S. (2011). Functional resting-state networks are differentially affected in schizophrenia. *Schizophrenia Research, 130*, 86-93. https://doi.org/10.1016/j.schres.2011.1.03.010

Xia, C. H., Ma, Z., Ciric, R., Gu, S., Betzel, R. F., Kaczkurkin, A. N., Calkins, M. E., Cook, P. A., García de la Garza, A., Vandekar, S. N., Cui, Z., Moore, T. M., Roalf, D. R., Ruparel, K., Wolf, D. H., Davatzikos, C., Gur, R. C., Gur, R. E., Shinohara, R. T., Bassett, D. S., & Satterthwaite, T. D. (2018). Linked dimensions of psychopathology and connectivity in functional brain networks. *Nature Communications, 9*, 3003. https://doi.org/10.1038/s41467-018-05317-y

Xu, L., Feng, J., & Yu, L. (2022). Avalanche criticality in individuals, fluid intelligence, and working memory. *Human Brain Mapping, 43,* 2534-2553. https://doi.org/10.1002/hbm.25802

Yeo, B. T. T., Krienen, F. M., Sepulcre, J., Sabuncu, M. R., Lashkari, D., Hollinshead, M., Roffman, J. L., Smoller, J. W., Zöllei, L., Polimeni, J. R., Fischl, B., Liu, H., & Buckner, R. L. (2011). The organization of the human cerebral cortex estimated by intrinsic functional connectivity. *Journal of Neurophysiology, 106*(3), 1125-1165. https://doi.org/10.1152/jn.00338.2011

Yin, W., Li, T., Hung, S.-C., Zhang, H., Wang, L., Shen, D., et al. (2020). The emergence of a functionally flexible brain during early infancy. *Proceedings of the National Academy of Sciences of the United States of America, 117*, 23904-23913. https://doi.org/10.1073/pnas.2002645117

Yörük, S., & Sen, S. (2023). A reliability generalization meta-analysis of the Creative Achievement Questionnaire. *Creativity Research Journal, 35*(4), 714-729. https://doi.org/10.1080/10400419.2022.2148073

Zalesky, A., & Breakspear, M. (2015). Towards a statistical test for functional connectivity dynamics. *NeuroImage, 114,* 466-470. https://doi.org/10.1016/j.neuroimag.2015.03.047

Zhang, Y., Brady, M., & Smith, S. (2001). Segmentation of brain MR images through a hidden markov random field model and expectation-maximization algorithm. *IEEE Transactions on Medical Imaging, 20*(1), 45-57. https://doi.org/10.1109/42.906424

Zhang, H., Meng, C., Di, X., Wu, X., & Biswal, B. (2023). Static and dynamic functional connectome reveals reconfiguration profiles of whole-brain network across cognitive states. *Network Neuroscience, 7*(3), 1034-1050. https://doi.org/10.1162/netn_a_00314

Zhang, Z., Telesford, Q. K., Giusti, C., Lim, K. O., Bassett, D. S., & Hayasaka, S. (2016). Choosing wavelet methods, filters, and lengths for functional brain network construction. *PLoS ONE, 11*(6), e0157243. https://doi.org/10.1371/journal.pone.0157243

Zhu, J., Li, Y., Fang, Q., Shen, Y., Qian, Y., Cai, H., & Yu, Y. (2021). Dynamic functional connectome predicts individual working memory performance across diagnostic categories. *NeuroImage: Clinical, 30,* 102593. https://doi.org/10.1016/j.nicl.2021.102593

Zhuang, K., Yang, W., Li, Y., Zhang, J., Chen, Q., Meng, J., Wei, D., Sun, J., He, L., Mao, Y., Wang, X., Vatansever, D., & Qiu, J. (2021). Connectome-based evidence for creative thinking as an emergent property of ordinary cognitive operations. *NeuroImage, 227*, 117632. https://doi.org/10.1016/j.neuroimage.2020.117632

Zingrone, N. L., Alvarado, C. S., & Agee, N. (2009). Psychological correlates of aura vision: Psychic experiences, dissociation, absorption, and synaesthesia-like experiences. *Australian Journal of Clinical & Experimental Hypnosis, 37*, 131-168.

Appendix

Table A1

Coefficients of models predicting intelligence, Openness/Intellect, and Plasticity from parcel flexibility

Parcel Index	Parcel Name	*g* cohesive, $\gamma = 1.1$	O/I overall, $\gamma = 1.2$	P overall, $\gamma = 1.2$
1	17Networks_LH_VisCent_ExStr_1	-0.15529	-0.01119	-0.12994
2	17Networks_LH_VisCent_ExStr_2	-0.21942		0.03100
3	17Networks_LH_VisCent_ExStr_3	-0.12247		0.02405
4	17Networks_LH_VisCent_ExStr_4	0.02647		0.02980
5	17Networks_LH_VisCent_ExStr_5	0.09985	0.05884	-0.07879
6	17Networks_LH_VisCent_ExStr_6	-0.06850		
7	17Networks_LH_VisCent_Striate_1	-0.10816		-0.01980
8	17Networks_LH_VisCent_ExStr_7	0.02972		-0.05151
9	17Networks_LH_VisCent_ExStr_8	0.26080		0.12406
10	17Networks_LH_VisCent_ExStr_9	0.19760		0.15918
11	17Networks_LH_VisCent_ExStr_10	0.12829	0.06472	-0.01698
12	17Networks_LH_VisCent_ExStr_11	0.00161		0.07046
13	17Networks_LH_VisPeri_ExStrInf_1	0.12239		0.00817
14	17Networks_LH_VisPeri_ExStrInf_2	0.11125		-0.03621
15	17Networks_LH_VisPeri_ExStrInf_3	-0.03709	-0.00734	
16	17Networks_LH_VisPeri_ExStrInf_4	-0.00005		-0.06416
17	17Networks_LH_VisPeri_ExStrInf_5	-0.20836	-0.02580	-0.24707
18	17Networks_LH_VisPeri_StriCal_1	-0.50069	0.02562	-0.00131
19	17Networks_LH_VisPeri_StriCal_2	0.11517		0.06445
20	17Networks_LH_VisPeri_ExStrSup_1	0.08498		0.02613
21	17Networks_LH_VisPeri_ExStrSup_2	0.12060	-0.06429	-0.07346
22	17Networks_LH_VisPeri_ExStrSup_3	-0.14037		0.09811
23	17Networks_LH_VisPeri_ExStrSup_4	0.16065		-0.01957
24	17Networks_LH_VisPeri_ExStrSup_5	0.04863		-0.00229
25	17Networks_LH_SomMotA_1	-0.09110		
26	17Networks_LH_SomMotA_2	0.08752		-0.00708
27	17Networks_LH_SomMotA_3	0.26537		
28	17Networks_LH_SomMotA_4	0.24930		-0.04822
29	17Networks_LH_SomMotA_5	0.03279		-0.06050
30	17Networks_LH_SomMotA_6	-0.02113	-0.09580	0.00995
31	17Networks_LH_SomMotA_7	0.08871		0.00517
32	17Networks_LH_SomMotA_8	0.13418		-0.04624
33	17Networks_LH_SomMotA_9	-0.04609	0.01330	-0.14636
34	17Networks_LH_SomMotA_10	0.06927		-0.06776
35	17Networks_LH_SomMotA_11	-0.17542	0.04897	-0.00453
36	17Networks_LH_SomMotA_12	0.21897	-0.05462	-0.10380
37	17Networks_LH_SomMotA_13	-0.04798	-0.04289	-0.03257
38	17Networks_LH_SomMotA_14	0.20171	-0.00516	-0.01158
39	17Networks_LH_SomMotA_15	-0.06959	-0.03353	-0.18015
40	17Networks_LH_SomMotA_16	0.26204	0.00450	-0.03857
41	17Networks_LH_SomMotA_17	0.01001		-0.00229
42	17Networks_LH_SomMotA_18	-0.15578		
43	17Networks_LH_SomMotA_19	0.15630	-0.05496	0.17749
44	17Networks_LH_SomMotB_Aud_1	-0.01306		-0.07154
45	17Networks_LH_SomMotB_Aud_2	0.01845	-0.00104	

46	17Networks_LH_SomMotB_Ins_1	0.12608	-0.00115	0.00745
47	17Networks_LH_SomMotB_S2_1	0.02124		-0.01542
48	17Networks_LH_SomMotB_S2_2	-0.03327		0.01043
49	17Networks_LH_SomMotB_Aud_3	-0.03603		-0.05234
50	17Networks_LH_SomMotB_Aud_4	0.38240	-0.01288	0.03577
51	17Networks_LH_SomMotB_S2_3	0.03664	-0.03896	-0.09547
52	17Networks_LH_SomMotB_S2_4	0.01167		0.08888
53	17Networks_LH_SomMotB_S2_5	-0.33093	0.00209	0.01738
54	17Networks_LH_SomMotB_S2_6	0.08933		0.01627
55	17Networks_LH_SomMotB_Cent_1	0.01518		0.07855
56	17Networks_LH_SomMotB_Cent_2	-0.03123		-0.02606
57	17Networks_LH_SomMotB_Cent_3	0.11671		0.06704
58	17Networks_LH_SomMotB_Cent_4	0.01470		-0.11432
59	17Networks_LH_SomMotB_Cent_5	0.00210		0.05691
60	17Networks_LH_DorsAttnA_TempOcc_1	-0.07137	0.06158	0.10386
61	17Networks_LH_DorsAttnA_TempOcc_2	-0.10595		-0.06974
62	17Networks_LH_DorsAttnA_TempOcc_3	-0.17231	-0.06055	-0.05897
63	17Networks_LH_DorsAttnA_TempOcc_4	0.13328		0.02097
64	17Networks_LH_DorsAttnA_ParOcc_1	0.15664		-0.22432
65	17Networks_LH_DorsAttnA_ParOcc_2	0.04685	0.03663	0.01365
66	17Networks_LH_DorsAttnA_SPL_1	-0.08221		-0.04804
67	17Networks_LH_DorsAttnA_SPL_2	0.18832		0.01082
68	17Networks_LH_DorsAttnA_SPL_3	0.07061		0.00810
69	17Networks_LH_DorsAttnA_SPL_4	0.16960		
70	17Networks_LH_DorsAttnA_SPL_5	-0.08248		0.06597
71	17Networks_LH_DorsAttnA_SPL_6	0.06950		0.13080
72	17Networks_LH_DorsAttnA_SPL_7	-0.28779		-0.10451
73	17Networks_LH_DorsAttnB_PostC_1	-0.01854		0.11657
74	17Networks_LH_DorsAttnB_PostC_2	-0.32680	-0.02415	-0.04770
75	17Networks_LH_DorsAttnB_PostC_3	-0.25563	-0.00149	
76	17Networks_LH_DorsAttnB_PostC_4	-0.07910	-0.04607	-0.00626
77	17Networks_LH_DorsAttnB_PostC_5	-0.16155		-0.04601
78	17Networks_LH_DorsAttnB_PostC_6	-0.00168	0.08044	0.08003
79	17Networks_LH_DorsAttnB_PostC_7	0.08948	0.00793	0.05929
80	17Networks_LH_DorsAttnB_PostC_8	-0.08841		0.06682
81	17Networks_LH_DorsAttnB_PostC_9	-0.02954	0.00084	-0.00576
82	17Networks_LH_DorsAttnB_FEF_1	0.06078	-0.06270	0.03306
83	17Networks_LH_DorsAttnB_FEF_2	-0.13476	-0.01159	0.06698
84	17Networks_LH_DorsAttnB_FEF_3	0.07529	0.00043	0.13523
85	17Networks_LH_DorsAttnB_PrCv_1	0.14631		0.01739
86	17Networks_LH_SalVentAttnA_ParOper_1	-0.18644		-0.00001
87	17Networks_LH_SalVentAttnA_ParOper_2	-0.06271		-0.06150
88	17Networks_LH_SalVentAttnA_ParOper_3	0.07441		-0.08637
89	17Networks_LH_SalVentAttnA_Ins_1	0.18995		0.03568
90	17Networks_LH_SalVentAttnA_Ins_2	-0.12333		-0.03216
91	17Networks_LH_SalVentAttnA_Ins_3	0.09112		0.05134

92	17Networks_LH_SalVentAttnA_Ins_4	0.17122		0.01512
93	17Networks_LH_SalVentAttnA_FrOper_1	0.01544		-0.07562
94	17Networks_LH_SalVentAttnA_FrOper_2	-0.06182		0.07080
95	17Networks_LH_SalVentAttnA_ParMed_1	-0.13797		0.03043
96	17Networks_LH_SalVentAttnA_ParMed_2	-0.05605	0.06478	-0.06406
97	17Networks_LH_SalVentAttnA_ParMed_3	0.01660		-0.02033
98	17Networks_LH_SalVentAttnA_FrMed_1	-0.12318		0.00055
99	17Networks_LH_SalVentAttnA_FrMed_2	0.12229	-0.02144	0.08080
100	17Networks_LH_SalVentAttnA_FrMed_3	-0.06912		-0.11813
101	17Networks_LH_SalVentAttnB_PFCl_1	-0.15935		0.08145
102	17Networks_LH_SalVentAttnB_PFCl_2	0.07124		
103	17Networks_LH_SalVentAttnB_PFCl_3	0.10365		-0.04037
104	17Networks_LH_SalVentAttnB_Ins_1	-0.03415		0.17159
105	17Networks_LH_SalVentAttnB_Ins_2	-0.16721		-0.06436
106	17Networks_LH_SalVentAttnB_Ins_3	-0.28048	0.01077	
107	17Networks_LH_SalVentAttnB_OFC_1	0.11958		
108	17Networks_LH_SalVentAttnB_PFCmp_1	-0.11090	-0.01210	-0.07327
109	17Networks_LH_LimbicB_OFC_1	0.01421		-0.00112
110	17Networks_LH_LimbicB_OFC_2	-0.07971	-0.00671	0.13669
111	17Networks_LH_LimbicB_OFC_3	-0.05837		
112	17Networks_LH_LimbicB_OFC_4	0.05360		0.10909
113	17Networks_LH_LimbicB_OFC_5	0.30033		-0.02301
114	17Networks_LH_LimbicA_TempPole_1	-0.15246	0.01106	0.05242
115	17Networks_LH_LimbicA_TempPole_2	-0.21812	-0.01962	-0.19257
116	17Networks_LH_LimbicA_TempPole_3	-0.07289		0.01062
117	17Networks_LH_LimbicA_TempPole_4	-0.04966	0.00317	-0.09300
118	17Networks_LH_LimbicA_TempPole_5	0.05048		0.02005
119	17Networks_LH_LimbicA_TempPole_6	-0.06302		-0.03550
120	17Networks_LH_LimbicA_TempPole_7	-0.04997		-0.08310
121	17Networks_LH_ContA_Temp_1	-0.17284	-0.07766	
122	17Networks_LH_ContA_IPS_1	-0.12141	-0.00087	0.02950
123	17Networks_LH_ContA_IPS_2	0.05768		0.06682
124	17Networks_LH_ContA_IPS_3	0.01242		0.07839
125	17Networks_LH_ContA_IPS_4	0.04700	0.02252	0.04524
126	17Networks_LH_ContA_IPS_5	0.16710		0.09136
127	17Networks_LH_ContA_PFCd_1	-0.16937		0.03044
128	17Networks_LH_ContA_PFClv_1	0.09136	0.02649	0.17000
129	17Networks_LH_ContA_PFClv_2	0.05377		
130	17Networks_LH_ContA_PFCl_1	0.24423	0.01293	-0.01619
131	17Networks_LH_ContA_PFCl_2	-0.13257		-0.08213
132	17Networks_LH_ContA_PFCl_3	0.20070		-0.11128
133	17Networks_LH_ContA_Cingm_1	-0.01154		
134	17Networks_LH_ContB_Temp_1	0.03550		0.02440
135	17Networks_LH_ContB_Temp_2	0.14464	-0.02137	0.10383
136	17Networks_LH_ContB_IPL_1	0.07519		0.05488
137	17Networks_LH_ContB_IPL_2	-0.09274		0.07490

138	17Networks_LH_ContB_IPL_3	0.04686		-0.03828
139	17Networks_LH_ContB_PFCd_1	-0.17899	-0.02177	
140	17Networks_LH_ContB_PFClv_1	0.05698	-0.00605	-0.06580
141	17Networks_LH_ContB_PFClv_2	0.09878		
142	17Networks_LH_ContB_PFClv_3	-0.08967	-0.01069	-0.00994
143	17Networks_LH_ContB_PFCmp_1	0.21021		0.06521
144	17Networks_LH_ContC_pCun_1	0.07763		0.09958
145	17Networks_LH_ContC_pCun_2	-0.03268		0.04372
146	17Networks_LH_ContC_pCun_3	-0.06835		0.01076
147	17Networks_LH_ContC_Cingp_1	0.16060		-0.03829
148	17Networks_LH_ContC_Cingp_2	-0.04416		0.00881
149	17Networks_LH_DefaultA_IPL_1	0.01196		0.18167
150	17Networks_LH_DefaultA_IPL_2	0.16212		-0.04959
151	17Networks_LH_DefaultA_PFCd_1	-0.02602		-0.01692
152	17Networks_LH_DefaultA_PFCd_2	0.11103		-0.03874
153	17Networks_LH_DefaultA_PFCd_3	0.08015		
154	17Networks_LH_DefaultA_pCunPCC_1	0.11065		0.04521
155	17Networks_LH_DefaultA_pCunPCC_2	-0.18081		0.09063
156	17Networks_LH_DefaultA_pCunPCC_3	0.16253		-0.01386
157	17Networks_LH_DefaultA_pCunPCC_4	0.13064		-0.00067
158	17Networks_LH_DefaultA_pCunPCC_5	0.01931	0.04148	0.07343
159	17Networks_LH_DefaultA_pCunPCC_6	0.05691		-0.00295
160	17Networks_LH_DefaultA_pCunPCC_7	-0.10598	-0.07816	0.02416
161	17Networks_LH_DefaultA_PFCm_1	-0.25485		
162	17Networks_LH_DefaultA_PFCm_2	-0.06410		-0.04995
163	17Networks_LH_DefaultA_PFCm_3	0.03176		-0.02900
164	17Networks_LH_DefaultA_PFCm_4	0.01516	0.05189	0.06485
165	17Networks_LH_DefaultA_PFCm_5	-0.05586	-0.01603	-0.02748
166	17Networks_LH_DefaultA_PFCm_6	0.04784	-0.02237	-0.09761
167	17Networks_LH_DefaultB_Temp_1	0.03204	0.04124	0.05702
168	17Networks_LH_DefaultB_Temp_2	0.07046	-0.00050	0.06194
169	17Networks_LH_DefaultB_Temp_3	-0.22292	-0.05148	0.03192
170	17Networks_LH_DefaultB_Temp_4	0.06252		
171	17Networks_LH_DefaultB_Temp_5	0.00117		-0.13981
172	17Networks_LH_DefaultB_Temp_6	0.02780	0.02411	-0.01173
173	17Networks_LH_DefaultB_IPL_1	-0.05205	0.00174	-0.03888
174	17Networks_LH_DefaultB_IPL_2	0.05609		
175	17Networks_LH_DefaultB_PFCd_1	-0.00374		-0.08947
176	17Networks_LH_DefaultB_PFCd_2	0.11835	0.08064	
177	17Networks_LH_DefaultB_PFCd_3	0.17294		0.02487
178	17Networks_LH_DefaultB_PFCd_4	-0.11619		0.04384
179	17Networks_LH_DefaultB_PFCd_5	-0.11412		
180	17Networks_LH_DefaultB_PFCd_6	0.00074	-0.00022	-0.02718
181	17Networks_LH_DefaultB_PFCl_1	-0.23930	-0.01095	
182	17Networks_LH_DefaultB_PFCl_2	-0.16810		0.03850
183	17Networks_LH_DefaultB_PFCv_1	0.02845	-0.08651	-0.03548

184	17Networks_LH_DefaultB_PFCv_2	0.01646		-0.00518
185	17Networks_LH_DefaultB_PFCv_3	0.14896	-0.01760	-0.11692
186	17Networks_LH_DefaultB_PFCv_4	0.05332		-0.05271
187	17Networks_LH_DefaultB_PFCv_5	-0.01386		-0.07040
188	17Networks_LH_DefaultC_IPL_1	-0.04294	0.02875	-0.08570
189	17Networks_LH_DefaultC_Rsp_1	-0.08430		0.05226
190	17Networks_LH_DefaultC_Rsp_2	-0.10094	0.00614	-0.16617
191	17Networks_LH_DefaultC_Rsp_3	-0.05227		0.05360
192	17Networks_LH_DefaultC_PHC_1	0.18875		0.02517
193	17Networks_LH_DefaultC_PHC_2	0.20811		0.03007
194	17Networks_LH_DefaultC_PHC_3	0.21761		0.07916
195	17Networks_LH_TempPar_1	0.01112		0.14225
196	17Networks_LH_TempPar_2	-0.11011		0.02259
197	17Networks_LH_TempPar_3	-0.00882	0.02735	-0.02950
198	17Networks_LH_TempPar_4	0.03090	0.05518	
199	17Networks_LH_TempPar_5	-0.06438		-0.02339
200	17Networks_LH_TempPar_6	0.01693		-0.20191
201	17Networks_RH_VisCent_ExStr_1	0.10717	0.04176	-0.04681
202	17Networks_RH_VisCent_ExStr_2	0.10018		0.05905
203	17Networks_RH_VisCent_ExStr_3	-0.24736		0.03925
204	17Networks_RH_VisCent_ExStr_4	0.33450		-0.02110
205	17Networks_RH_VisCent_ExStr_5	0.28975		-0.11073
206	17Networks_RH_VisCent_ExStr_6	-0.10868	-0.00580	0.04934
207	17Networks_RH_VisCent_Striate_1	-0.04224		-0.07257
208	17Networks_RH_VisCent_ExStr_7	-0.24883		
209	17Networks_RH_VisCent_ExStr_8	-0.08897	-0.07673	-0.00332
210	17Networks_RH_VisCent_ExStr_9	-0.06096		-0.02854
211	17Networks_RH_VisCent_ExStr_10	-0.02312	0.11683	-0.13146
212	17Networks_RH_VisCent_ExStr_11	-0.15465		0.05545
213	17Networks_RH_VisPeri_ExStrInf_1	0.13282	-0.00437	-0.05660
214	17Networks_RH_VisPeri_ExStrInf_2	0.22730		-0.03172
215	17Networks_RH_VisPeri_ExStrInf_3	-0.05233		0.04193
216	17Networks_RH_VisPeri_ExStrInf_4	0.10387		-0.00512
217	17Networks_RH_VisPeri_ExStrInf_5	0.02189	-0.04050	0.01095
218	17Networks_RH_VisPeri_StriCal_1	0.07147		0.06429
219	17Networks_RH_VisPeri_StriCal_2	-0.16691	-0.03469	-0.11210
220	17Networks_RH_VisPeri_ExStrSup_1	-0.22468		0.05100
221	17Networks_RH_VisPeri_ExStrSup_2	0.16073		0.08623
222	17Networks_RH_VisPeri_ExStrSup_3	0.01431		-0.07421
223	17Networks_RH_VisPeri_ExStrSup_4	-0.01447		
224	17Networks_RH_SomMotA_1	-0.07014		0.04082
225	17Networks_RH_SomMotA_2	-0.25650		-0.00473
226	17Networks_RH_SomMotA_3	0.09950		-0.01671
227	17Networks_RH_SomMotA_4	-0.08411		0.08040
228	17Networks_RH_SomMotA_5	0.08693		0.02909
229	17Networks_RH_SomMotA_6	-0.17726	0.00436	0.17158

230	17Networks_RH_SomMotA_7	0.00012		-0.00350
231	17Networks_RH_SomMotA_8	-0.22486	-0.01301	-0.03174
232	17Networks_RH_SomMotA_9	-0.10767		
233	17Networks_RH_SomMotA_10	0.20588	0.01981	
234	17Networks_RH_SomMotA_11	0.12673		-0.07255
235	17Networks_RH_SomMotA_12	0.09434		0.02071
236	17Networks_RH_SomMotA_13	-0.11915	-0.04628	-0.06243
237	17Networks_RH_SomMotA_14	-0.14472		0.09551
238	17Networks_RH_SomMotA_15	0.12969		-0.05271
239	17Networks_RH_SomMotA_16	0.16914	0.08612	
240	17Networks_RH_SomMotA_17	-0.02780	0.04763	0.00960
241	17Networks_RH_SomMotA_18	0.08506	0.01399	0.00569
242	17Networks_RH_SomMotA_19	-0.09870	0.01884	-0.06431
243	17Networks_RH_SomMotA_20	-0.20774	-0.00164	0.03163
244	17Networks_RH_SomMotB_Aud_1	0.10818	-0.00080	-0.01402
245	17Networks_RH_SomMotB_Aud_2	-0.18720	-0.00322	0.03077
246	17Networks_RH_SomMotB_Ins_1	0.11566		-0.12703
247	17Networks_RH_SomMotB_S2_1	-0.09934		0.16468
248	17Networks_RH_SomMotB_S2_2	-0.01207	0.01049	0.08711
249	17Networks_RH_SomMotB_Aud_3	0.06088	-0.01133	
250	17Networks_RH_SomMotB_S2_3	0.12528		-0.00156
251	17Networks_RH_SomMotB_S2_4	-0.05341		0.12646
252	17Networks_RH_SomMotB_S2_5	-0.13523		0.08156
253	17Networks_RH_SomMotB_S2_6	0.09839	0.01209	-0.01712
254	17Networks_RH_SomMotB_S2_7	-0.05174		-0.04113
255	17Networks_RH_SomMotB_S2_8	-0.10825	0.03352	-0.01277
256	17Networks_RH_SomMotB_Cent_1	0.04756	0.00213	0.08769
257	17Networks_RH_SomMotB_Cent_2	0.07541		-0.02630
258	17Networks_RH_SomMotB_Cent_3	-0.04448		-0.11144
259	17Networks_RH_DorsAttnA_TempOcc_1	0.01101		-0.16583
260	17Networks_RH_DorsAttnA_TempOcc_2	-0.01817		-0.00630
261	17Networks_RH_DorsAttnA_TempOcc_3	-0.12782	0.00192	0.09124
262	17Networks_RH_DorsAttnA_ParOcc_1	0.12400		-0.04986
263	17Networks_RH_DorsAttnA_ParOcc_2	0.15310		-0.09187
264	17Networks_RH_DorsAttnA_ParOcc_3	0.05177		
265	17Networks_RH_DorsAttnA_SPL_1	-0.02777		-0.13680
266	17Networks_RH_DorsAttnA_SPL_2	-0.08224		-0.05638
267	17Networks_RH_DorsAttnA_SPL_3	-0.02828		-0.11869
268	17Networks_RH_DorsAttnA_SPL_4	0.13398		
269	17Networks_RH_DorsAttnA_SPL_5	0.02549	-0.02383	-0.01961
270	17Networks_RH_DorsAttnA_SPL_6	-0.22298	0.03122	0.05697
271	17Networks_RH_DorsAttnA_SPL_7	0.33253		-0.01419
272	17Networks_RH_DorsAttnA_SPL_8	-0.01294	-0.03975	-0.07331
273	17Networks_RH_DorsAttnB_TempOcc_1	0.12802		0.05035
274	17Networks_RH_DorsAttnB_PostC_1	0.13755		-0.11033
275	17Networks_RH_DorsAttnB_PostC_2	0.09828	-0.02113	

276	17Networks_RH_DorsAttnB_PostC_3	-0.14670		0.03026
277	17Networks_RH_DorsAttnB_PostC_4	-0.14977		0.03260
278	17Networks_RH_DorsAttnB_PostC_5	0.15341	-0.01497	
279	17Networks_RH_DorsAttnB_PostC_6	0.16502	-0.03583	0.06801
280	17Networks_RH_DorsAttnB_PostC_7	0.17001		-0.07958
281	17Networks_RH_DorsAttnB_PostC_8	-0.04518	-0.00064	0.04612
282	17Networks_RH_DorsAttnB_FEF_1	-0.19569	0.05374	-0.04736
283	17Networks_RH_DorsAttnB_FEF_2	0.10601		-0.06851
284	17Networks_RH_DorsAttnB_FEF_3	-0.21820		
285	17Networks_RH_SalVentAttnA_ParOper_1	0.16642		0.07306
286	17Networks_RH_SalVentAttnA_ParOper_2	-0.20680		
287	17Networks_RH_SalVentAttnA_ParOper_3	0.08021	-0.00418	-0.01175
288	17Networks_RH_SalVentAttnA_PrC_1	0.02942	-0.00096	0.07741
289	17Networks_RH_SalVentAttnA_Ins_1	0.02506	0.06136	0.05218
290	17Networks_RH_SalVentAttnA_Ins_2	-0.03457	-0.02093	0.17589
291	17Networks_RH_SalVentAttnA_Ins_3	-0.02310		-0.01250
292	17Networks_RH_SalVentAttnA_Ins_4	-0.09125		0.06318
293	17Networks_RH_SalVentAttnA_FrOper_1	-0.16513	-0.08622	-0.04020
294	17Networks_RH_SalVentAttnA_FrOper_2	0.09800		0.00029
295	17Networks_RH_SalVentAttnA_FrOper_3	-0.07319		0.06364
296	17Networks_RH_SalVentAttnA_FrMed_1	0.04620		0.09509
297	17Networks_RH_SalVentAttnA_ParMed_1	-0.20129		0.19743
298	17Networks_RH_SalVentAttnA_ParMed_2	0.09599	0.02455	0.02499
299	17Networks_RH_SalVentAttnA_FrMed_2	0.17576		-0.00920
300	17Networks_RH_SalVentAttnA_ParMed_3	-0.01725		-0.02645
301	17Networks_RH_SalVentAttnA_ParMed_4	0.04950	-0.00500	0.08442
302	17Networks_RH_SalVentAttnA_FrMed_3	-0.20115		
303	17Networks_RH_SalVentAttnA_FrMed_4	0.00957		0.03410
304	17Networks_RH_SalVentAttnB_IPL_1	0.18952		0.06841
305	17Networks_RH_SalVentAttnB_PFClv_1	-0.09144		-0.08051
306	17Networks_RH_SalVentAttnB_PFCl_1	0.18347	0.00166	0.11287
307	17Networks_RH_SalVentAttnB_PFCl_2	0.12304	-0.02424	0.03984
308	17Networks_RH_SalVentAttnB_PFCl_3	-0.10955	0.00021	0.10134
309	17Networks_RH_SalVentAttnB_Ins_1	-0.19957		0.03468
310	17Networks_RH_SalVentAttnB_Ins_2	0.07973		
311	17Networks_RH_SalVentAttnB_PFCmp_1	-0.02488		0.01417
312	17Networks_RH_SalVentAttnB_PFCmp_2	0.09145	0.00439	-0.07014
313	17Networks_RH_LimbicB_OFC_1	-0.05257		-0.02130
314	17Networks_RH_LimbicB_OFC_2	-0.05506		
315	17Networks_RH_LimbicB_OFC_3	0.11342		0.04210
316	17Networks_RH_LimbicB_OFC_4	-0.02926		0.10066
317	17Networks_RH_LimbicB_OFC_5	-0.00851		0.10770
318	17Networks_RH_LimbicB_OFC_6	0.25541		0.06031
319	17Networks_RH_LimbicA_TempPole_1	-0.07884		-0.02836
320	17Networks_RH_LimbicA_TempPole_2	0.05084		-0.07772
321	17Networks_RH_LimbicA_TempPole_3	-0.04927		0.01505

322	17Networks_RH_LimbicA_TempPole_4	0.17030		-0.04294
323	17Networks_RH_LimbicA_TempPole_5	-0.06986		-0.12919
324	17Networks_RH_LimbicA_TempPole_6	0.26075	-0.02753	-0.00164
325	17Networks_RH_ContA_IPS_1	-0.19243	-0.01702	
326	17Networks_RH_ContA_IPS_2	-0.04278		-0.19404
327	17Networks_RH_ContA_IPS_3	-0.02591		0.04209
328	17Networks_RH_ContA_IPS_4	0.00555	0.00303	-0.08365
329	17Networks_RH_ContA_PFCd_1	-0.11759	-0.05397	-0.18499
330	17Networks_RH_ContA_PFCl_1	0.02583		-0.06633
331	17Networks_RH_ContA_PFCl_2	-0.23080		0.01906
332	17Networks_RH_ContA_PFCl_3	0.15391		-0.00833
333	17Networks_RH_ContA_PFCl_4	-0.02352	-0.00047	-0.08266
334	17Networks_RH_ContA_PFCl_5	0.03232	0.03757	
335	17Networks_RH_ContA_Cingm_1	0.00166		0.06280
336	17Networks_RH_ContB_Temp_1	0.02275		
337	17Networks_RH_ContB_Temp_2	-0.12565		
338	17Networks_RH_ContB_IPL_1	-0.06590		0.03129
339	17Networks_RH_ContB_IPL_2	-0.08129	-0.04203	0.00344
340	17Networks_RH_ContB_IPL_3	-0.09822		-0.04158
341	17Networks_RH_ContB_IPL_4	-0.02176		-0.11478
342	17Networks_RH_ContB_PFCld_1	-0.20433		0.04853
343	17Networks_RH_ContB_PFCld_2	-0.04910		0.05554
344	17Networks_RH_ContB_PFCld_3	-0.15946	0.05108	-0.13917
345	17Networks_RH_ContB_PFCld_4	-0.10286	-0.03312	0.01314
346	17Networks_RH_ContB_PFClv_1	0.02379	0.03570	0.10401
347	17Networks_RH_ContB_PFClv_2	-0.16687	-0.07158	
348	17Networks_RH_ContB_PFClv_3	-0.01536	0.04327	0.13266
349	17Networks_RH_ContB_PFClv_4	0.24574		0.02212
350	17Networks_RH_ContB_PFCmp_1	0.09696		-0.08224
351	17Networks_RH_ContC_pCun_1	-0.11390	0.05449	
352	17Networks_RH_ContC_pCun_2	0.07589		-0.07933
353	17Networks_RH_ContC_pCun_3	-0.17943		0.04361
354	17Networks_RH_ContC_pCun_4	0.03431		
355	17Networks_RH_ContC_pCun_5	-0.28442		0.00013
356	17Networks_RH_ContC_Cingp_1	-0.04977		0.02538
357	17Networks_RH_ContC_Cingp_2	-0.23534		
358	17Networks_RH_DefaultA_Temp_1	-0.00651		-0.07641
359	17Networks_RH_DefaultA_IPL_1	0.01496	0.00458	0.03536
360	17Networks_RH_DefaultA_IPL_2	0.14523	-0.04729	-0.06277
361	17Networks_RH_DefaultA_PFCd_1	-0.07140	0.02273	-0.01670
362	17Networks_RH_DefaultA_PFCd_2	0.03732		-0.04482
363	17Networks_RH_DefaultA_pCunPCC_1	-0.01170		-0.06381
364	17Networks_RH_DefaultA_pCunPCC_2	-0.06036		0.10447
365	17Networks_RH_DefaultA_pCunPCC_3	-0.01696	-0.01374	0.03037
366	17Networks_RH_DefaultA_pCunPCC_4	-0.04454	0.03758	-0.08932
367	17Networks_RH_DefaultA_pCunPCC_5	0.19967		-0.06755

368	17Networks_RH_DefaultA_PFCm_1	-0.02114		0.00566
369	17Networks_RH_DefaultA_PFCm_2	0.10972		-0.06574
370	17Networks_RH_DefaultA_PFCm_3	-0.15875	-0.00434	-0.06200
371	17Networks_RH_DefaultA_PFCm_4	-0.09596		0.13014
372	17Networks_RH_DefaultA_PFCm_5	-0.02026		-0.02547
373	17Networks_RH_DefaultA_PFCm_6	-0.18837		0.02290
374	17Networks_RH_DefaultB_Temp_1	-0.03037		-0.09426
375	17Networks_RH_DefaultB_Temp_2	0.20746		0.06884
376	17Networks_RH_DefaultB_AntTemp_1	0.06668		-0.09555
377	17Networks_RH_DefaultB_PFCd_1	0.09940	0.00814	-0.07228
378	17Networks_RH_DefaultB_PFCd_2	0.22675		0.02884
379	17Networks_RH_DefaultB_PFCd_3	-0.03418		-0.05879
380	17Networks_RH_DefaultB_PFCd_4	0.04521	0.02414	0.11602
381	17Networks_RH_DefaultB_PFCd_5	-0.04842		0.10466
382	17Networks_RH_DefaultB_PFCv_1	-0.06587		-0.05317
383	17Networks_RH_DefaultB_PFCv_2	0.04563	0.01949	
384	17Networks_RH_DefaultB_PFCv_3	0.10712		-0.00143
385	17Networks_RH_DefaultC_IPL_1	-0.10683		0.03512
386	17Networks_RH_DefaultC_IPL_2	-0.16704		
387	17Networks_RH_DefaultC_Rsp_1	0.23760		-0.18553
388	17Networks_RH_DefaultC_Rsp_2	0.16865		0.11538
389	17Networks_RH_DefaultC_PHC_1	-0.00024		0.00096
390	17Networks_RH_DefaultC_PHC_2	0.02677		-0.02273
391	17Networks_RH_TempPar_1	0.13487		0.00436
392	17Networks_RH_TempPar_2	-0.07804		0.15691
393	17Networks_RH_TempPar_3	0.13622		0.03492
394	17Networks_RH_TempPar_4	-0.10941		-0.09649
395	17Networks_RH_TempPar_5	0.10326		0.00420
396	17Networks_RH_TempPar_6	0.02397		0.15102
397	17Networks_RH_TempPar_7	-0.21588		0.03220
398	17Networks_RH_TempPar_8	-0.10373		0.00093
399	17Networks_RH_TempPar_9	0.07788		-0.03894
400	17Networks_RH_TempPar_10	0.13032	-0.01032	-0.08560

Note. VisCent = central visual, VisPeri = peripheral visual, SomMot = somatomotor, DorsAttn = dorsal attention, SalVentAttn = salience/ventral attention, Cont = frontoparietal control, TempPar = temporoparietal. *g* = general intelligence. O/I = Openness/Intellect, P = Psychoticism

Table A2

Performance metrics of models using flexibility of all parcels as predictors in the γ = 1 partition

	Type			Training Sample			Test Sample		
		α	λ	RMSE	MAE	R^2	RMSE	MAE	R^2
O/I	Overall	0.1	.00903	1.87	1.48	.040	1.84	1.45	.001
	Cohesive	1	.11012	1.01	.79	.032	.99	.80	.000
	Disjoint	0.8	.15751	.99	.78	.066	1.00	.80	.000
g	Overall	0.3	.00006	3.12	2.45	.023	2.40	1.91	.003
	Cohesive	1	.05186	1.05	.83	.025	1.03	.84	.001
	Disjoint	0.9	.05799	1.02	.80	.020	1.02	.83	.001

Note. g = general intelligence. O/I = Openness/Intellect. α = mixing parameter, λ = penalty parameter, RMSE = root-mean-square error. MAE = mean absolute error

Predicting Plasticity from Parcel Flexibility

Metatrait Plasticity scores were computed by averaging participants' Extraversion and Openness/Intellect scores. Scores of the metatrait Stability were also computed by averaging Conscientiousness, Agreeableness, and the inverse of Neuroticism scores to be included as a covariate. We repeated the procedure described in the main text predicting Plasticity scores from each of the flexibility measures. These models included age, gender, mean relative RMS movement, handedness, total brain volume, the type of image reconstruction algorithm, *g,* and metatrait Stability scores as covariates. Stability was included as a covariate to account for the influence of evaluative consistency bias (Feeley 2002; Anusic et al. 2009). Results from these tests are described in Table A3.

Table A3

Performance metrics of models predicting metatrait Plasticity from parcel flexibility

Community	Type			Training Sample			Test Sample		
		α	λ	RMSE	MAE	R^2	RMSE	MAE	R^2
γ = 1.1	Overall	1	.10796	1.00	.78	.032	1.00	.78	.002
	Cohesive	0.8	.09679	1.01	.79	.050	1.00	.79	.000
	Disjoint	1	.02148	1.17	.93	.029	1.10	.88	.004
γ = 1.2	Overall	0.1	.11325	1.08	.84	.040	1.17	.93	.000
	Cohesive	0.7	.00006	2.48	2.00	.041	2.89	2.25	.001
	Disjoint	0.1	.11763	1.15	.91	.019	1.17	.93	.000

Note. α = mixing parameter, λ = penalty parameter, RMSE = root-mean-square error. MAE = mean absolute error

Supplementary References

Anusic I., Schimmack U., Pinkus R. T., & Lockwood P. (2009). The nature and structure of correlations among Big Five ratings: The halo-alpha-beta model. *Journal of Personality and Social Psychology, 97*(6), 1142-1156. https://doi.org/10.1037/a0017159

Feeley, T. H. (2002). Comment on halo effects in rating and evaluation research. *Human Communication Research, 28*(4), 578-586. https://doi.org/10.1111/j.1468-2958.2002.tb00825.x